

THE FIRE ENDURANCE OF REINFORCED CONCRETE STRUCTURES

THE FIRE ENDURANCE OF REINFORCED CONCRETE STRUCTURES

by

Edward F. Vickers, B.Eng.

A Thesis

Submitted to the Faculty of Graduate Studies

in Partial Fulfillment of the Requirements

for the Degree

Master of Engineering

McMaster University

Hamilton, Ontario

Canada

1974

MASTER OF ENGINEERING (1974)

McMaster University
Hamilton, Ontario
Canada.

TITLE: The Fire Endurance of Reinforced Concrete Structures

AUTHOR: Edward F. Vickers, B.Eng. (McMaster University)

SUPERVISOR: Dr. R.G. Drysdale

NUMBER OF PAGES: XI , 155

SCOPE: The material behaviour of concrete at elevated temperatures has been investigated. A series of tests was performed to verify and add to information available in the literature. This information has been used to model the behaviour of pinned end columns and the behaviour of columns in a building frame when subjected to fire exposure. A computer program was written to analyze rigid frames. This program employs an iterative procedure to approximate the inelastic behaviour of the frame.

ACKNOWLEDGEMENTS

The author wishes to convey his sincere appreciation to Dr. R.G. Drysdale for his guidance and comments during the course of this study. It has been a pleasure to work under his supervision.

The author would like to take this opportunity to thank the following:

- (1) D.E. Allen and T.T. Lie of the National Research Council of Canada for their contribution of temperature related information
- 92) The department of Metallurgical Engineering, McMaster University, for the use of their test facilities.
- (3) McMaster University for providing financial support in the form of a teaching assistantship and the National Research Council of Canada for additional support.

The author also wishes to express his appreciation to his wife, Barbara for her encouragement during the course of this study. Her assistance in the final preparation of this thesis was invaluable.

TABLE OF CONTENTS

| | <u>PAGE</u> |
|---|-------------|
| Chapter 1 <u>INTRODUCTION TO FIRE ENDURANCE</u> | 1 |
| 1.1 General Introduction | 1 |
| 1.2 Remarks on Fire Endurance | 2 |
| 1.3 Theory of Fires | 7 |
| 1.4 Standard Fire Curves | 10 |
| 1.5 Temperature Gradient in a Square Concrete Column | 11 |
| 1.6 Objectives | 14 |
| Chapter 2 <u>THERMAL AND MECHANICAL PROPERTIES OF REINFORCED CONCRETE</u> | 15 |
| 2.1 Introduction | 15 |
| 2.2 Thermal and Deformation Properties of Concrete | 15 |
| 2.2.a Aggregate | 18 |
| (i) Expansion | 18 |
| (ii) Thermal Conductivity | 18 |
| 2.2.b Cement Paste | 20 |
| (i) Expansion | 20 |
| (ii) Thermal Conductivity | 21 |
| 2.2.c Combined Aggregate and Cement | 21 |
| 2.3 Strength Properties of Reinforced Concrete | 22 |
| 2.3.a Concrete Properties | 22 |
| (i) Strength | 22 |
| (ii) Modulus of Elasticity | 25 |
| (iii) Creep | 25 |
| (iv) Spalling | 26 |
| 2.3.b Steel Properties | 27 |
| (i) Strength | 27 |
| (ii) Elastic Modulus | 27 |
| (iii) Expansion and Creep | 27 |

| | | |
|-----------|--|----|
| 2.4 | Concrete Cylinder Fire Tests | 28 |
| 2.4.a | Introduction | 28 |
| 2.4.b | Test Program | 29 |
| 2.4.c | Concrete and Specimen Preparation | 30 |
| 2.4.d | Forms and Preparation of Sample | 30 |
| 2.4.e | Concrete Mix | 31 |
| 2.4.f | Unstressed Cylinder Test Program | 33 |
| 2.4.g | Stressed Cylinder Tests | 34 |
| 2.4.h | Results and Observations | 36 |
| | (i) Unstressed Tests | 36 |
| | (ii) Stressed Tests | 39 |
| 2.5 | Selection of Material Properties | 41 |
| 2.6 | Mathematical Representation of Material Properties | 42 |
| 2.7 | Summary | 46 |
| Chapter 3 | <u>FIRE ENDURANCE OF REINFORCED CONCRETE COLUMNS</u> | 47 |
| 3.1 | Study of Design Parameters on Fire Endurance | 47 |
| 3.2 | Calculation of Column Strength | 48 |
| 3.3 | Variable Normalization | 50 |
| 3.4 | Standard Cross Section | 51 |
| 3.5 | Interaction Diagrams | 52 |
| 3.6 | Thermal Protection of Steel | 54 |
| 3.6.a | Concrete Cover | 56 |
| 3.6.b | Column Size | 58 |
| 3.6.c | Placement of Steel | 59 |
| 3.7 | Effect of Steel Percentage | 61 |
| 3.8 | Column Slenderness | 64 |
| 3.9 | Summary | 66 |

| | | |
|------------|---|-----|
| Chapter 4 | <u>FIRE ENDURANCE OF REINFORCED CONCRETE FRAMES</u> | 67 |
| 4.1 | Concept of Stiffness Properties Based on Transformed Areas | 67 |
| 4.2 | Calculation of Stiffness Properties | 70 |
| 4.3 | Load-Deformation Relationships | 71 |
| 4.3.a | Moment-Curvature Relationship | 73 |
| 4.3.b | Axial Load-Axial Strain Relationship | 75 |
| 4.3.c | Axial Load-Curvature Relationship | 77 |
| 4.4 | Variation of EA and EI with External Loads | 79 |
| 4.4.a | Variation of EA and EI with Moment | 82 |
| 4.4.b | Variation of EA and EI with Axial Load | 86 |
| 4.5 | Method of Structural Analysis | 89 |
| 4.6 | Results and Observations of Frames Subjected to Fire Exposure | 94 |
| 4.6.a | Frame Details | 94 |
| 4.6.b | Force Redistribution Due to Fire Exposure | 97 |
| 4.6.c | Thermal Restraint Equation | 101 |
| 4.6.d | Deflection of Fire Exposed Columns | 104 |
| 4.7 | Summary | 104 |
| Chapter 5 | <u>CONCLUSIONS AND RECOMMENDATIONS</u> | 107 |
| 5.1 | Conclusions | 107 |
| 5.2 | Recommendations | 108 |
| References | | 109 |
| Appendix A | <u>COMPUTER PROGRAM FOR FIRE ENDURANCE</u> | 111 |
| A.1 | Introduction | 111 |
| A.2 | Program FIRE | 111 |
| A.3 | Subroutine TEMPER | 111 |
| A.4 | Subroutine ITERATE | 115 |

| | <u>PAGE</u> |
|-------------------------------------|-------------|
| A.5 Subroutine STIFF | 123 |
| A.6 Structural Analysis Subroutines | 124 |
| A.6.a Subroutine COLUMN | 124 |
| A.6.b Subroutine FRAME | 127 |
| A.6.c Subroutine RIGID | 133 |
| A.7 Program Listing | 134 |

LIST OF FIGURES

| <u>FIGURE</u> | <u>TITLE</u> | <u>PAGE</u> |
|---------------|--|-------------|
| 1.1 | Temperature Course of a Fire | 9 |
| 1.2 | ASTM E-119-71 Fire Curve | 9 |
| 1.3 | Temperature Gradient Surface | 13 |
| 2.1 | Variation of Concrete Strength at Elevated Temperatures | 24 |
| 2.2 | Variation of Concrete Strength at Elevated Temperatures | 24 |
| 2.3 | Recovery of Concrete Strength | 24 |
| 2.4 | Bounds on E_c | 24 |
| 2.5 | Creep of Concrete and Steel | 28 |
| 2.6 | Aggregate Sieve Analysis | 32 |
| 2.7 | Aggregate Mix Composition | 32 |
| 2.8 | Apparatus for Loaded While Heating Tests | 35 |
| 2.9 | Small Cylinder Load Tests at Elevated Temperatures | 37 |
| 2.10 | Experimental Load-Deflection Curves for Unstressed Tests | 40 |
| 2.11 | Concrete Temperature Dependence | 45 |
| 2.12 | Concrete Stress-Strain | 45 |
| 2.13 | Steel Temperature Properties | 45 |
| 2.14 | Steel Stress-Strain | 45 |
| 2.15 | Concrete Stress-Strain with Expanded Strain Axis | 45 |
| 3.1 | Interaction Diagram for the Standard 16 Inch Square Column | 53 |
| 3.2 | Interaction Diagram for a 12 Inch Square Column | 55 |
| 3.3 | Ultimate Load of 16 x 16 Columns | 57 |
| 3.4 | Ultimate Load of 12 x 12 Columns | 57 |
| 3.5 | Interaction Diagram Using Mid-depth Steel | 60 |

| <u>FIGURE</u> | <u>TITLE</u> | <u>PAGE</u> |
|---------------|---|-------------|
| 3.6 | Comparison for Steel Placement | 62 |
| 3.7 | Variation of Steel Percentage | 63 |
| 3.8 | Variation of Steel Percentage | 63 |
| 3.9 | Variation of Column Length | 65 |
| 4.1 | Interaction Diagram and Material Properties for Standard 16 Inch Column | 72 |
| 4.2 | Moment-Curvature Relationship | 74 |
| 4.3 | Axial Load-Axial Strain Relationship | 76 |
| 4.4 | Axial Load-Curvature Relationship | 78 |
| 4.5 | Variation of EA at Constant Axial Load | 80 |
| 4.6 | Variation of EI at Constant Axial Load | 81 |
| 4.7 | Comparison for EI Method of Calculation | 84 |
| 4.8 | Plot of M_{xt} versus M_{cg} | 85 |
| 4.9 | Variation of EI at Constant Moment | 87 |
| 4.10 | Variation of EA at Constant moment | 88 |
| 4.11 | Frame Analysis based on Centroid Axis | 90 |
| 4.12 | P-Δ Effect | 92 |
| 4.13 | Details of Frames Analyzed | 96 |
| A.1 | Calculations for Subroutine ITERATE | 113 |
| A.2. | Illustration of Transformed Areas | 114 |
| A.3 | Calculation Procedures for Stress and E | 120 |
| A.4 | Joint and Member Numbering | 129 |

LIST OF TABLES

| <u>TABLE</u> | <u>TITLE</u> | <u>PAGE</u> |
|--------------|--|-------------|
| 4.1 | Eight Storey Frame Analysis | 98 |
| 4.2 | Four Storey Frame Analysis | 99 |
| 4.3 | Two Storey Frame Analysis | 100 |
| 4.4 | Thermal Expansion Effects on Column Line 2 | 102 |
| 4.5 | Thermal Restraint Force at Column Base 2 | 102 |
| 4.6 | Vertical Deflection at Top of Lower Column 2 | 105 |

Nomenclature

Notation

- A - area, in².
- c - concrete cover to steel stirrups, inches.
- d - distance on cross section to point under consideration measured from subscript location, inches.
- e - eccentricity of load, inches.
- E - modulus of elasticity, ksi.
- EA - axial stiffness, kips.
- EI - flexural stiffness, in²-kips.
- f - material stress, ksi.
- f'_c - 28 day concrete compressive strength, ksi.
- I - moment of inertia, in⁴.
- L - length of column, feet.
- m - number of steel bars.
- M - bending moment, in-kips.
- n - number of divisions of the square cross section depth and width.
- p - steel area as percentage of concrete area, %.
- P - axial load, kips.
- t - dimension of square cross section, inches.
- T - temperature in thousands of °C.
- x,y - coordinates on face of cross section, define frame geometry.

Greek

- φ - curvature
- ξ - strain, in/in.
- Δ - deflection, inches.
- Σ - summation

Subscripts

- b - balanced conditions.
- c - of concrete.
- cg - at elastic centroid.
- ext,int - external, internal.
- i,j - of concrete element i,j.
- k - of steel bar k.
- min,max - minimum, maximum.
- s - of steel.
- u - ultimate.
- y - at steel yield
- xt - at cross section mid-depth.

Superscripts

- ' - normalized value, (except f'_c).
- T - at elevated temperature.

Chapter 1

INTRODUCTION TO FIRE ENDURANCE1.1 General Introduction

Exposure to high temperature in a building fire will have detrimental effects on the load capacity and on the deformation characteristics of a building element. The effect of fire exposure on an unprotected steel column or on an entire steel framed building can be readily calculated. This is due to the availability of knowledge of the thermal effect on steel properties^(10,13) and also due to the elastic behaviour of the steel which permits conventional matrix structural analysis of the frame. If the building has a large degree of redundancy it may require the use of a computer as a design aid but the methods involved are common knowledge to most engineers. For the steel framed building fire endurance can be readily determined.⁽¹⁵⁾

Unlike the steel framed building it is very difficult to analytically determine the fire endurance of a reinforced concrete building. This is due in part to the lack of quantitative information of the effect of high temperature on the mechanical properties of concrete, especially the effects on deformation related properties such as creep, shrinkage and expansion. It is not possible to determine analytically the mechanical properties for all concretes. However, it is possible to determine the mechanical properties for a specific test concrete in the laboratory. The laboratory results which are available although not as thorough or as complete as would be desired have been used in this investigation

to obtain the fire endurance of pin-ended unrestrained reinforced concrete columns.

Concrete exhibits non-linear, inelastic behaviour at almost any strain intensity. Conventional stiffness matrix analysis cannot be used because the modulus of elasticity of the concrete is dependent on the strain and on the stress in the element. This inelastic behaviour can be estimated by a succession of elastic approximations. By a process of iteration, the internal stresses and strains on the elements comprising the assumed elastic frame can be adjusted to represent the actual behaviour of the inelastic frame. The actual stress and strain distributions over the cross section are used to obtain the axial section property (EA) and the flexural section property (EI) by a numerical summation over the area. These two parameters are adjusted due to changes in stress and strain until the behaviour of the frame has been approximated within some allowable tolerance.

The effect of expansion must be included when there is any restraint to free movement. This is true for pin-ended columns as well as for a rigid frame. In the case of a rigid frame there can be substantial increases in column axial load as a result of expansion. The harmful effect of this increase is alleviated to some extent by the simultaneous moment re-distribution brought about by changes in member axial and flexural stiffnesses.

1.2 Remarks on Fire Endurance

The only performance requirement related to fire endurance

its load carrying capacity during fire exposure. The fire rating required by building codes is the length of time that a structural beam, column, floor or wall can support the design load when exposed to a standard fire.

Past practice has been to base the fire endurance of reinforced concrete structures on actual testing if not too expensive, or on the application of empirical data to check the fire worthiness of a design. This data has been obtained from many varied and perhaps unrelatable sources. With reinforced concrete a column test will have a large number of material variables, some of which are type of aggregate, initial water-cement ratio and degree of hydration at the time of testing. As well a large number of structural variations such as depth of cover to steel, size and shape of concrete cross section, degree of restraint and amount of reinforcing steel exist. These possibilities for variation make it unlikely that designs being carried out at present will exactly fit the design parameters of the previously tested columns. Designers should be cautioned against the attitude that the similarities are "close enough". There can be significant changes in the fire endurance for seemingly small differences in say, percentages of hydration or degree of restraint.

It is the opinion of the author that present checks for fire endurance based on pin-ended columns, have little validity when the column is used in a frame. All the structural members of a frame will be restrained by frame action. As the temperature environment changes, a redistribution of forces in all members that is different from the original design will occur. This

interaction with the remainder of the structure can be beneficial or non-beneficial depending on the position of each member in the frame and depending on the extent of the fire in the frame. For a reinforced concrete column that is designed principally for axial load there could be a detrimental increase in axial load due to expansion. However, for a reinforced concrete beam, an increase in axial load due to expansion with a constant bending moment will usually increase the factor of safety in the beam. Beams and columns in areas of a frame adjacent to the fire could have adverse increases in bending moments due to expansion and moment redistribution by the members affected by the fire.

Although the use of pin-ended columns for the checking of designs may not be totally satisfactory for a rigid frame the use of pin-ended columns provides a good means to study the effects of different variables on the fire endurance of reinforced concrete structures.

Previous work, by Clark⁽⁴⁾ for example, was hindered by a lack of knowledge of material properties. This resulted in very empirical methods for predicting the fire endurance of concrete columns.

With a better understanding of material behaviour, it could be possible to use fewer simplifying assumptions. At present, research is being carried out in many countries along the lines of testing the individual components of reinforced concrete. Studies into areas such as aggregate composition, thermal induced creep or thermal conductivity have yielded data that has recently increased the knowledge of concrete thermal and

mechanical properties. (1,2,5,7,9,18,19) This has permitted numerical modelling of column and frame behaviour which is as reliable as much of the empirical data available.

In the present study, some variables that should be included in the overall analysis have been excluded. It is felt that this work should provide a basis for furthering the design of reinforced concrete structures so that they are actually designed and not just checked for fire endurance.

As Canada and other countries adopt national design codes based on limit state design, it is necessary that a consistent safety factor be used in all aspects of design. The use of computer aided design allows a set of calculations to be performed to check the actual safety factor of a structural element. The numerical analysis and design of an entire reinforced concrete building for fire endurance as well as design loads could be performed in a fraction of the time and cost required for the experimental testing of a single structural element.

The ultimate reason for studies in this area is to prevent loss of life and also loss of financial investment. A full study on structural fires would include fire prevention methods, fire extinguishing methods, structural integrity assurance, smoke control and means of ensuring occupant egress.

Only structural integrity will be investigated now but this does not mean that other aspects of a structural fire are not important. In a reinforced concrete structure, which by nature has a high latent fire endurance and hence high structural integrity, problems of smoke control and egress may be more

Major fires in high rise reinforced concrete buildings have shown that the problems of smoke control and egress are more important to prevent loss of life. These same fires have shown that the possibility of a reinforced concrete building actually collapsing during a fire is probably minimal. This could be explained by the fact that not all columns or beams in a building will be exposed to the same maximum temperature at the same time, thus allowing adjoining members to share the load on a member that is undergoing the maximum temperature. Also the interior design of many apartments or office buildings tend to isolate the effects of the fire from other areas.

Building fires can result in structural collapse as evidenced by recent fires in two buildings. A large one-storey data warehouse operated by the General Services Administration in the United States was exposed to a severe building fire. The structure enclosed an acre of floor space under a continuous roof. The expanding concrete roof deck exerted enormous column base shear loads, resulting in a base displacement after failure of several feet.

As reported in recent publications, a hotel in the United States was exposed to a fire while under construction. Although several floors collapsed along many frame lines, the remainder of the construction was deemed to be sound and reconstruction followed.

Although the building may not collapse, there is the economic question of utility after the fire. Excessive permanent set deformations and spalled surfaces of beams, columns or walls will affect the appearance and the structural

adequacy of the building. Less obvious problems that will affect member strength arise from hidden details such as surface layers of concrete which may have yielded and crushed slightly, interior areas of a cross section which may have cracked due to differential thermal expansion and material transformation of the concrete and steel which may have occurred due to thermal activation. These structural problems could all be minimized by proper design allowances.

1.3 Theory of Fires

It is necessary to have some understanding of the characteristics of a building fire in order that the seriousness of such fires can be appreciated. The severity of a fire has been estimated by various means over the years. The severity is a means of expressing the temperature course of a fire, that is, how high the temperature will rise and how long the fire will be sustained at high temperatures.

The calorific value of the combustible material in an enclosure used to be the only means of estimating fire severity. Actual fire tests were found to yield greatly varying maximum attained temperature for the same amount of combustible material. This led to the consideration of the ventilation area of the enclosure and of the thermal properties of the enclosure walls, floors and ceilings.

The temperature course of a fire has three major portions i.e. growth, burning and decay, as shown in figure 1.1. The growth period begins when the heat source ignites some combustible material in the room. There is a slow increase in as the fire is the

when a fire can be extinguished easily or escape can be made. As the temperature increases, heat transferred in the enclosure will cause volatile gases to be evolved from the combustible material. The evolved gases mix with the air to form a combustible mixture which ignites, causing "flashover", spreading the fire and rapidly raising the temperature. The duration of the growth period is affected by many factors. A low ignition temperature and a large surface area with little material depth will cause rapid flame spread. A shallow material depth means that heat from the flames will not be absorbed by a large material mass, but will tend to spread along the surface or irradiate to other objects. With some materials which are not shallow in depth, an insulating char will develop on the surface which inhibits flame spread. The shape of the enclosure, location of ventilation sources and the quantity of air movement is also essential in determining whether the fire's growth will be limited by the available combustible material or by the ventilation source. The amount of combustible materials is important as is the spacing of the combustible material with respect to each other and to the ignition source.

The burning stage begins at flashover. All of the combustible materials begin to burn rapidly, pushing the temperature in the enclosure up until the heat produced by the fire equalizes with the heat lost from the enclosure. The maximum temperature in figure 1.1 is where the heat production just begins to drop. At all points on the curve the heat produced by the fire is balanced with the heat brought in with the intake ventilation

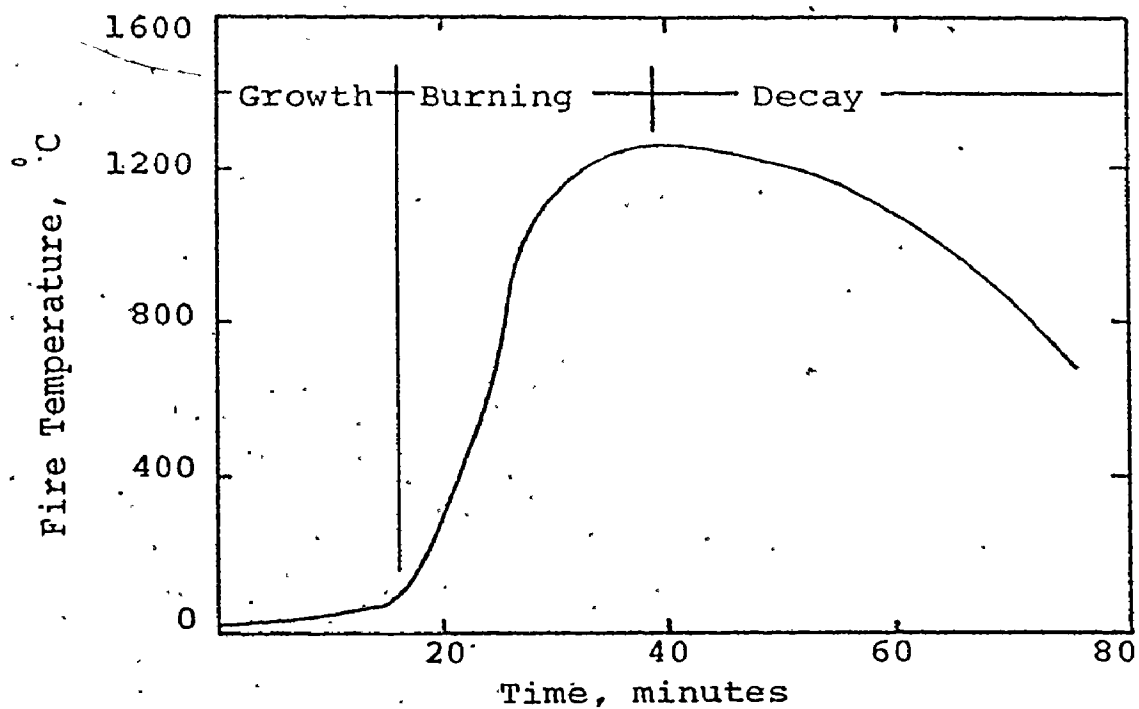


Figure 1.1
Temperature Course of a Fire

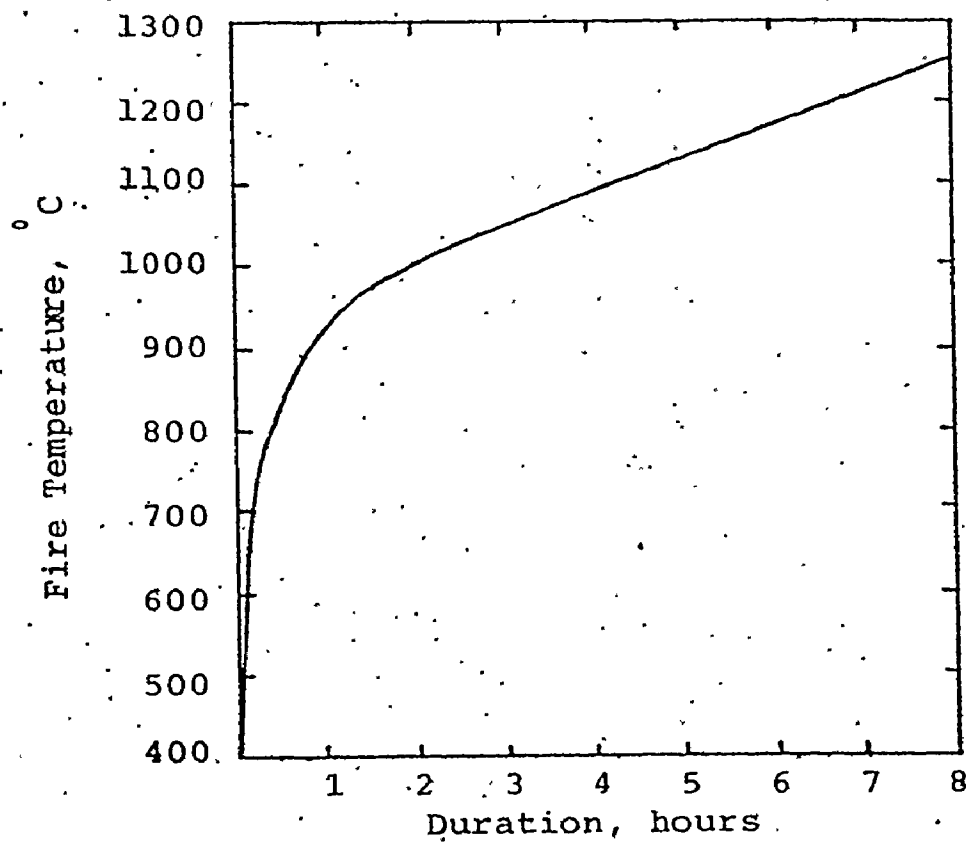


Figure 1.2

air must balance against all heat losses. Heat is absorbed by the surfaces of the enclosure and by the air in the enclosure. Heat is also lost by radiation through openings and by convection in the outgoing gases. The better the enclosure is insulated, the higher will be the maximum attained temperature. With the extremely high heat produced, the fire can spread to surrounding rooms by flame spread and by penetration. The fire can also spread to adjacent buildings by the collapse of barrier walls or by radiation through windows and doorways.

During the burning and decay periods the rate of burning is controlled by the amount of ventilation up to the point where there is an excess of air available for combustion. When the air supply is unlimited then the surface area of the combustible material will govern the maximum temperature. The decay period, when temperature begins to lower, is caused by excessive charring which restricts the area available for combustion.

1.4 Standard Fire Curves

A modern building usually has large windows, ensuring adequate ventilation for a fire. The walls, floor and ceiling are often concrete or block work providing good isolation of the fire but which allows very high temperatures to develop in a localized portion of a building. Every room in a building will have different amounts of combustible material which will likely change with time due to occupant usage, therefore, the fire severity in a building will be very difficult to ascertain.

Each room could have its own fire temperature course curve which would make actual testing to determine the fire endurance a very costly affair. Recognizing the variability possible in the fire load and ventilation, standard curves have been developed to represent the expected temperature course of a fire. Although most countries have developed their own standard fire test curves, these curves are quite similar between countries. For the present study, the standard fire curve used is described by ASTM E119-71,⁽⁴⁾ shown in figure 1.2. This curve can be approximated by the following equation.⁽¹⁴⁾

$$T = 530 + 1350(1 - \exp(-3.79553\tau^{1/2})) + 306.74\tau^{1/2} \quad 1.1$$

The actual fire temperature curve may not be the same as the standard curve but at least a uniform standard will be applied to the design of building elements for high temperatures.

1.5 Temperature Gradient in a Square Concrete Column

For this study all of the temperature information has supplied by T.T. Lie of the National Research Council of Canada. Lie,⁽¹²⁾ in his work to determine the temperature gradient in concrete has developed an accurate method of obtaining internal concrete temperature when the specimen is exposed to external heat at the surface. The study at hand has been restricted to the analysis of square concrete cross sections. Due to the four axes of symmetry, the number of calculations for thermal and mechanical properties is greatly reduced. The temperature related calculations are required for a pie-shaped wedge over only one eighth of the cross section.

The column cross section is exposed on all four sides to a

fire that follows the temperature course of ASTM E119-71. (see equation 1.1) It has been assumed that the column will act as a black body and absorb all heat developed by the fire that is incident on its surface. The thermal gradients are calculated by a finite-element technique. The results of the finite-element analysis are tabulated in matrix form with each element of the square matrix corresponding to the midpoint of the respective element on the cross section. The temperature gradient surface over a sixteen inch square quartz aggregate concrete column is shown in figure 1.3. Since this cross section is quite large, there is a great differential between the temperature at the surface and that at the centre point. Along grid lines in the central portion of the cross section, the temperature drops rapidly as distance from the outer surface increases. Near the corners of the cross section the temperature gradient is more shallow, resulting in higher temperatures in the four corners. This is the result of heating on all four surfaces. There is a greater flow of heat on the corners.

Since the fire exposure is uniform the temperature of the outer layer of concrete is the same all around the cross section. The shape of this temperature surface will affect later considerations on design parameters such as, cover to reinforcing steel or the location of the steel in the cross section.

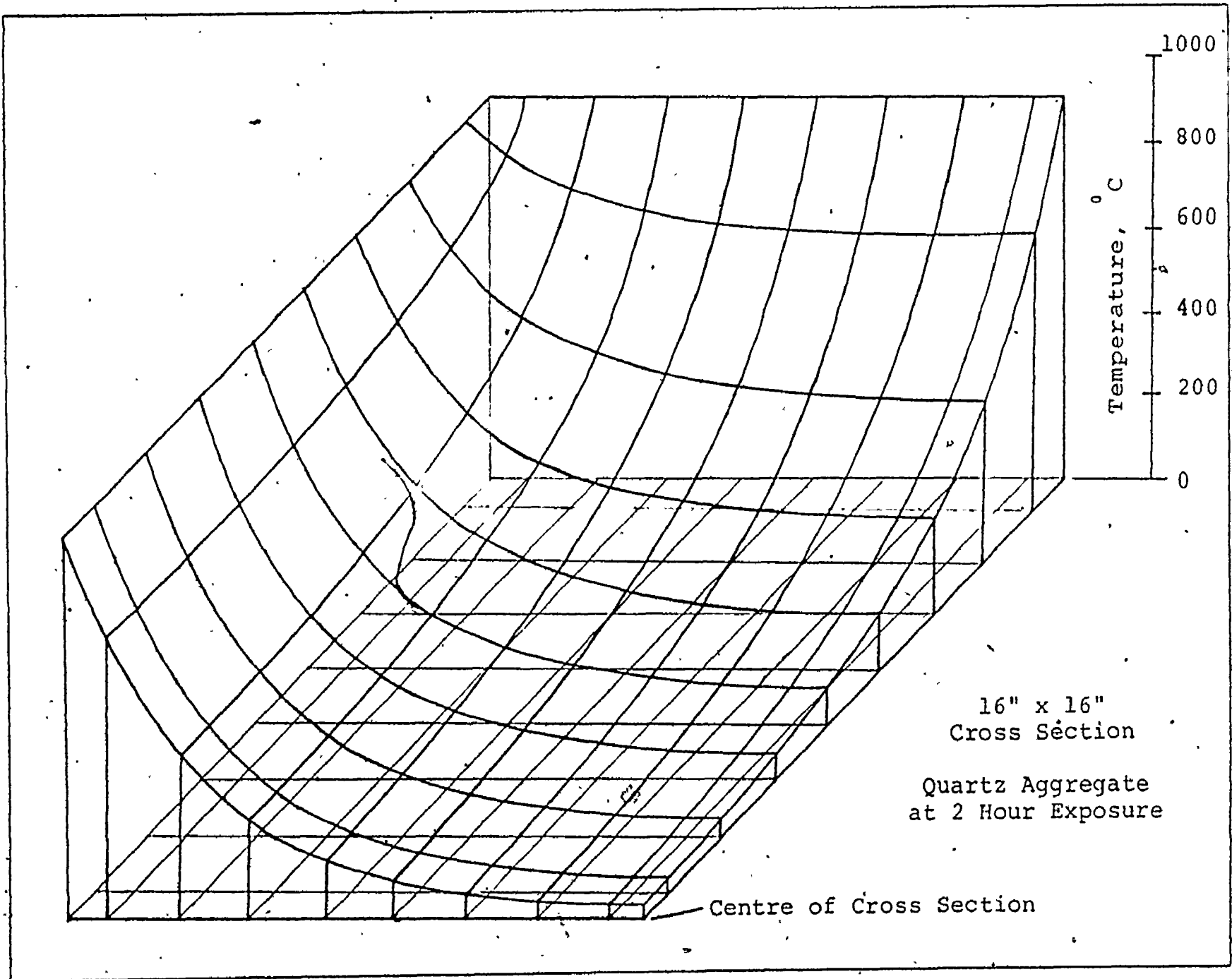


Figure 1.3 - Temperature Gradient Surface

1.6 Objectives

This study will attempt to verify by testing, some of the existing information on the material behaviour of concrete. This will be done in a qualitative manner to discover any abnormalities in the literature.

With the material properties either accepted or questioned, a representative set of material properties will be selected for following column and frame analysis.

Short and slender columns will be analyzed to determine the effects of variation of design parameters such as concrete cover, on the fire endurance. Finally, building frames will be exposed to fire to examine the effect of frame continuity on the fire endurance.

Chapter 2

THERMAL AND MECHANICAL PROPERTIES OF REINFORCED CONCRETE2.1 Introduction

To determine the strength and deformation characteristics of a compound building material exposed to a fire, it is necessary to understand the behaviour and the thermal properties of the constituent material at the temperature attained in a fire. The thermal properties determine the temperature increase over the cross section of the member. This temperature rise causes a change in the mechanical properties; strength and deformation. These mechanical properties will be temperature-dependent and may also be stress-dependent and time-dependent.

In sections 2.2 and 2.3, the thermal and mechanical properties of the components of reinforced concrete will be outlined. In the following section, the results of a limited test program, performed to generally verify the data in the literature will be given. Finally, the properties selected to represent a standard quartz aggregate concrete will be discussed. This standard concrete will be used in all calculations.

2.2 Thermal and Deformation Properties of Concrete

The thermal and deformation properties of concrete can be determined by appropriate testing methods. However, due to the possible wide variations in aggregate composition and water-cement-aggregate ratios, it becomes necessary to generalize about the effects of each variable.

It is important to note that all of the testing to determine

the thermal properties of concrete performed in the past has been done on small specimens, usually oven-dried prior to testing. The specimen is heated to an elevated temperature with or without an applied load, allowed to heat equalize at this temperature and then tested to rapid failure by a force controlled device.

Material properties obtained in this manner may not be truly indicative of the actual behaviour of reinforced concrete assemblies in a fire. Due to the size of columns and beams, the temperature gradient over the cross section is always in a state of dynamic flux. Over the cross section this results in unequal thermal expansion, unequal stress-strain characteristics and the entrapment of both pore-water and released crystallization-water within the hot, dried outer layer of concrete. Testing in this dynamic state, which would require the costly testing of whole assemblies, needs to be performed to verify the design usage of information obtained by testing on small specimens at static temperature. It has been assumed in this study that this usage is allowable. In fact, others ⁽¹⁴⁾ have shown reasonable agreement between results of experiments on assemblies compared with calculated predictions.

Elevated temperatures result in two types of design; steady state and transitory. Steady state occurs when the assembly is in thermal equilibrium. The design can proceed using usual methods with proper reductions for strength and modulus of elasticity. The expanded shape should be taken into account.

Transitory design occurs when the temperature is changing up or down, resulting in non-uniform stressing due to differential

thermal expansion and due to the variation of maximum strengths and the stress-strain relationships over the cross section. A large construction subjected to an extreme temperature gradient may crush in the hot zone and pull apart in the cold zone. For this phase of design, thermal expansion must be accurately defined for all temperatures. A linear coefficient is not sufficient.

In the following section, the effect of thermal expansion and conductivity will be examined to indicate how they affect the components of concrete. Thermal expansion is common to all materials. In concrete, the apparent expansion is the sum of all of the expansions of the individual components. Due to different rates of expansion large internal stresses and strains can develop between the components. Thermal conductivity needs to be completely defined especially for the transitory design stage. Thermal conductivity of concrete is affected by the conductivities of the cement and aggregate, by the mix ratios, by the compactness (lack of porosity) and by the moisture content.

The physical meaning of the factors affecting heat flow through the concrete cross section, that is, conductivity, specific heat and diffusivity will not be explained in detail. Information on these variables can be found in reference (13). The effects of temperature and material composition on these has been included in the derivation of the temperature gradients by Lie. The temperature rise at the position of the steel reinforcing is a function of the concrete thermal properties and is considered to be unaffected by the steel

thermal properties.

2.2 (a) Aggregate

(i) Expansion

The mineral composition and structure of the aggregate is the major factor in determining the thermal expansion coefficient of the concrete. Due to the low cement to aggregate ratio, the thermal characteristics of the hardened concrete are very close to those of the aggregate.

It should be noted that rocks with high quartz content such as quartzite and sandstone have the highest coefficient of thermal expansion (about 12×10^{-6} in/in/ $^{\circ}$ C at temperatures of 10° C to 65° C). Limestone (carbonate) rocks with no quartz content have the lowest coefficient of expansion (about 5×10^{-6} in/in/ $^{\circ}$ C). Igneous rocks such as granite with low quartz content have a thermal expansion in between the two extremes. As temperature is increased, the coefficient of thermal expansion will increase non-linearly. Thus, for later use in stress-strain calculations, the coefficient of thermal expansion must be changed continuously as the temperature is increased.

Water content plays a part in aggregate expansion. Air dry rocks may have a 10% higher apparent expansion than water saturated rocks. This is the result of initial drying shrinkage of the saturated rocks decreasing the true aggregate expansion.

(ii) Thermal Conductivity

Thermal conductivity is higher for quartz aggregate than

As would be

elementary thermodynamics, a crystalline aggregate such as quartz will have a higher thermal conductivity, due to increased molecular order than would an amorphous aggregate. As temperature is increased, there is usually a drop in thermal conductivity. In general, aggregates with a high thermal expansion which could result in increased micro-cracking (rupturing of intercrystalline bonds in the aggregate) are those rocks which undergo the largest decrease in thermal conductivity as the temperature increases. Lightweight aggregates with a high degree of porosity have a low thermal conductivity. Other factors affecting the heat flow in the aggregate are the possibility of thermally activated transformations of the aggregate or the release of any crystal water. Limestone aggregate will transform to a soft chalk at 600°C , while quartz will undergo several phase transformations. Usually associated with these transformations is a large increase in the specific heat which has the effect of slowing the thermal conductivity.

The relationship between thermal conductivity and expansion is important. For quartz which has a high thermal conductivity, the temperature gradient is not as steep as would be expected for anorthosite aggregate. Although the thermal expansion is greater for quartz than for anorthosite, due to the smaller differences in temperature between the inner core and outer layer, the strain differential will be less for quartz than for anorthosite. It is this strain differential which is responsible for tension-cracking in the concrete core while the surface concrete is being crushed.

This leads to weakening of the concrete and could be a cause of spalling. Although a number of temperature gradients for different aggregate concretes were made available by T.T. Lie and D.E. Allen of the National Research Council of Canada, only those gradients dealing with quartz aggregate have been used.

2.2 (b) Cement Paste

(i) Expansion

The actual expansion of cement is the super-imposed sum of the true and apparent expansion. True expansion caused by increased kinetic molecular action is essentially constant at 10.0×10^{-6} in/in/ $^{\circ}$ C. Apparent or hygrothermal expansion is a hygrothermal volume change caused by movement of internal moisture from the cement capillaries to the gel pores. The movement is caused by capillary forces produced by temperature changes without any change in total water content in the specimen. Apparent expansion depends primarily on the moisture content and as well on the capillary structure and quantity of cement.

Certain moisture contents have the effect of increasing the thermal expansion so that a maximum is obtained at 65% to 70% saturation for a six months old sample or at 45% to 50% saturation for a sample many years old. Minimum expansions occur at zero and 100% saturation.

Hygrothermal expansion of neat cement paste may exceed true expansion since total thermal expansion can vary from 9.0×10^{-6} up to 21.6×10^{-6} in/in/ $^{\circ}$ C. at room temperature. The different rates depend on differences in cement fineness, cement

with age of cement.

Cement paste expands rapidly up to the boiling point of water and then begins to contract as water is given off at a constant temperature of 100°C . This contraction is greater than initial expansion. Shrinkage is due to the removal of the water of hydration. This shrinkage is time-dependent due to the length of the path that the water must follow to escape. Contraction will continue up to 500°C to 700°C where expansion will again occur.

(ii) Thermal Conductivity

As with the aggregate the thermal conductivity of the cement paste lowers as the temperature of the cement is increased. This decrease in conductivity is caused by micro-cracking due to aggregate expansion and cement contraction at elevated temperature. Increased porosity due to loss of pore water will also cause a decrease in conductivity. Pore water has a high specific heat which adversely affects conductivity but the air void remaining after the water is driven off has an even lower conductivity,

2.2 (c) Combined Aggregate and Cement.

The thermal properties and expansion of the combined cement paste and aggregate can be estimated by using their relative proportions in the concrete mix. Due to possible variations in moisture content, porosity or age, the taking of actual measurements is the most reliable means of determining these values.

At temperatures up to 100°C the cement matrix that holds the aggregate in place will expand faster than the aggregate. This expansion places the cement paste-aggregate bonds in compression. At higher temperatures the cement shrinks while the aggregate expands. Now the internal bonds undergo tension or they must crack. The addition of external stress on the specimen will reduce the strain differential between the cement and aggregate. This reduced strain differential results in less internal cracking. With fewer cracks the concrete will retain a higher compression strength at the elevated temperature. To avoid the detrimental effects of this cracking, the external stress must be present while the specimen is being heated.

2.3 Strength Properties of Reinforced Concrete

The strength of concrete and steel at elevated temperatures must be determined by testing. For concrete the usual test is a cylinder compression test. Steel strengths are usually determined by a tension test. These tests must be performed at a number of temperatures.

2.3 (a) Concrete Properties

(i) Strength

Although the method of testing has little effect on the steel strength, there are a large number of factors related to methods of testing to be considered when testing to determine concrete strength. The rate and duration of heating, size and shape of the specimen, load intensity during heating and whether

the specimen was tested hot or cold are all aspects of the method of testing. The factors that affected the thermal properties discussed in section 2.2, that is, aggregate type and water-cement-aggregate ratios will also affect the concrete strength.

The effects on concrete strength of the cement to aggregate ratio and the load intensity during heating are shown in figure 2.1. Loss of strength is slower for a high aggregate content. As temperature is increased, the rate of loss of strength accelerates. This is partly due to increased expansion causing more cracks and due to material transformation. Work by Abrams⁽¹⁾ shows that the addition of load during heating is beneficial to the compressive strength of the concrete. His work indicates that the actual load intensity is not important but rather that the addition of any load possibly in the range of 0.25 to $0.5 \cdot f_c$ is the controlling factor.

Figure 2.2 shows the effects of high temperatures on the unstressed residual strength, that is, the strength of the core after heating in an unstressed state, allowing it to cool and then testing. This indicates that the concrete continues to lose its strength after the heating has stopped. Possibly, a structure should be checked for its after-fire worthiness as well as its behaviour during the fire.

During the fire in an actual building, the concrete and steel both lose strength. After the fire the steel regains its strength as it cools except as noted in section 2.3 (b). Therefore, the reinforced concrete assembly would have a large

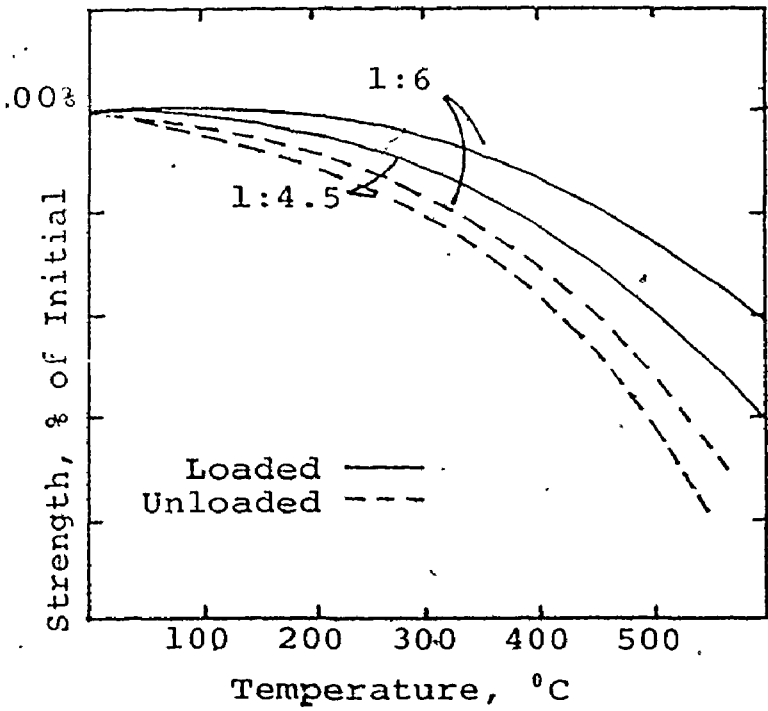


Figure 2.1

Variation of Concrete Strength at Elevated Temperatures

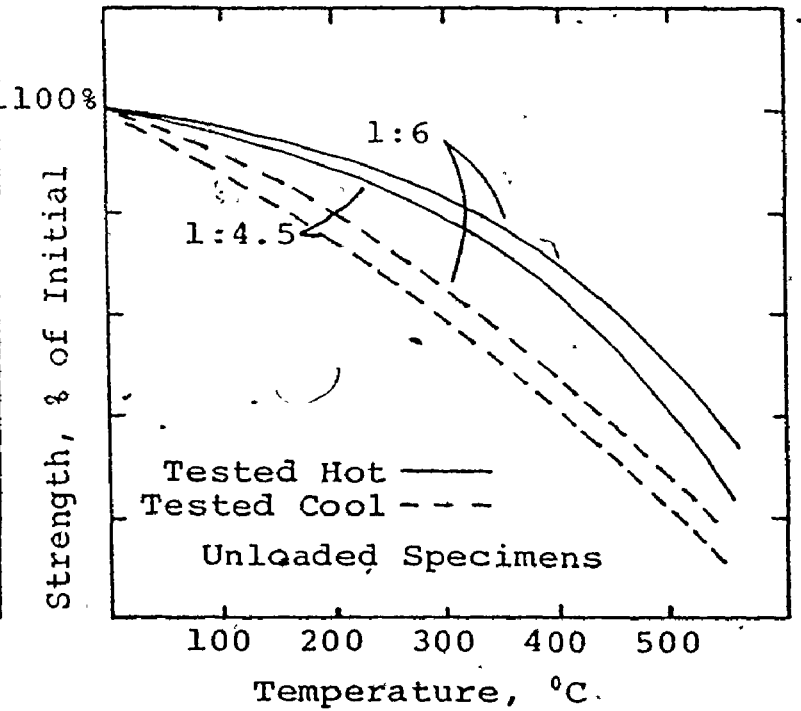


Figure 2.2

Variation of Concrete Strength at Elevated Temperatures

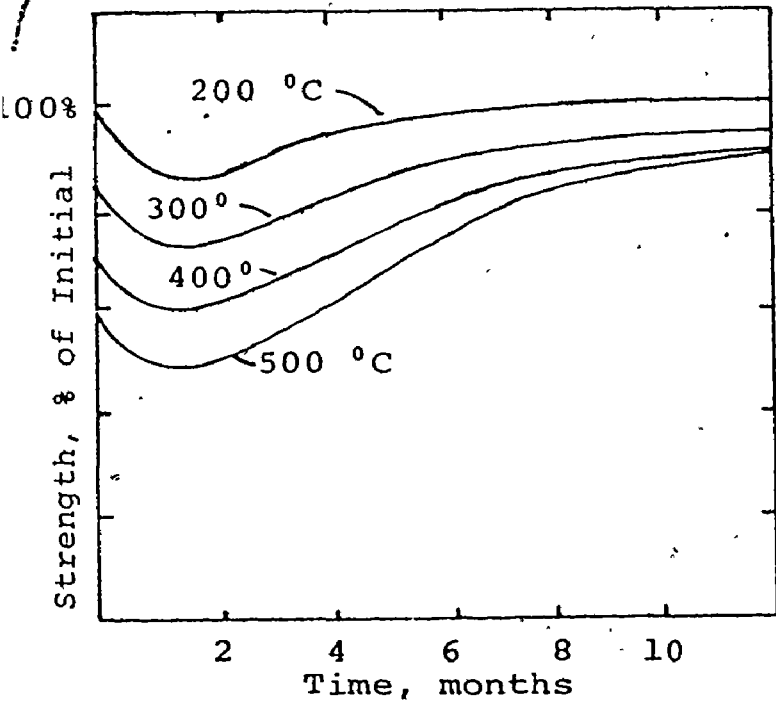


Figure 2.3

Recovery of Concrete Strength

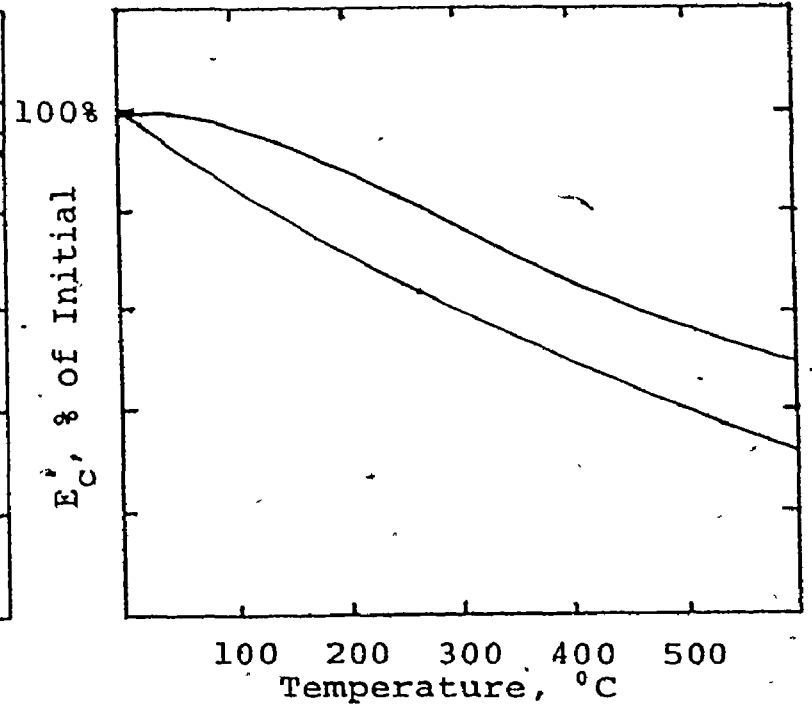


Figure 2.4

Bounds on E_c

proportion of its initial strength after the fire even though the concrete is weak.

Following initial losses, the concrete will begin to regain after heating, a large proportion of its strength over a period of several months. This applies to concrete heated up to about 500°C. Above this temperature, permanent material transformations occur which inhibit any regaining of strength. The gain in strength after heating is due to recovery of the water of hydration lost during heating. (see figure 2.3)

(ii) Modulus of Elasticity

The modulus of elasticity of concrete exhibits behaviour similar to the strength of concrete. Figure 2.4 shows the upper and lower bounds for the elastic modulus that can be expected for normal weight concrete. As was the case with strength, the modulus of elasticity declines when heated and continues to decline for a period after cooling. Then it slowly begins to regain a portion of its initial strength and modulus of elasticity.

(iii) Creep

The creep rate of concrete will increase at high temperatures. The work by Cruz⁽⁵⁾ (modified by Lie⁽¹³⁾) shown in figure 2.5 indicates the effect of temperature on the creep rate of normal weight concrete for a 4,000 psi concrete stressed to 1,200 psi. The creep rate increases as the stress level is increased for a constant temperature. Creep at high temperatures would be very difficult to measure due to gradual heat flow to other portions of the test apparatus resulting in expansion and creep of those

(iv) Spalling

Concrete structures have a tendency to lose layers off of their outer surfaces when exposed to elevated temperatures. This phenomenon is usually caused by either high compression strains in the outer layer due to differential expansion, or caused by high vapour pressures resulting from boiling of entrapped pore water beneath the surface or caused by a combination of these two factors.

Thermal expansion strains can develop large stresses in the outer layers of a concrete assembly if the assembly is restrained by the edges or by the reinforcing steel. A steep temperature gradient in the outer layer will result in very rapidly decreasing expansions with the depth away from the surface. Unless the interior can crack in tension, the exterior will fail in compression. Spalling as a result of restraint will result in a gradual loss of concrete.

Moisture is also responsible for spalling. A concrete with a high moisture content and low porosity is susceptible to explosive spalling. As the temperature is increased, water in the outer layers will either be evaporated or be attracted to the cooler concrete pores deeper in the concrete. An outer layer of dry concrete forms which traps the free water in the filled pores. As the temperature is increased, this water begins to vaporize. If the dry layer is porous, the steam can escape. Otherwise an explosive spalling will take place to release the steam.

2.3 (b) Steel Properties

(i) Strength

The yield strength of steel decreases as the temperature is increased. The shape of the typical stress-strain curve is affected also. The definite yield point for mild steel becomes a gradual curve for higher temperatures. For mild steel there is an initial increase in ultimate strength as the temperature is raised, then a rapid drop after 400°C . For high strength steels both yield stress and ultimate strength drop rapidly as the temperature is increased. Cold drawn and heat treated steels lose their strength more rapidly than high strength alloy steel or mild steel. As would be expected, cold drawn and heat treated steels do not regain their initial strength after fire exposure.

(ii) Elastic Modulus

Previous test data show a large variation in experimental results concerning the changes in the elastic modulus. All results indicate that the elastic modulus decreases at a slightly slower rate than the yield strength.

(iii) Expansion and Creep

The coefficient of thermal expansion increases very slowly with increasing temperature. The only irregularity in the expansion of steel is the transformation to austenite at about 700°C , resulting in a small contraction. This has little importance since the steel has lost almost all of its strength at this temperature.

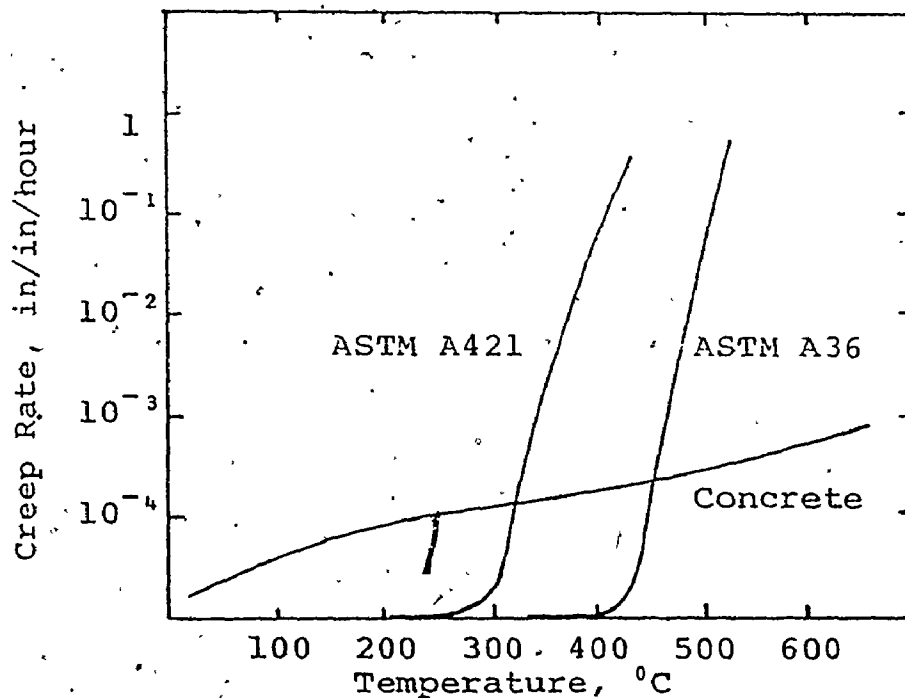


Figure 2.5
Creep of Concrete and Steel

The creep rate for steel is practically zero up to a certain temperature which depends on the load intensity and type of steel. At this point, the creep rate increases dramatically as is shown in figure 2.5. For high strength steels, the critical temperature is lower than for mild steel. In figure 2.5, the applied stress on the ASTM A36 steel is 21.6 ksi (0.6 Fy) and the applied stress on the ASTM A421 is 100 ksi, (approximately 0.5 Fy).

2.4 Concrete Cylinder Fire Tests

2.4 (a) Introduction

Abrams⁽¹⁾ et al^(2,5,13) have investigated the strength of concrete at temperatures up to 850°C. In this area there has been a great deal of conflict over results and observations. This is due in small part to the many variations possible of

ratio, plasticity of concrete, rate of heating, strain-rates and other factors. It is extremely difficult to obtain a meaningful relationship with so many factors to be considered. Thus, it is more plausible to obtain a set of test results which are as close as possible to the actual situation that will be investigated. The author was interested in the material properties in a building which has been erected on a job site. Therefore, niceties such as humid room for controlled environment curing are not to be expected. A more realistic case is moist curing for a few days followed by continual drying in the open air. This will produce somewhat poorer concrete but will yield a more realistic picture.

Many investigators have attempted to dry their specimens before heating to eliminate any chance of spalling that may occur due to boiling of trapped pore water. This spalling might also have been caused by differential expansion of the concrete as explained in section 2.3 (a) (iv). Artificial preheating to dry the sample is not representative of an actual building fire, which will likely have a rapid rise in temperature to a more or less constant temperature.

2.4 (b) Test Program

A limited test program was carried out to observe the behaviour of concrete specimens heated to a high temperature. Due to limitations on the availability of the testing machinery, especially for testing specimens under load while heating, it was not possible to obtain conclusive evidence. However, the few tests performed were valuable to the author in aiding the

understanding of previous information mentioned in sections 2.1 to 2.3.

2.4 (c) Concrete and Specimen Preparation

It was decided to avoid thermocouples buried in the centre of the test specimens. To ensure rapid and uniform heating through the specimen, the size of the specimen had to be smaller than the usual six inch diameter test cylinder. Additional limitations were placed on size by the oven used for the loading while heating tests and by the testing machine itself. The diameter of the cylinder was restricted to one and three quarter inches. Therefore, a maximum height of $2xD$ or three and one half inches was used. The cross section area was 2.41 square inches. Although it was necessary to use a small diameter, it was important to keep the length as long as possible so that expansion and creep effects could be easily measured.

2.4 (d) Forms and Preparation of Sample

The forms for the small cylinders were made from two inch outside diameter plastic tubing. The tubing was cut into three and one half inch lengths to make the forms. To facilitate removal of the concrete specimen, each section of tube had one longitudinal cut made into it and was coated internally with form oil before casting. The specimens were cast on a smooth surface to provide one good end for placing in the test machine. Although care was taken to ensure that the upper end of the cylinder was trowelled smooth and vibrated, it was necessary to have the second end saw cut to provide a good testing surface.

Standard practice for preparing six inch diameter cylinders is to cap the ends with a sulphur compound. However, due to the high heat that the specimens would be exposed to, this was not possible and saw cut surfaces had to be used.

2.4 (e) Concrete Mix

The aggregate size was limited to three eighths inch maximum due to the small cylinder size. The aggregate sieve analyses in figure 2.6 were performed for the lakeshore sand and for the limestone aggregate. The combined curve shown in figure 2.7 is in the aggregate mix proportion 1.54:1.0 fine to coarse aggregate, that is, the fine aggregate is 60.5% of the total aggregate. The water-cement ratio was 0.65:1.0 and the cement to aggregate ratio was 1:5.5. The mix design was 0.65:1.0:5.5, water to cement to aggregate ratios yielding an average 28 day strength (f'_c) of 4,006 psi. The following six inch diameter cylinders were tested to obtain f'_c .

| <u>Cylinder</u> | <u>P</u> <u>Axial (lbs)</u> | <u>σ</u> <u>Stress (psi)</u> |
|-----------------|--------------------------------|---|
| #1 | 119,000 | 4,220 |
| #2 | 110,000 | 3,900 |
| #3 | 111,600 | 3,960 |
| #4 | 113,500 | 4,030 |
| #5 | 110,500 | 3,920 |
| | | <u>20,030</u> |

$$f'_c = \frac{20,030}{5} = 4,006 \text{ psi.}$$

$$\text{maximum deviation} = \frac{(4,220 - 4,006)}{4,006} \times 100\% = 5.3\%$$

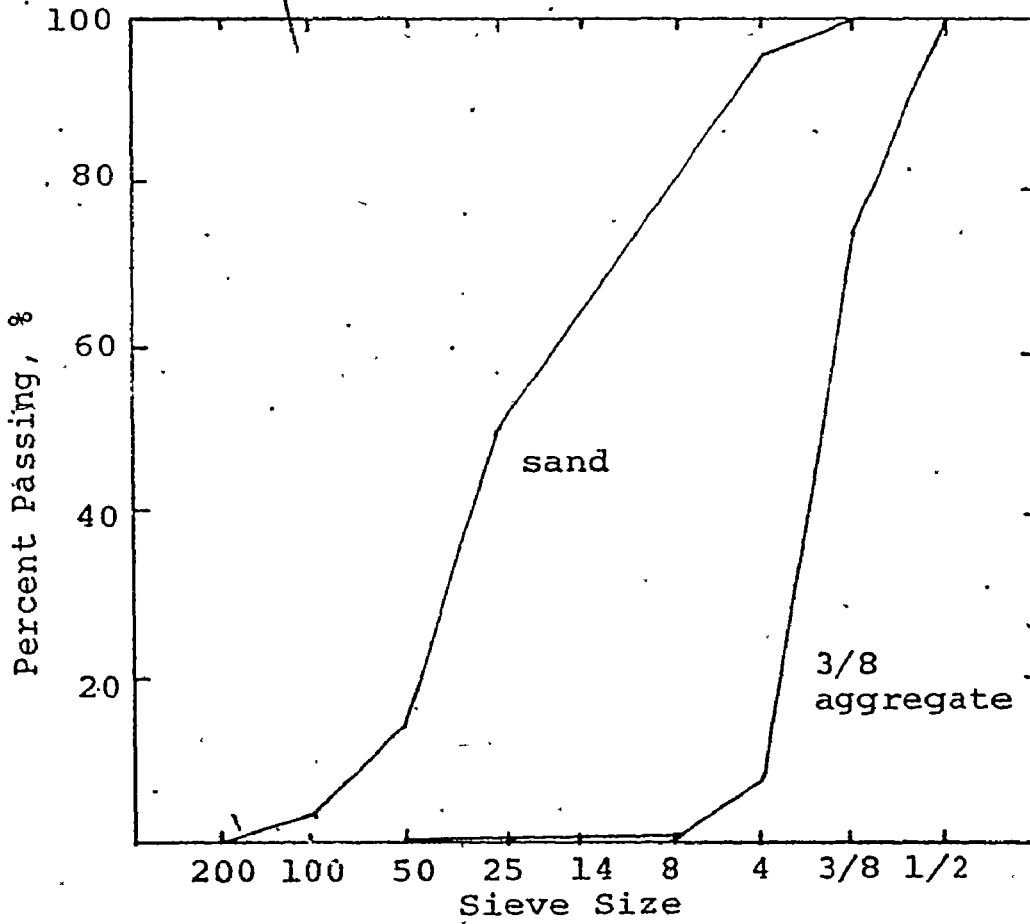
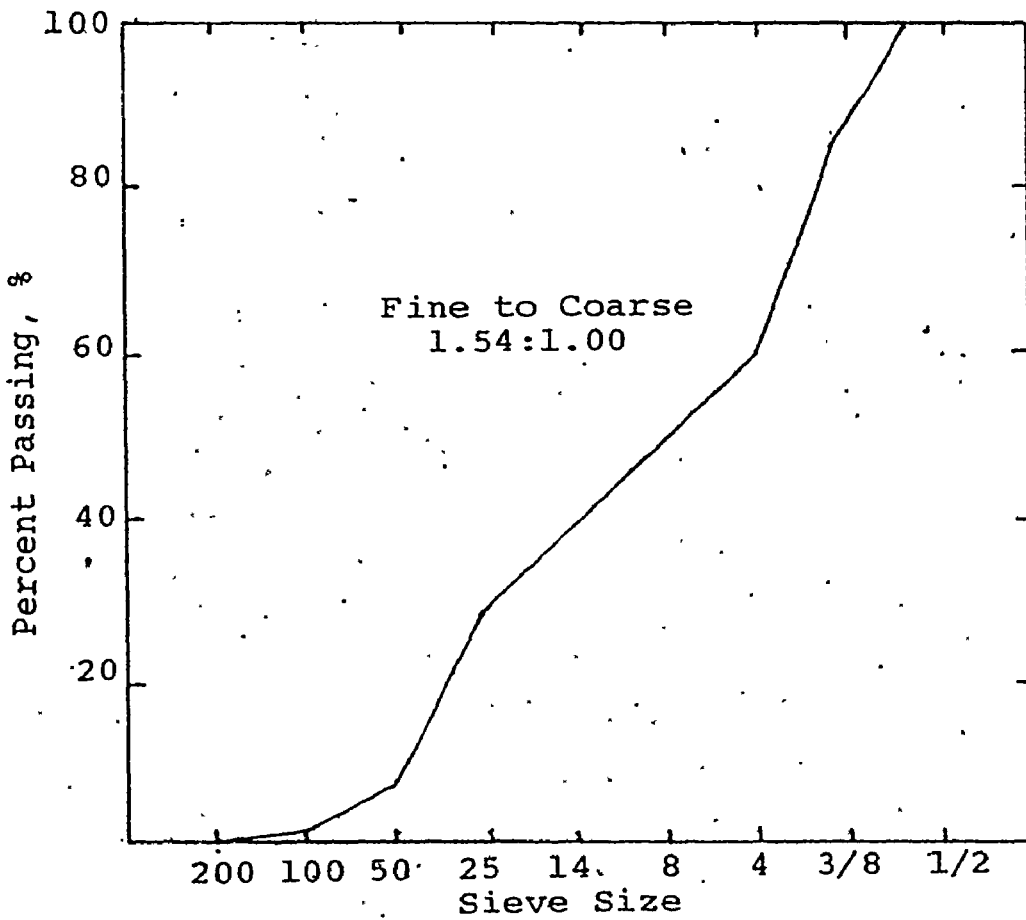


Figure 2.6
Aggregate Sieve Analysis



2.4 (f) Unstressed Cylinder Test Procedure

At each designated temperature level, four types of heat treatment were carried out on specimens that were not loaded while being heated. In the first test, the specimen was heated in the oven and tested while still hot. Secondly, a different specimen was similarly heated and then allowed to cool in air for 24 hours before testing. Two other test specimens were subjected to a quenching bath of cold water after heating. This was to represent the effect of a concrete assembly being subjected to cold water from a fire hose in an actual fire. For both of these quenching tests, the specimens were immersed in cold water for only 10 seconds. One specimen was then tested immediately while the second one was allowed to cool for 24 hours before testing.

The specimens were all heated in an electric oven to the desired temperature by heating a $5^{\circ}\text{C}/\text{minute}$. This slow rate of heating allows the entire cylinder to reach nearly the same temperature. An arbitrarily chosen period of ten minutes for heat soaking was allowed at the desired temperature to ensure uniform heating. The thermocouple was placed near the test specimen so that any effects of radiation would be very nearly the same on both objects. The temperature in the oven fluctuated only a few degrees and did not move above the set point.

The specimens after appropriate heat treatments were placed on a 300 kip Tinius-Olsen compression testing machine. The specimens were quickly removed from the oven, placed under the ram of the machine and tested to failure. The maximum load

was noted for each specimen.

Specimens that were quenched were removed from the oven, held in the water bath for ten seconds and then quickly tested in compression. The two specimens that were tested cold were removed from the oven, quenched if required, allowed to cool for 24 hours and then tested.

2.4 (g) Stressed Cylinder Tests

For specimens which were under load during heating, a small three-zone electric furnace was mounted on an Instron Universal testing machine. The size of the oven and the capacity of the test machine limited the cylinder diameter to one and three quarter inches and maximum load to ten kips. Due to restrictions on machine usage, very few of these tests could be carried out. (Approximately one day was required for set up and carrying out of a single test). The oven contained three heating zones: upper, middle and lower. By appropriate setting of the upper and lower heating zones, the middle zone would automatically turn off after the desired temperature was reached. This prevented any cycling of the temperature. The concrete cylinder was placed in the middle zone, supported top and bottom by long, dense alumide rods. The rods in turn were placed in stainless steel holders attached to the testing machine. One rod was attached to the load cell. To prevent any flow of heat to the load cell or to the cross-head, the steel holders were wrapped with copper tubing through which cold tap water flowed. The control electronics for the oven required air cooling due to the confined work area and high temperatures. (see figure 2.8).

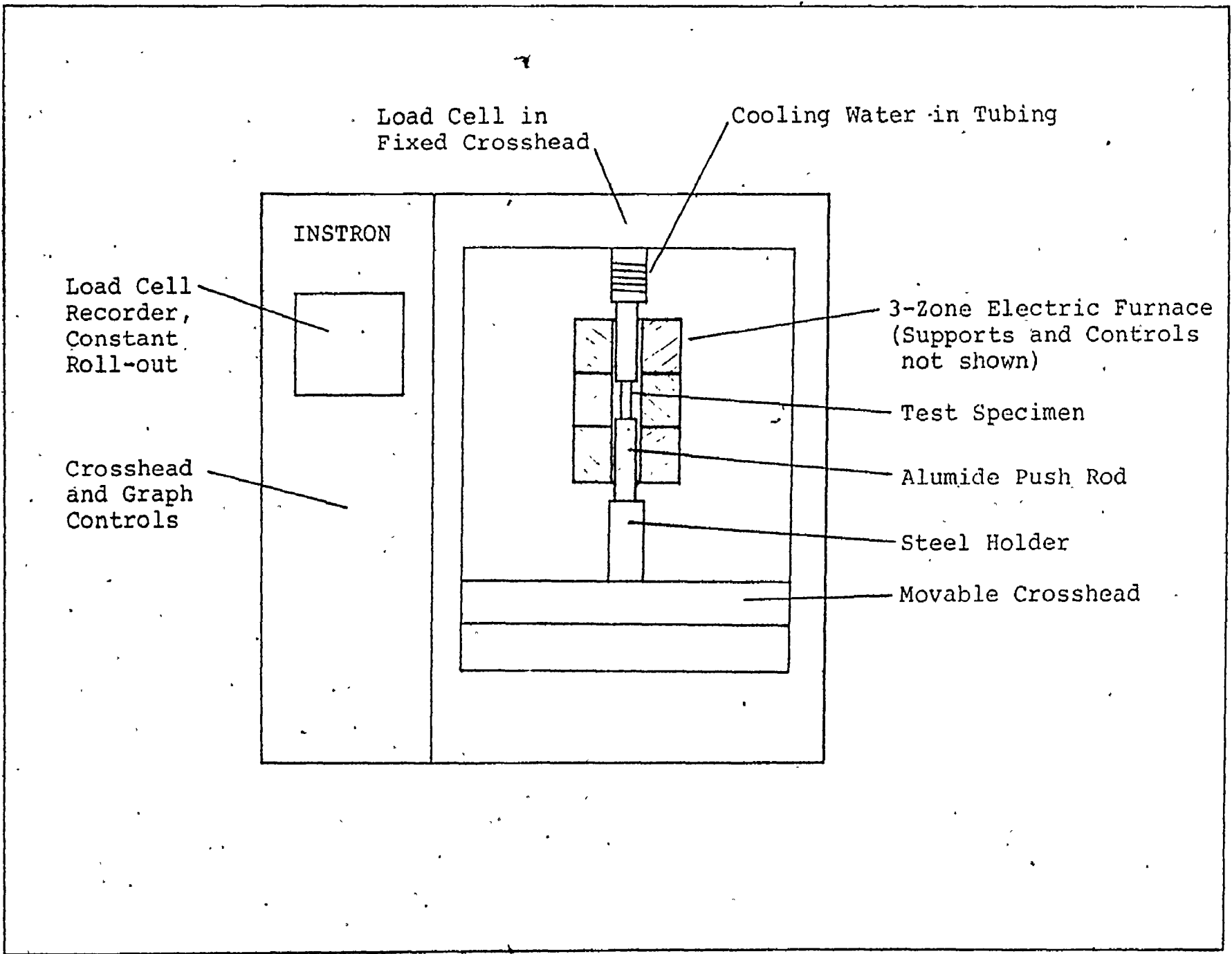


Figure 2.8 Apparatus for Loaded While Heating Tests

various rates. The machine had an automatic graphing system, plotting load cell reading against paper roll-out. The paper roll-out could be transformed into a deflection axis by synchronizing the paper rate of movement and the rate of cross-head travel.

As was the case for the unstressed cylinder tests, the rate of heating was 5°C per minute. While the specimen was heated under load, expansion took place requiring the gradual backing off of the cross-head to prevent over-stressing. Care had to be exercised to prevent the axial load from exceeding ten kips in order to avoid any damage to the load cell.

2.4 (h) Results and Observations

The results of the tests are given in figure 2.9. The values of maximum load at room temperature are plotted against a temperature scale. The curves for the unstressed tests are fairly complete but the curve for the stressed while heating case was necessarily incomplete. Due to machine load capacity limitations, maximum load points for the stressed while heating tests could not be reached for temperatures below 600°C . As noted in the work by Abrams⁽¹⁾, some concretes will actually show an increase in strength, for heating up to a certain point, if they have been under an initial stress.

(i) Unstressed Tests

The tests of initially unstressed hot cylinders all exhibited a slow failure. That is, there was no sudden rupture of the cylinder. Up to 700°C , all of these cylinders had a cone shaped

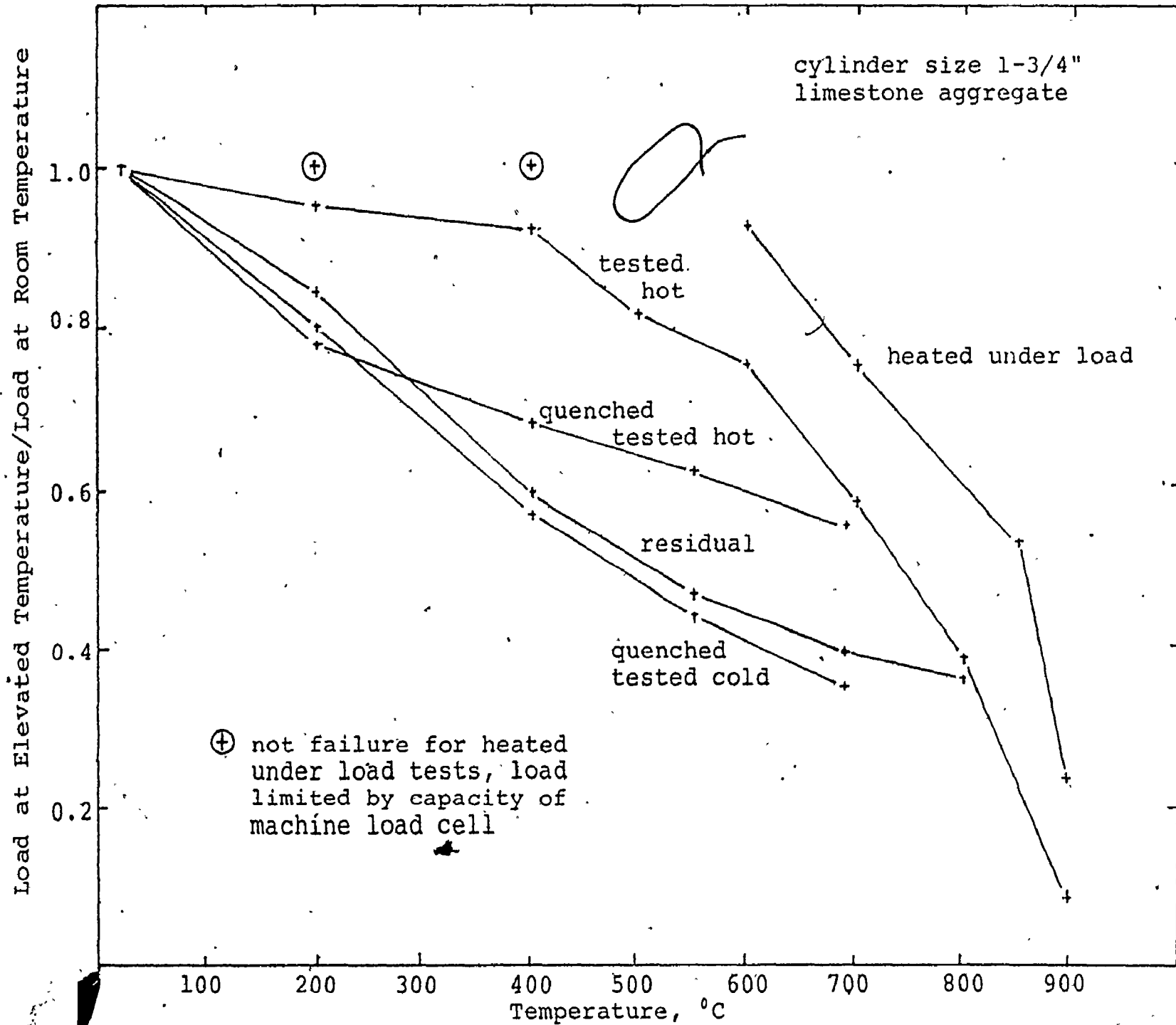


Figure 2.9 Small Cylinder Load Tests at Elevated Temperatures

failure. With increasing temperatures above room temperature there was less aggregate failure and more bond rupturing. At the higher temperatures, the concrete cylinders visibly "barreled out" (bulged at mid-height) as failure began to occur. As the temperature increased, the concrete cylinder exhibited more ductility as it fractured. The tests for residual strength after cooling show a decrease in strength compared with the companion specimens that were tested while hot. As noted in section 2.3 (a)(i) this is most likely due to the effects of the continual loss of the water of hydration after heating. The differences between results for testing while remaining hot compared to after cooling decrease with increasing temperature. The drop in "hot" strength at high temperatures is due to the sudden loss of crystallization-water in the hot specimens. For specimens heated above 700°C , the dark grey limestone aggregate transforms to a white chalk-like substance.

When the specimens are quenched, surface cracks appear. For both quenched tests (tested hot or cold), the maximum load is lower than the corresponding unquenched test. The thermal shock of quenching must rupture a large number of the bonds between aggregate and cement. Quenching also serves to indicate the extent of cracking in the specimen. For the specimen heated to a low temperature, the wetted area after quenching is only a ring around the cylinder but for the high temperature, the cylinder is wetted throughout even though it is very hot and should repel water. This indicates the occurrence of more extensive and larger cracks as the temperature is increased.

The load-deflection curve for small cylinders was obtained at three different temperatures. Figure 2.10 is the plot of the experimental observations. The drop in maximum load is apparent at increased temperature. The deflection at which maximum load occurs is shown to increase with a rise in temperature.

(ii) Stressed Tests

The data points obtained for maximum load are plotted in figure 2.9. These clearly indicate that application of a load during heating is beneficial to the maximum stress.

At low stress levels, it is necessary to back off the cross-head as the temperature increases and hence, the expansion increases. However, at high stress levels with high temperature, it is necessary to advance the cross-head in order to maintain the constant load. This indicates that creep strain is larger than expansion strain. Relaxation occurs very rapidly under these particular conditions. Failures of the cylinders were gradual and failed shapes were similar to the unstressed tests.

These tests are correct for the maximum load. Failure is easily defined and as long as the other components of the system are not damaged then the failure was definitely in the concrete. However, the effects of expansion and creep as previously mentioned, are open to criticism. One cannot state that the expansion and creep as witnessed is only due to the concrete. The expansion of the alumide rods and portions of the steel holders must also be considered. Alumide, by nature, has a low thermal expansion but it is a refractory ceramic type of material hence, it is probably susceptible to creep as is concrete. Again due to

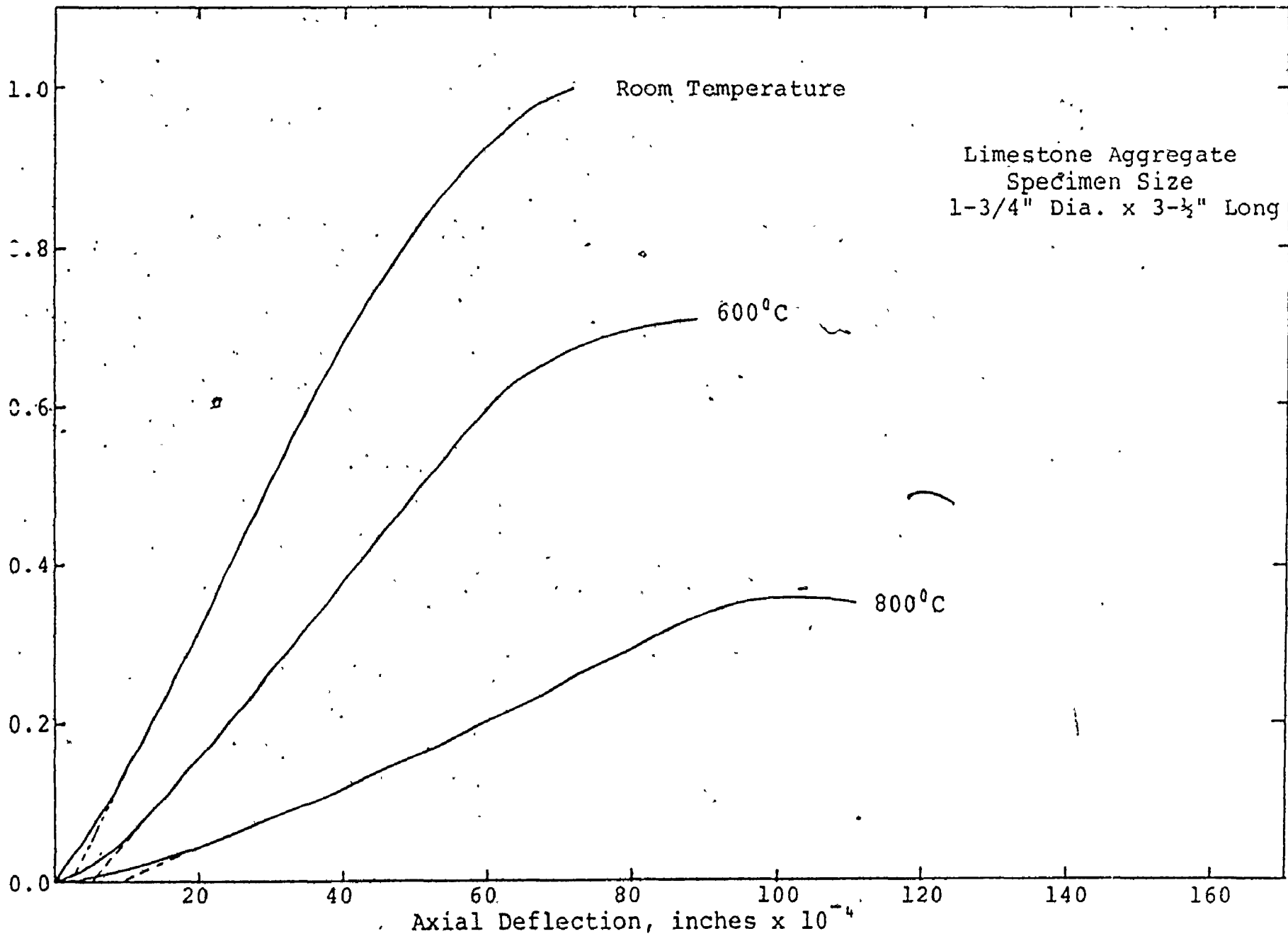


Figure 2.10 Experimental Load-Deflection Curves for Unstressed Tests

physical limitations, it was not possible to test the alumide rods by themselves to determine the magnitudes of expansion and creep. Since the alumide rods were each fifteen inches long compared to only three and one half inches for the concrete cylinder, the creep observed could principally be that of the alumide and not of the concrete.

2.5 Selection of Material Properties

Up to now, fire resistance has been determined by testing of whole assemblies. Now, since the behaviours of the individual components of concrete are known, an attempt can be made to calculate the fire resistance (a much cheaper alternative). As other investigators have realized, the predominant factor in reinforced concrete fire resistance is the temperature of the reinforcing steel. Although the concrete may shrink or creep, as long as the steel does not reach its critical temperature for the stress level involved, concrete beams or columns should be able to carry their service load.

To determine fire resistance by calculation, a mathematical model of the assembly must be derived that is as closely representative of the assembly as possible. However, computing time, computer storage capacity, and expense forces one to examine each variable in order to determine its importance to the overall model and in order to consider the complexity of each variable. The stress-strain characteristics of steel and concrete and how they change with temperature are necessary. Expansion is very important when considering interaction with the remainder of a building. Expansion also affects a compound

material internally due to different rates of expansion. Expansion strains are very high for concrete and steel and hence, have a large effect on the structure.

Creep and shrinkage for concrete could be important, however, conclusive information is not available in a quantitative form. Since the following investigations are for a short time period, only two to three hours, creep and shrinkage have been neglected. Creep would be very difficult to account for in any calculations since creep is time, stress and temperature dependent. Stress and temperature vary over the entire cross section and change with time. The history of one cross section would be difficult to ascertain let alone the history of an entire structure. For these reasons, the direct effects of creep and shrinkage have been ignored. However, the stress-strain curves for concrete will indirectly include some effects of creep and shrinkage since they have been obtained over a short time period.

2.6 Mathematical Representation of Material Properties

The following equations are used to represent reinforced concrete. These equations are also used by D.E. Allen^(12,14) of the National Research Council of Canada. Use of similar equations should give comparable results. Reference should be made to the Nomenclature. All temperatures for equations 2.2 to 2.13 are in thousands of degrees Celsius above room temperature.

$$T = \frac{(^{\circ}\text{C} - 20)}{1,000}$$

for quartz aggregate concrete

$$f_{C_{max}}^T = f'_C \text{ if } T < 0.429 \quad 2.2$$

$$f_{C_{max}}^T = f'_C (2.011 - 2.353T) \text{ for } 0.429 \leq T \leq 0.855 \quad 2.3$$

for steel

$$f_Y^T = f_Y (1 - 0.78T - 1.89T^4) \quad 2.4$$

$$E_S^T = E_S (1 - 2.04T^2) \quad 2.5$$

concrete stress-strain

$$f_C = \frac{1}{2} f_{C_{max}}^T \left(\left(\left((-1.797 \times 10^{10} \xi + 2.126 \times 10^8) \xi - 9.304 \times 10^5 \right) \xi + 1.2 \times 10^3 \right) \xi + 3.529 \right) \quad 2.6$$

$$\xi = \xi_C - 0.00127367 \quad 2.7$$

steel stress-strain

$$f_S = E_S^T (|\xi_S + \xi_Y^T| - |\xi_S - \xi_Y^T|) / 2.0 \quad 2.8$$

$$\xi_Y^T = f_Y^T / E_S^T \quad 2.9$$

concrete fracture strain

$$\xi_{C_{max}} = 0.004 \text{ if } T \leq 0.1 \quad 2.10$$

$$\xi_{C_{max}} = 0.00274 + 0.01276T \text{ if } T \leq 0.1 \quad 2.11$$

thermal expansion.

$$\xi_C^T = (0.008T + 0.006)T \quad 2.12$$

$$\xi_S^T = (0.004T + 0.012)T \quad 2.13$$

Equations 2.2 and 2.3 for maximum concrete stress are illustrated in figure 2.11. Shown with this equation is an example of maximum stress taken from the literature. Concrete stress-strain behaviour represented by equations 2.2, 2.3 and 2.6 are shown in figure 2.12. Equations 2.4 and 2.5 for maximum steel stress and modulus of elasticity are illustrated in figure 2.13. The steel stress-strain relationships described by 2.8 and 2.9 are shown in figure 2.14 for several temperatures. When thermal expansion is considered, the maximum concrete fracture strain must be adjusted. To achieve this effect, the strain axis is scaled producing an elongated stress-strain curve. This is tantamount to the inclusion of creep. If this adjustment was not made, calculations indicate that the concrete would rapidly crush due to thermal expansion. The combined effect of equations 2.2, 2.3, 2.6, 2.10 and 2.11 is shown in figure 2.15 for various temperatures.

The calculations in the following chapters are made assuming that the bond between the concrete and steel reinforcing bars is maintained. It is also assumed that any shear in the cross section is supported by adequate stirrups, thus only axial and flexural forces will be considered.

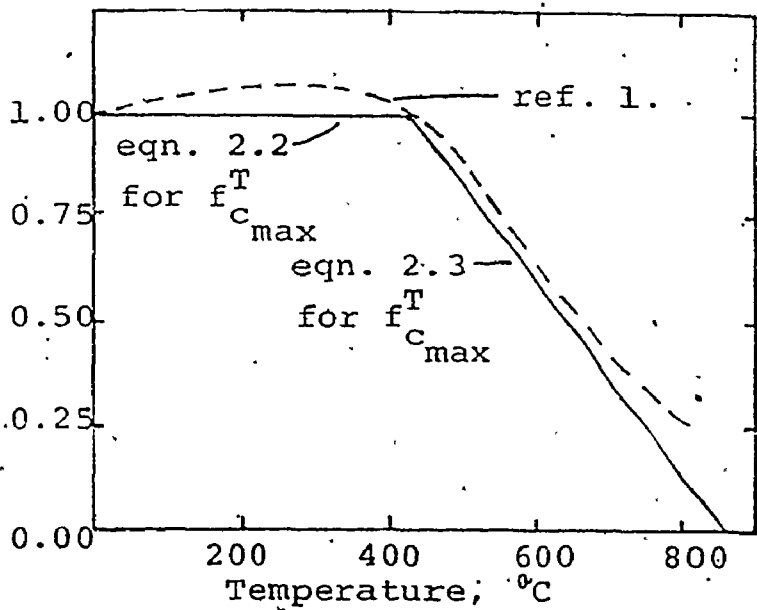


Figure 2.11
Concrete Temperature Dependence

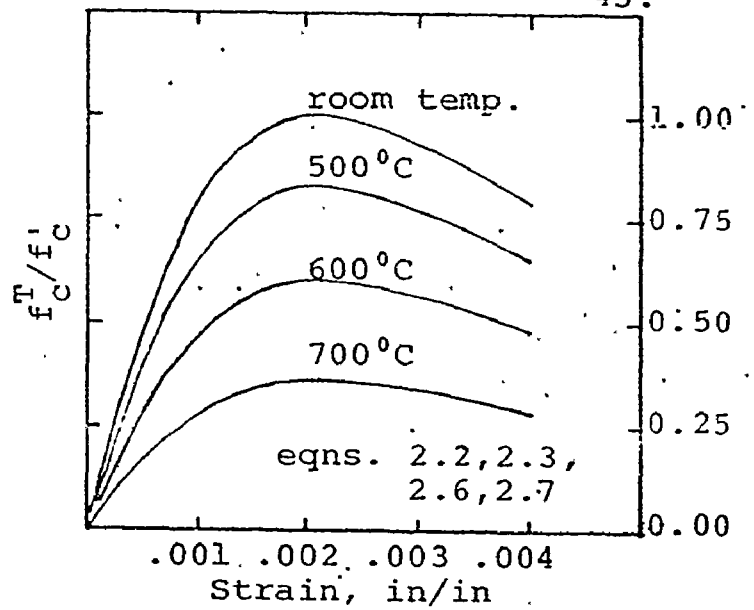


Figure 2.12
Concrete Stress-Strain

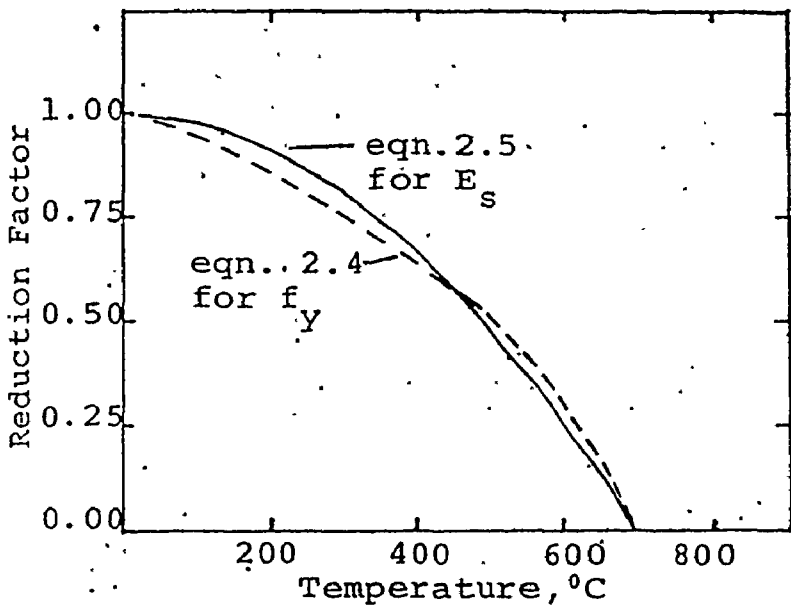


Figure 2.13
Steel Temperature Properties

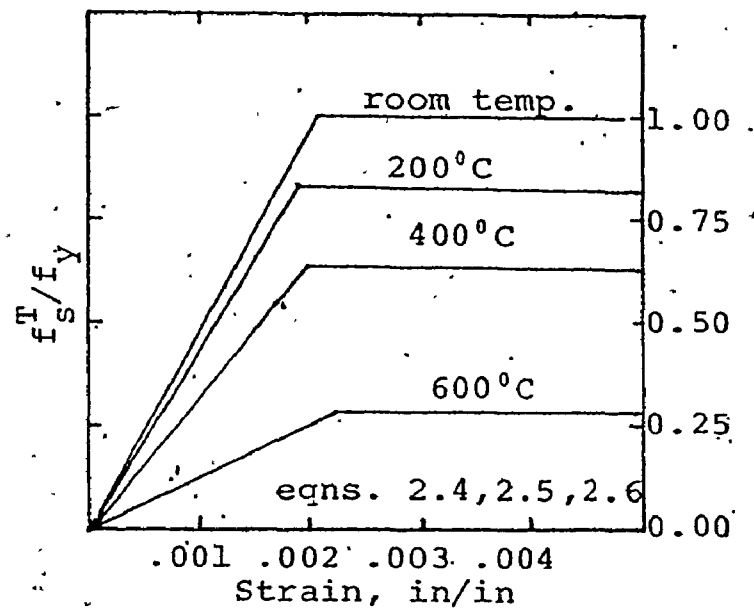
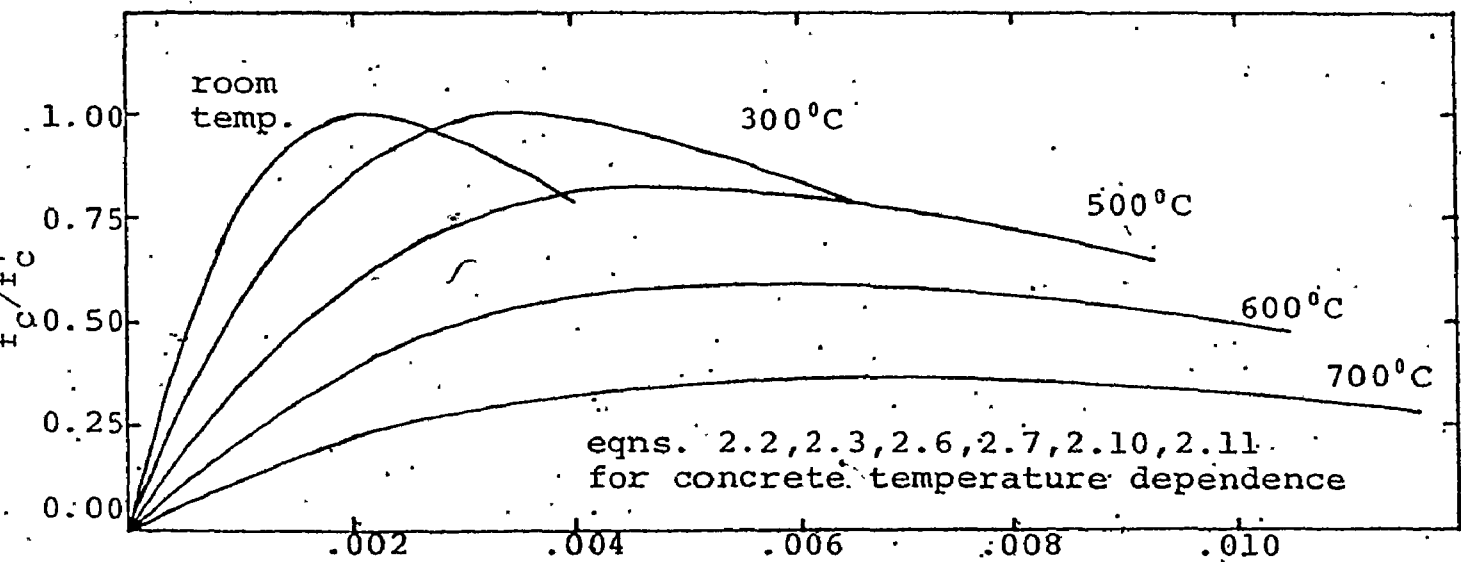


Figure 2.14
Steel Stress-Strain



2.7 Summary

Material properties as reported in the literature have been outlined. The properties selected for use in structural analysis have been defined. The limited test program was carried out to supplement the available information and to gain insight in defining the above material properties.

Although the information available is not as comprehensive as ideal, it is considered adequate to enable this investigation to provide additional insight into the behaviour of reinforced concrete under fire load.

Chapter 3

FIRE ENDURANCE OF REINFORCED CONCRETE COLUMNS3.1 Study of Design Parameters on Fire Endurance

Having defined the mathematical models of concrete and steel behaviour, a study was undertaken to determine how different design parameters affect fire endurance. The following parameters were selected for evaluation of their effect on the fire endurance of columns:

- concrete cover to steel
- steel as percentage of concrete area
- column size
- load eccentricity
- column slenderness
- placement of steel

The column analysis was based completely on theoretical behaviour of the concrete and steel. Many of the simplifications assumed in standard design procedures were not incorporated into the analysis. The only assumptions made for this study regarding strength and deformation were:

- (1) plane sections remain plane
- (2) concrete strength at any strain and temperature is defined by equations 2.2, 2.3, 2.6, 2.7, 2.10, 2.11.
- (3) steel strength at any strain and temperature is defined by equations 2.4, 2.5, 2.8, 2.9.
- (4) concrete has no tensile strength
- (5) concrete fracture occurs at an ultimate strain of 0.004.
- (6) failure of the cross section is defined by the inability

to achieve convergence, that is, balance between external and internal forces cannot be obtained.

- (7) the application of cross section mechanics is valid for the determination of section capacities and strains at room temperature and at elevated temperatures.

3.2 Calculation of Column Strength

The capacity of a short column, that is, a column of such length that buckling will not occur, is determined by the strength of the materials and the dimensions of the cross section. High temperatures in a fire will produce a transitory temperature gradient over the column cross section. The material properties have been assumed to vary uniformly over the cross section due to this temperature gradient.

The temperature gradient as supplied by T.T. Lie is based on one half inch or one inch square elements. This size limitation sets the grid division for all calculations. The material properties are redefined for each element as the temperature changes.

With a linear strain distribution for applied loads, the strain at each element can be calculated. By using the stress-strain curve for concrete or steel defined at the temperature of the element, the appropriate stress can be found. It must be borne in mind that the stress in the concrete and the steel for this study is a function of strain and temperature.

$$f_c = f_c(\xi_c, T_c) \quad 3.1$$

$$f_s = f_s(\xi_s, T_s) \quad 3.2$$

With the stress defined for each element, an integration could be carried out over the cross section to determine internal axial and bending forces.

$$P_{int} = \int_A (f_c(\xi_c, T_c) dA) + \sum_{k=1}^m (f_{sk}(\xi_{sk}, T_{sk}) A_{sk}) \quad 3.3$$

$$M_{int} = \int_A (f_c(\xi_c, T_c) d_c dA) + \sum_{k=1}^m (f_{sk}(\xi_{sk}, T_{sk}) d_{sk} A_{sk}) \quad 3.4$$

Since the temperature gradient was supplied as a series of points and not an equation defining the temperature surface, it was not possible to perform these integrations. Even if equations for the temperature gradient surface were developed, to perform the integrations by hand would be uneconomical in light of the availability of computers. The stresses in each element can be defined numerically quite easily, therefore, a numerical integration can be carried out over the surface of the cross section, using cross section mechanics to obtain the desired forces as follows:

$$P_{int} = \sum_{i=1}^n \sum_{j=1}^n (f_{cij} A_{cij}) + \sum_{k=1}^m (f_{sk} A_{sk}) \quad 3.5$$

$$M_{int} = \sum_{i=1}^n \sum_{j=1}^n (f_{cij} d_{cij} A_{cij}) + \sum_{k=1}^m (f_{sk} d_{sk} A_{sk}) \quad 3.6$$

Use of equations 3.5 and 3.6 will permit determinations of the actual forces with an accuracy that is acceptable for structural design. Due to the non-linearity of the material behaviours and of the temperature gradient, it is necessary to determine the correct strain magnitude and curvature by a trial

and error process. Acceptance of the final strain pattern is given by:

$$P_{int} = P_{ext} \pm \text{tolerance} \quad , \quad 3.7$$

$$M_{int} = M_{ext} \pm \text{tolerance} \quad 3.8$$

For this chapter which deals with short and slender columns only, the effects of thermal expansion have not been included. There is little effect of expansion on the cross section capacity if the column is not restrained (as assumed here). The effect of expansion is secondary to the other design parameters being considered in this chapter.

The detailed description of the computer program in Appendix A gives more information as to the method of determination of forces and strains. It should be noted that the subroutine descriptions apply to this chapter and to Chapter 4, therefore; some information particularly concerning expansion and section properties may be confusing until Chapter 4 has been read.

3.3 Variable Normalization

All variables will be normalized to facilitate comparisons with the results in this study and other studies. Any variable concerning length units will be divided by the dimension of the square cross section. All axial force values will be divided by the gross concrete axial force at room temperature. Similarly, bending moment forces will be divided by the product of the gross concrete section modulus and the maximum concrete stress. The following symbols represent the normalized variables. (see

| | | |
|----------------|----------------------------|------|
| Axial Load | $P' = P / (f'_c t^2)$ | 3.9 |
| Bending Moment | $M' = M / (f'_c t^3 / 6)$ | 3.10 |
| Eccentricity | $e' = \frac{e}{t}$ | 3.11 |
| Column Length | $L' = \frac{L}{t}$ (in/in) | 3.12 |

On all graphs, these normalized values will be used unless otherwise indicated.

3.4 Standard Cross Section

One column cross section has been studied in detail to obtain the complete axial load versus bending moment interaction diagram and for all the results in Chapter 4. The effects of changes in cover, steel percentage, steel placement and column length will be compared using this column cross section as much as possible.

The size for this standard cross section is sixteen by sixteen inches. The percentage of steel reinforcing is three and one half percent and the concrete cover to the outer edge of the stirrups is one and one half inches.

The sixteen inch square size of column was chosen as a realistic practical size. It also provided two hundred and fifty-six elements of the cross section, which is a fine enough mesh to yield an accurate numerical integration, even in the case where thermal expansion was considered. The large percentage of steel meant that the loss of steel strength had a predominant influence on the loss in section capacity, especially for large eccentricities. The selection of one and one half inches for

concrete cover was made to coincide with normal design practice. This also ensured that the steel would lose all of its strength because of increased temperature by an elapsed time of exposure of three hours. Therefore, this standard section had changing properties which covered the full spectrum of behaviour. It is suggested that this standard column provides a realistic model for comparison of effects of the various parameters.

3.5 Interaction Diagrams

By the selection of a large number of e' ratios, it is possible to obtain a complete interaction diagram for a reinforced concrete cross section. Figure 3.1 shows this for the standard sixteen inch square column for room temperature and for every half hour of standard fire exposure up to three hours. As would be expected, the interaction diagram "shrinks" as the elapsed time of exposure increases. This is due to the previously mentioned decrease in material strengths at elevated temperatures. The maximum bending moment decreases much more rapidly than does the maximum axial compressive load. Also, the case of bending moment with zero axial load and the case of pure tension with no bending moment decrease to zero at the three hour limit. The reason behind these two observations is that the steel strength has decreased to zero at the three hour (180 minutes) exposure time.

Since all bending moments are positive, it is necessary to use a negative e' ratio to obtain a negative force. The interaction diagram in the tensile axial load region is not a straight line but is actually curved. Near the maximum load

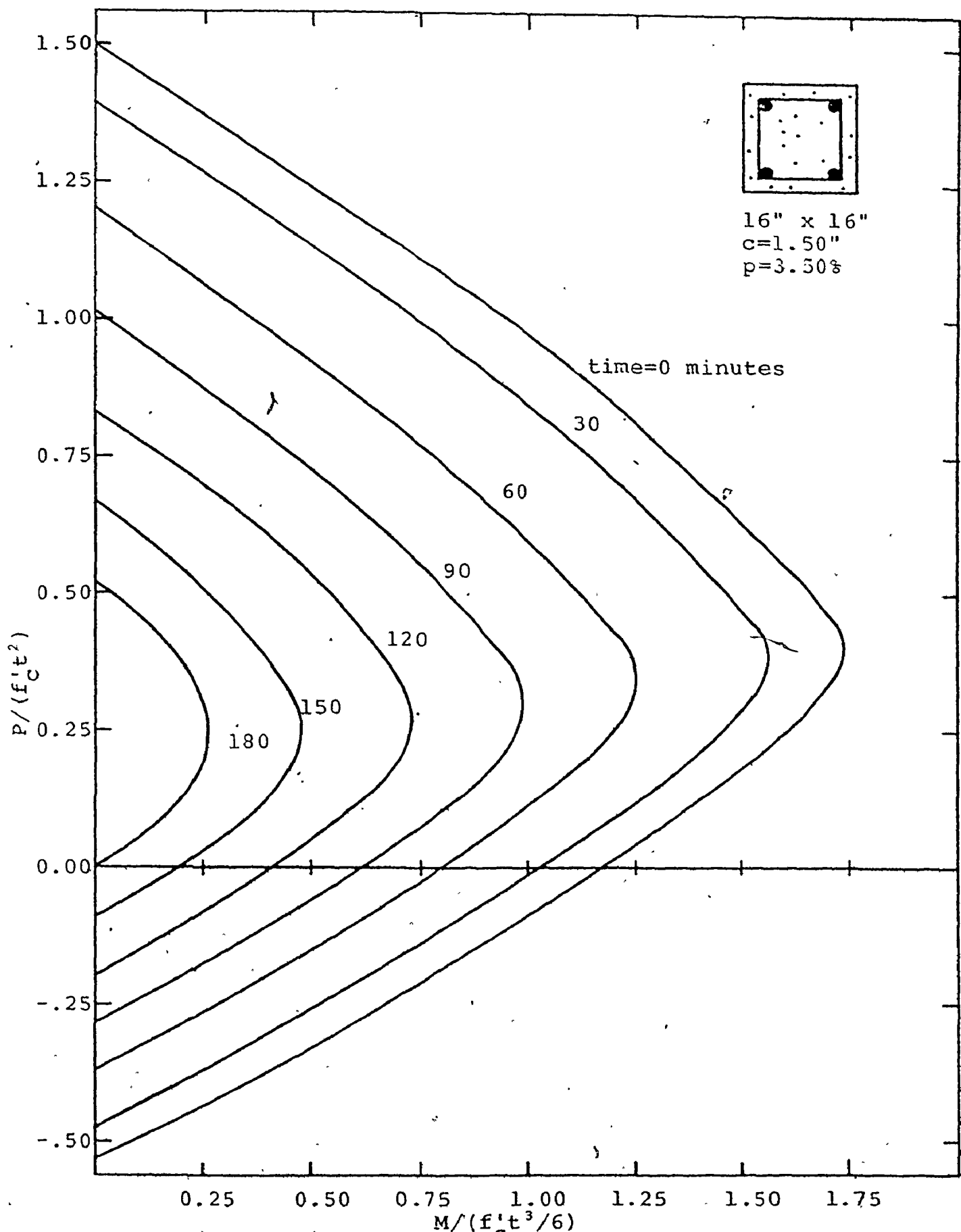


Figure 3.1
Interaction Diagram for the Standard 16 Inch Square Column

point for a given eccentricity and tensile force, the concrete section will contribute some strength to the compressive force of the bending moment couple and also cause a shift in the force centroid. Hence, the interaction diagram is curved in this region.

At room temperature, the balanced conditions (simultaneous yielding of steel and crushing concrete) occur at an e'_b ratio of approximately 0.7. This eccentricity shifts as the exposure is increased. At one and one half hours the value of e'_b is about 0.5 and this reduces further to 0.175 at a time of three hours. This shifting of e'_b indicates the loss of strength in outer layers of concrete. The effective area is being reduced.

A second interaction diagram is shown in figure 3.2. It can be seen in this second figure that changing the steel percentage or cross section size will only affect the magnitude and not the general shape of the interaction diagram.

3.6 Thermal Protection of Steel

Referring back to figure 1.3, it can be seen how the temperature in the concrete varies over the cross section. The temperature is high near any outer edge but drops rapidly as the distance from the edge increases. There is a large flow of heat incident on the cross section in the corner areas. This results in the concrete in the corners being hotter than any other point on the cross section at a similar distance from the outer edge. These observations indicate that the steel reinforcing should be kept at a maximum distance from the outer surface or from the corners. This restriction on steel location may have a

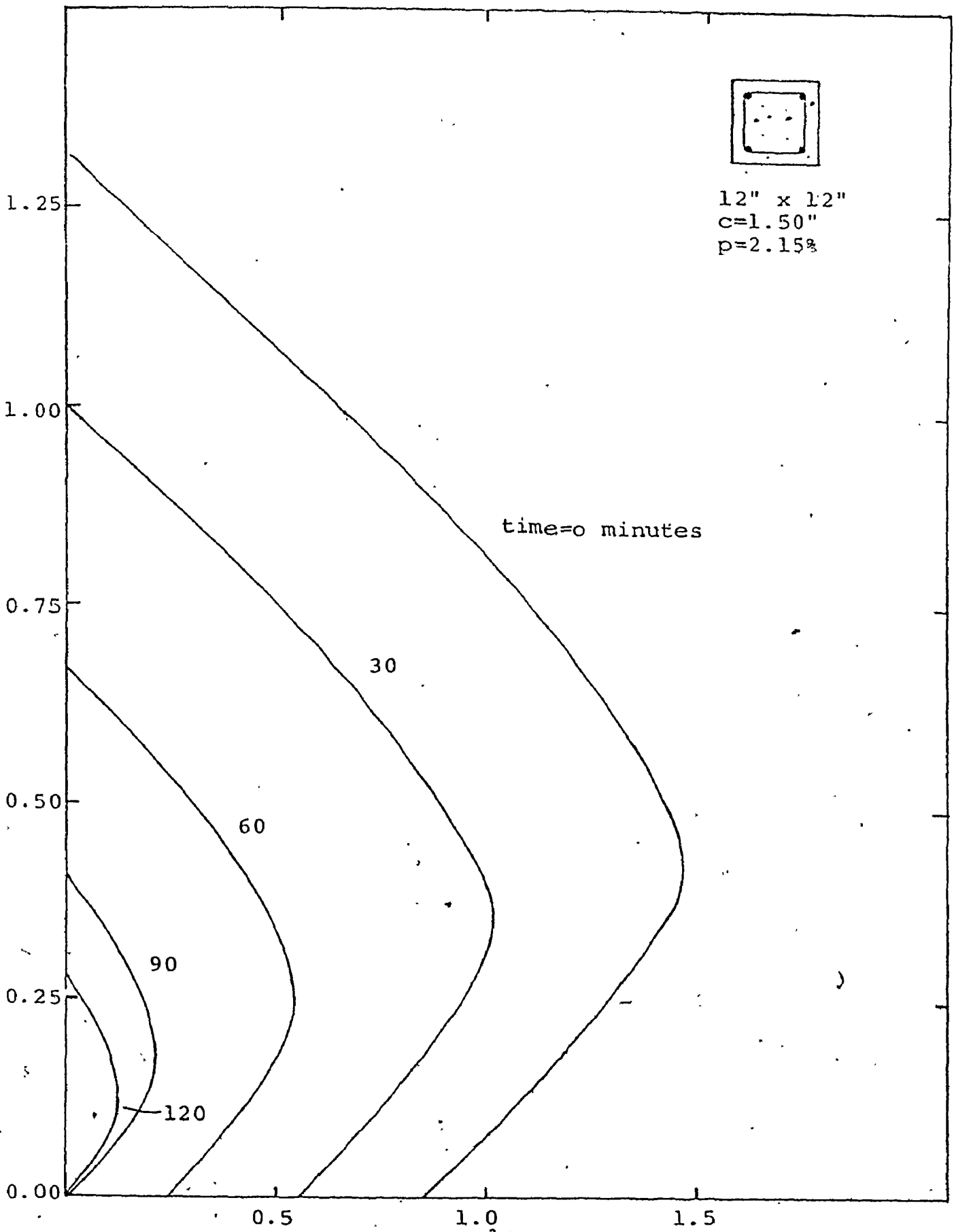


Figure 3.2
Interaction Diagram for a 12-inch Square Column

significant effect on the structural design. The steel can be protected by increasing the concrete cover to the depth of the steel, by increasing the column outer dimensions or by re-arranging the steel to avoid high temperature regions.

3.6 (a) Concrete Cover

The depth of concrete cover over the steel reinforcement is the single most important factor in fire endurance of reinforced concrete. Figures 3.3 and 3.4 illustrate the effect of cover on the ultimate load for a sixteen inch square column and a twelve inch square column respectively. Curves are plotted for a constant steel percentage of 3.5% and for three values of loading eccentricity and for three values of concrete cover.

At zero time, the minimum cover corresponds to the maximum normalized load. The moment lever arm increases as the cover decreases hence, the increase in ultimate load for minimum cover.

The temperature in the steel will be high for a shallow cover. For all eccentricities, there is a rapid decrease in the ultimate load for a cover of 0.75 inches. If the eccentricity is greater than or near balanced load conditions, then the ultimate load will drop to zero when the steel strength drops to zero due to excessive temperature. When the eccentricity is low, the ultimate load curve for 0.75 inch cover will not drop to zero but will begin to decline at a less steep slope. Although the steel has no strength, the interior concrete can continue to resist loads for a long time before the concrete completely loses its strength.

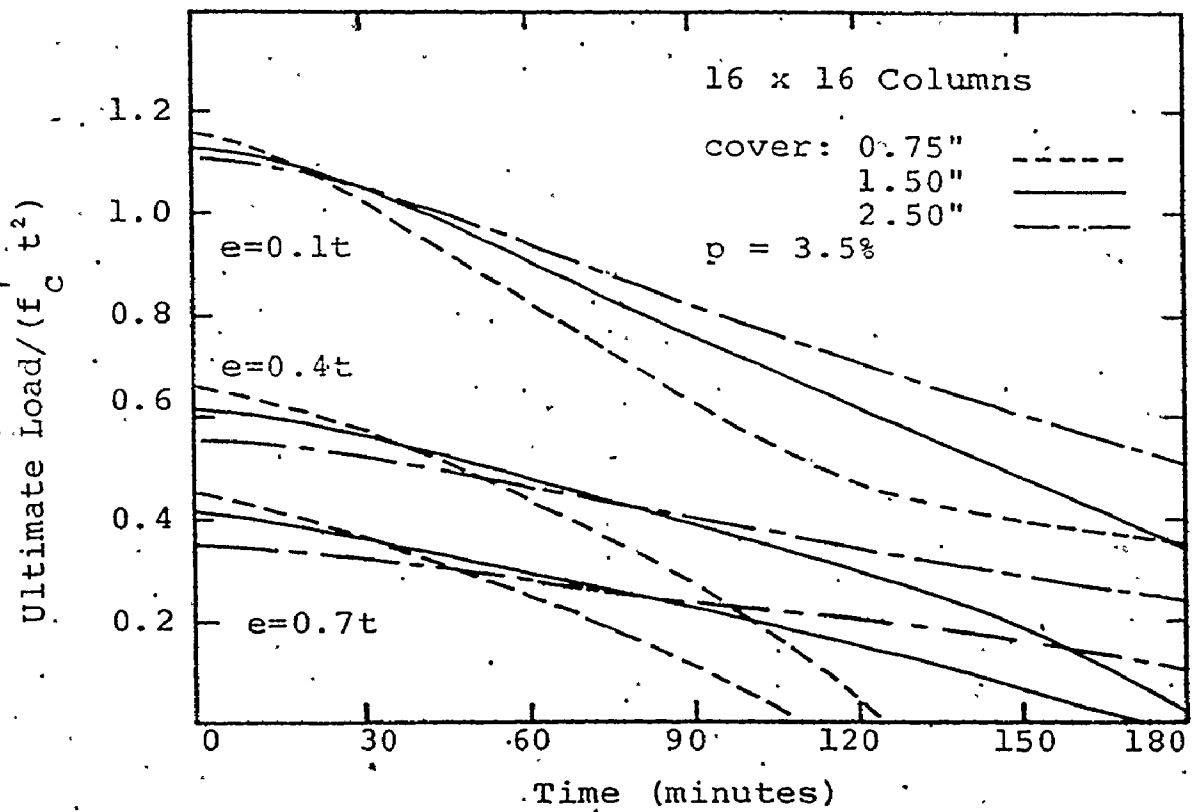


Figure 3.3

Ultimate Load of 16 x 16 Columns

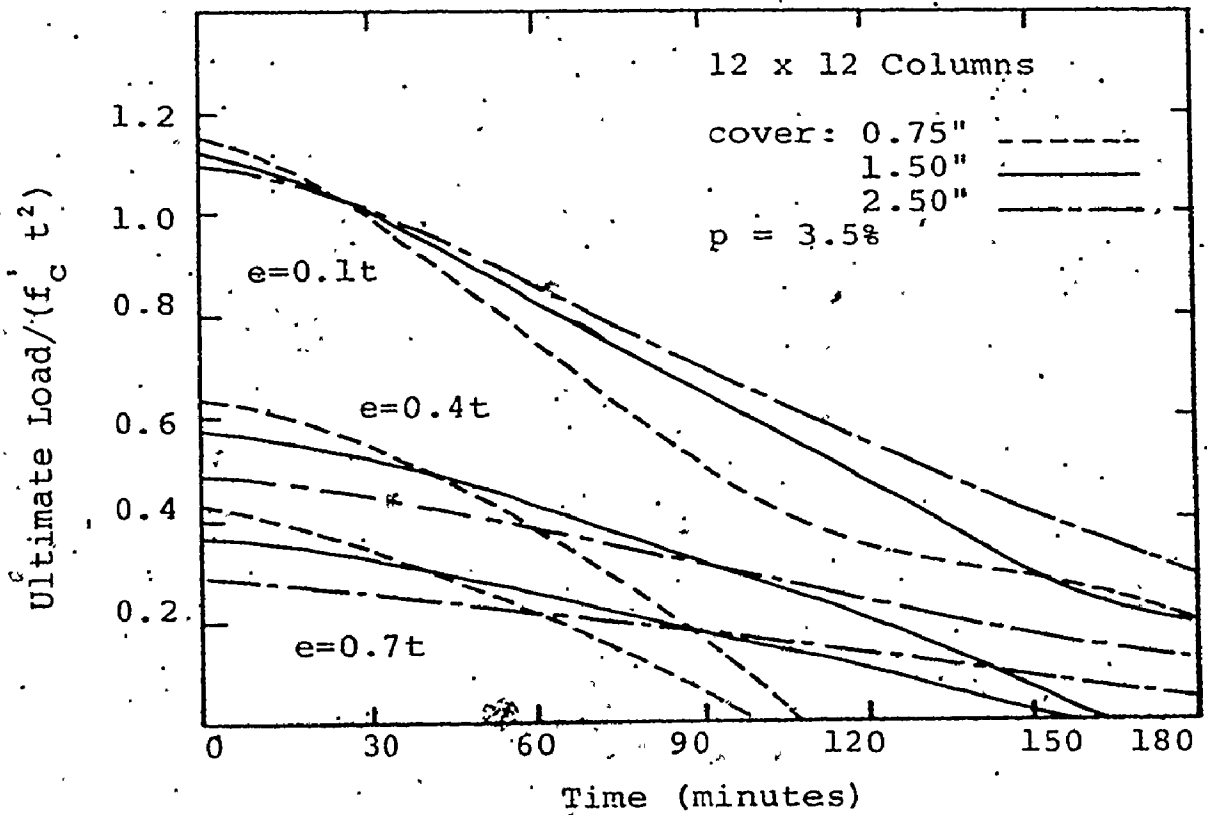


Figure 3.4

Ultimate Load of 12 x 12 Columns

For 1.50 inches cover, the slope of the ultimate load curves are similar to the 0.75 inch cover. The time at which steel loses its strength is greater for 1.50 inches cover, thereby resulting in a greater endurance of the column. For the sixteen inch square column, the steel then fails at about 170 minutes as evidenced by the failure at 0.7t eccentricity. Once the steel has failed, it does not contribute to the ultimate load.

At an eccentricity of 0.1t, curves for both 0.75 and 1.50 inches of cover approach a common strength. For the twelve inch square column with $e = 0.1t$, the graph shows the ultimate load for the 1.50 inches cover to be slightly less than the load for the 0.75 inch, even though these two curves should be coincident after steel failure. This apparent anomaly was calculated using the computer program which correctly deducts for the concrete area which is displaced by the steel (see Appendix A). The concrete at the level of the steel is slightly stronger for the cover of 1.50 inches, resulting in a greater deduction.

The curves for 2.50 inches of cover exhibit no failures up to 180 minutes. At 180 minutes, the ultimate load is about 47% of the corresponding load at zero time for the sixteen inch square column. Clearly, increasing cover increases the fire endurance of a concrete column.

3.6 (b) Column Size

The larger the column, the greater will be its fire endurance for identical depths of cover. As a square column is increased in size, the ratio of internal area of concrete to exposed

perimeter of concrete increases. This results in an increased heat capacity for the larger section. The incident heat is "spread over" a larger area which results in smaller temperature rises at the steel locations. This effect can be seen by comparing results in figure 3.3 and figure 3.4. At the time of 180 minutes, the sixteen inch square has a strength of 47% of the initial strength for $e = 0.1t$ and 2.50 inches cover. Using similar design parameters, the twelve inch square column has only 26% of its initial strength. Use of a smaller cross section results in greatly reduced fire endurance.

In the design stage of a concrete member, the effects of cover should be remembered. A heavily reinforced member with minimum cover will have a low fire endurance. However, a larger column with the same or even less area of steel at the same steel bar separation, will have a longer fire endurance and less reduction of capacity.

3.6 (c) Placement of Steel

The temperature in the steel is a function of the steel location in the cross section. For a given depth of cover to steel, the temperature will be higher in the corners than at any other location in the cross section. Figure 3.5 shows an interaction diagram with the position of the steel re-arranged from the usual 4-bar corner layout. In figure 3.5 half of the steel area is concentrated at the mid-depth of the cross section. The remaining one-half of the steel is in the standard 4-corner position.

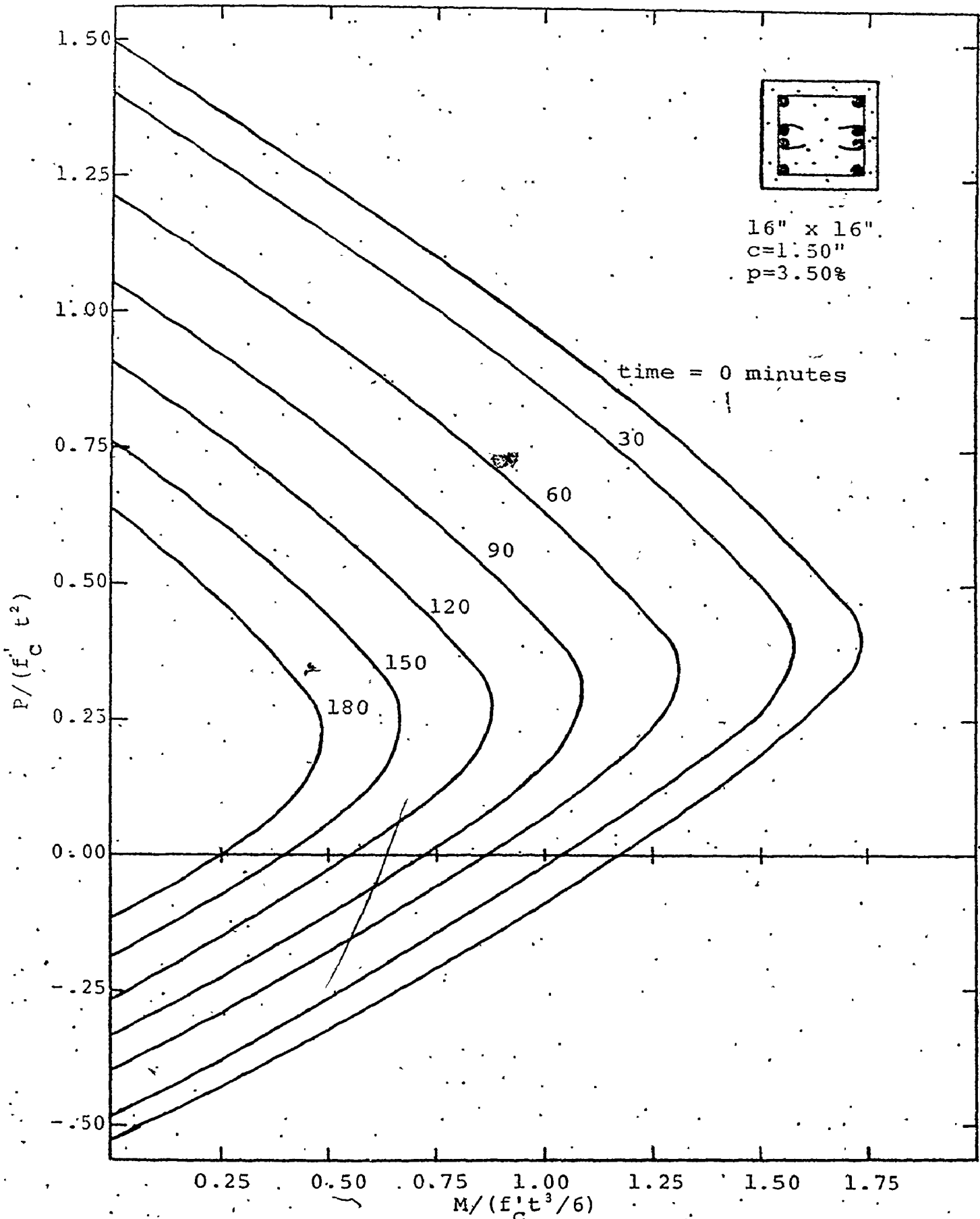


Figure 3.5
Interaction Diagram Using Mid-depth Steel

Figure 3.6 shows a partial comparison between the results shown in figures 3.1 and 3.5. At three hours of fire exposure there is a significant increase in the strength of the cross section with the mid-depth steel compared to the simple 4-bar corner steel layout. If the steel was positioned on a circular pattern which would avoid the high temperature locations, the period of fire endurance could be further increased.

3.7 Effect of Steel Percentage

Increasing the areas of the corner steel reinforcing bars will not lengthen the fire endurance period for a column. The maximum steel strength is dependent on its location in the cross section.

Figures 3.7 and 3.8 show the effect of variation of the steel percentage on the ultimate load for sixteen inch square and twelve inch square columns, respectively. As expected, the ultimate load at zero time, increases as the percentage of steel increases. However, the loads for all three percentages of steel approach the same ultimate load when the steel strength goes to zero. As previously noted, the computer program deducts for area of concrete displaced by the steel. For this reason, the twelve inch square column with $e = 0.1t$ and only 1.5% steel reinforcing is stronger than the cross section with more steel after 150 minutes. When the concrete at the level of the steel loses its strength also, then the results for all three percentages of steel will have a common point.

When a column is heavily reinforced, the steel carries a large portion of the total axial load. At the 180 minute exposure time,

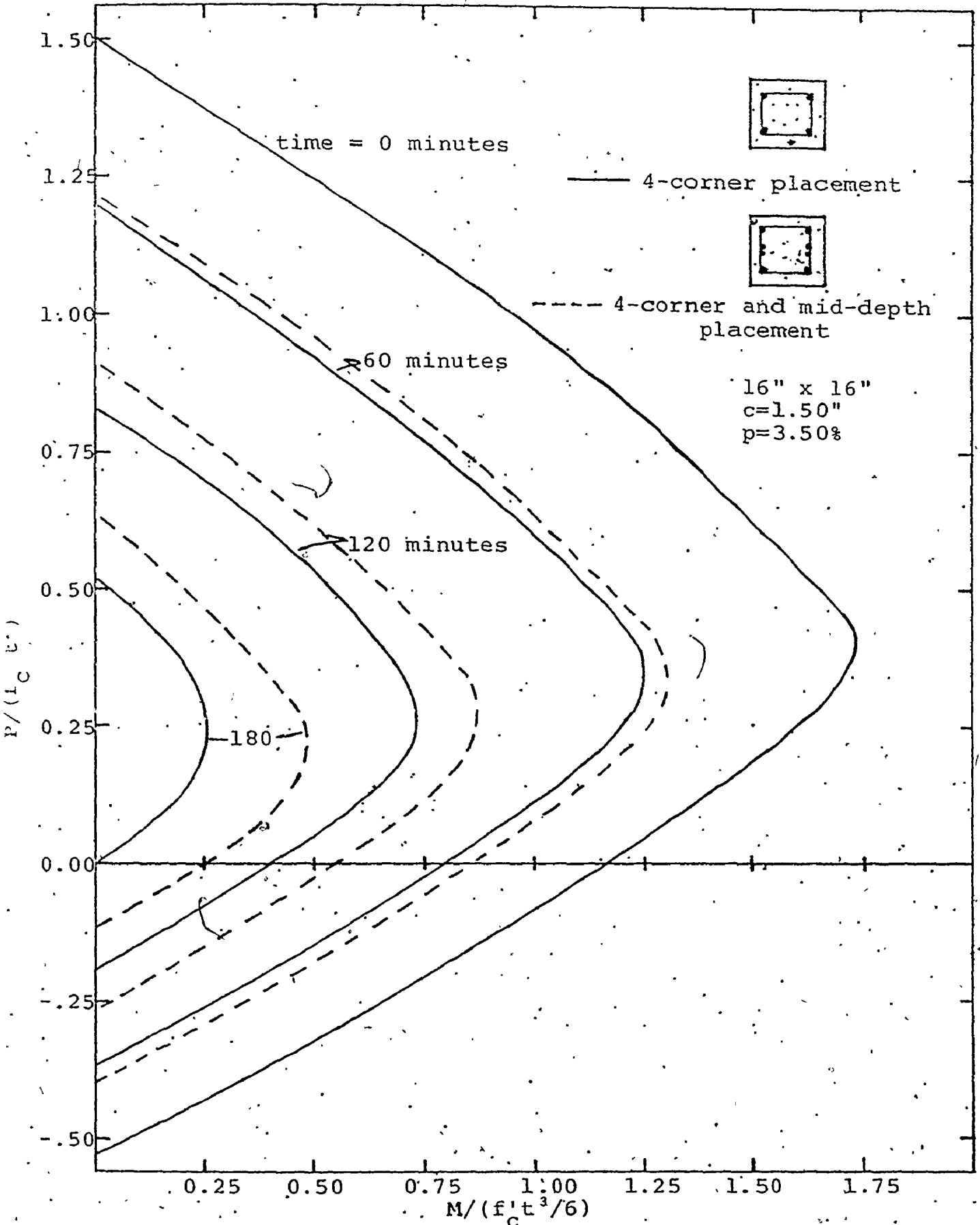


Figure 3.6
for P

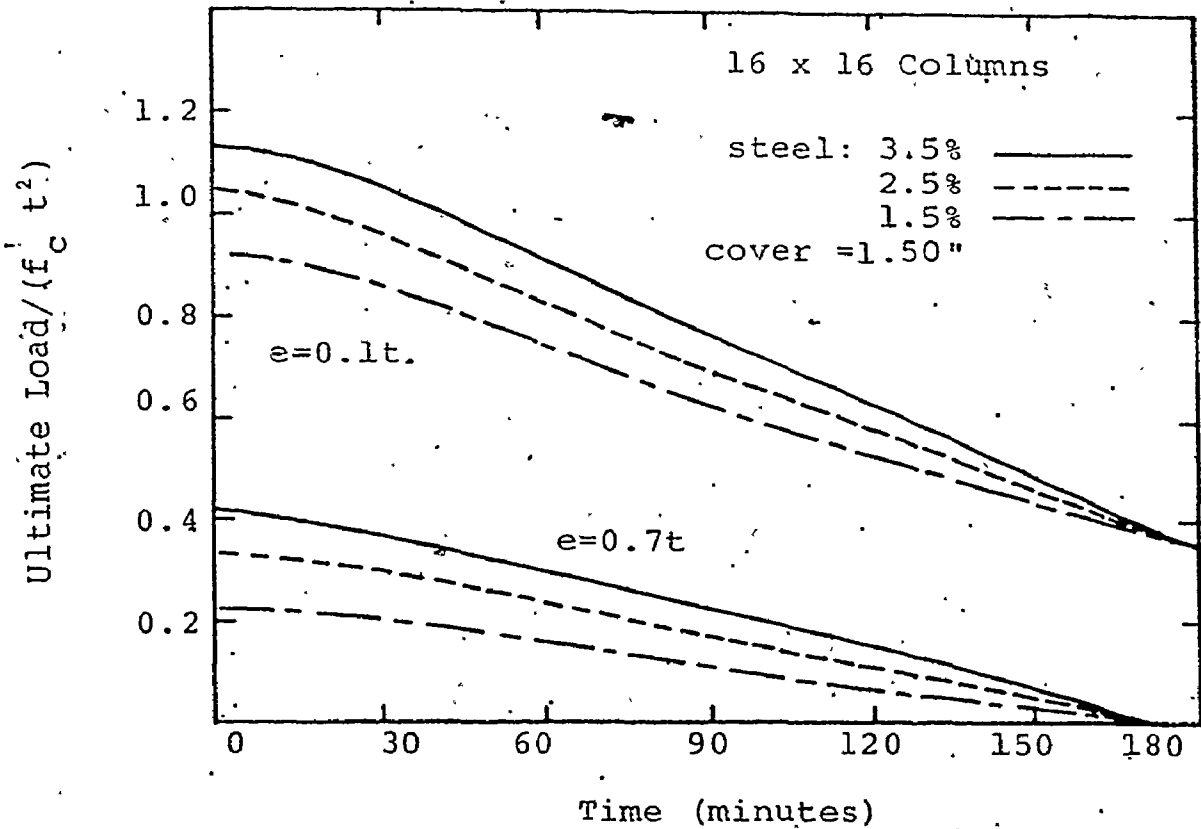


Figure 3.7
 Variation of Steel Percentage

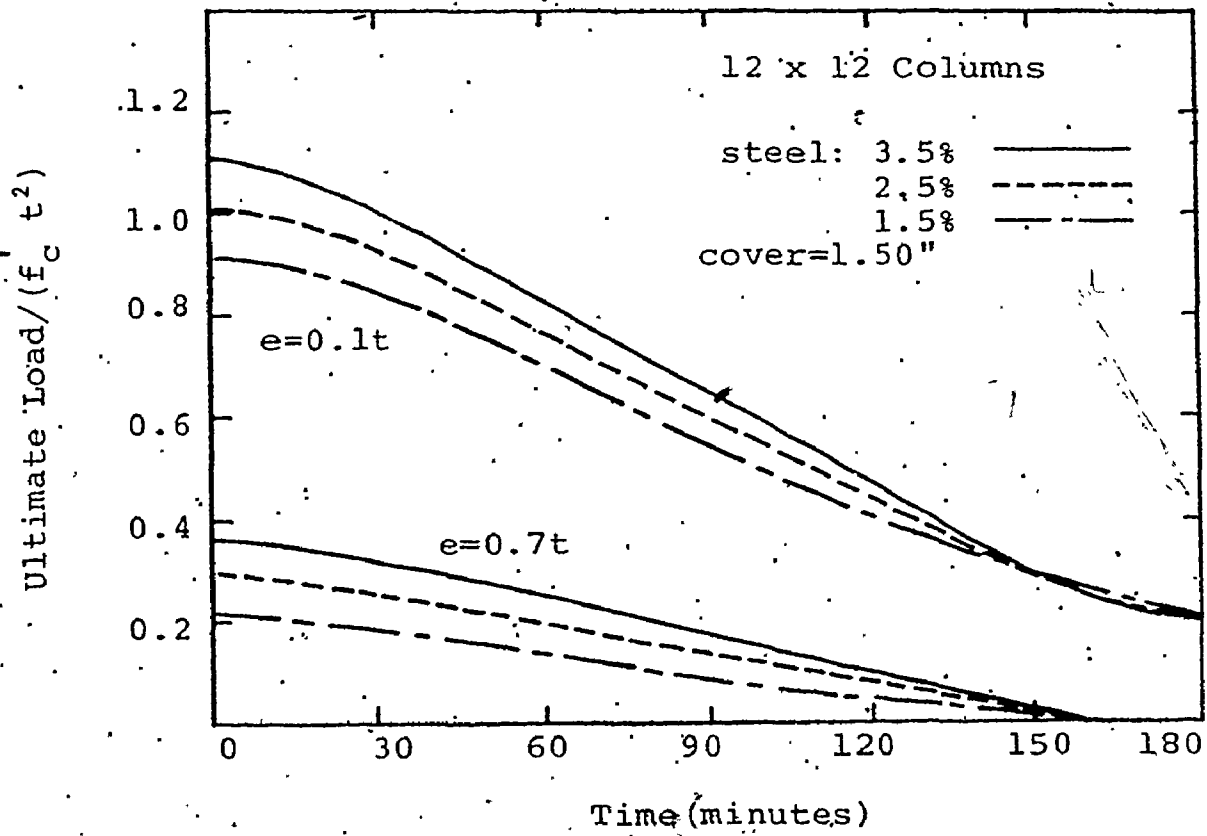


Figure 3.8

the sixteen inch square with 3-1/2% steel has an ultimate axial load of 30.0% of its original strength for $e = 0.1t$. The sixteen inch square column with 1-1/2% steel has an ultimate load of 39.0% of its original strength under similar conditions. This indicates that a heavily reinforced column will fail under design load sooner than a lightly reinforced column. As can be seen in figures 3.7 and 3.8, the fire endurance decreases much more rapidly with increasing eccentricity of load. High eccentricity results in a failure when the steel strength drops to zero.

3.8 Column Slenderness

As the column length is increased, the secondary bending moments, (P- Δ effects) reduce the capacity of the pin-ended column. The effect of column length can be investigated by the program in Appendix A. The results in figure 3.9 show the effect of column length on the ultimate cross section load for zero and for 120 minutes of fire exposure. Increased column slenderness lowers the maximum axial load for all three cases shown.

For the sixteen inch square standard column with the properties described in figure 3.9 (a), the ultimate load at 120 minutes is 55% of the load at zero time for no slenderness effect and $e = 0.1t$. For a slenderness ratio of 30, the ultimate load at 120 minutes is only 40% of the load at zero time. This decrease in capacity is explained by the loss of flexural stiffness (EI) due to heating of both concrete and steel. As the concrete is heated, the effective depth of the cross section will be less than t . As the effective depth decreases, secondary effects

Period of fire: 0.0 minutes ———
 120.0 minutes - - - - -

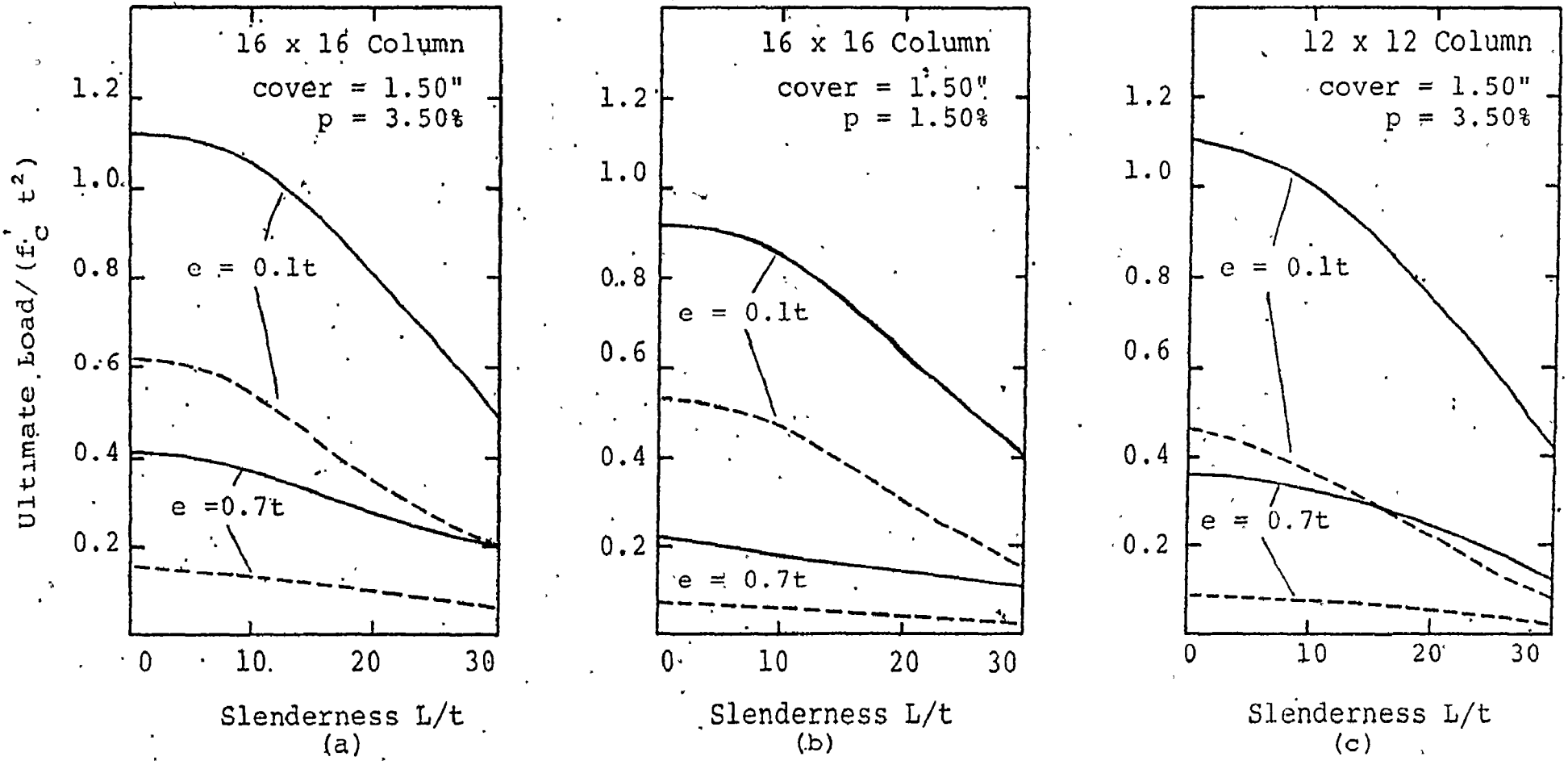


Figure 3.9
 Variation of Column Length

When the percentage of steel is reduced there is a decrease in the maximum load for all column lengths. This can be seen by comparing results in figure 3.9 (b) for 1.5% steel with figure 3.9 (a) for 3.5% steel. Similarly, for a decrease in column cross section size, the normalized forces also decrease with increasing slenderness. The twelve inch square column has a greater reduction in capacity for small eccentricities at increased temperature and slenderness than does the sixteen inch square column.

3.9 Summary

This chapter has presented the results of analysis of individual columns subjected to various durations of exposure to fire. It is thought that these results provide important information on the effect of various parameters on column capacity. Also it is suggested that in a general way the results provide evidence of column fire endurance. However, isolated columns which are unaffected by the remainder of the structure are seldom found in practice. Therefore, a more realistic evaluation of the effect of fire on column capacity may be found by analyzing columns as part of a continuous frame. This subject is discussed in Chapter 4.

Chapter 4

FIRE ENDURANCE OF REINFORCED CONCRETE FRAMES4.1 Concept of Stiffness Properties Based on Transformed Areas

The calculations performed in Chapter 3 are not dependent on the reference position on the cross section. As long as the external and internal bending moments are calculated about the same point, usually the mid-depth, the two forces are related.

In this chapter, the same relation between external and internal forces exists. However, there is also a relationship between the forces, the stiffness properties and the internal strains. For an elastic section, this relationship is as follows:

$$EA = P/\xi_{cg} \quad \text{or} \quad P = EA \xi_{cg} \quad 4.1$$

$$EI = M/\phi \quad \text{or} \quad M = EI \phi \quad 4.2$$

These relationships are the basis of structural analysis. As before, the values for forces, stiffness properties and strains must be calculated about a common point. What is this common point? The arbitrary selection of the mid-depth is as valid as selecting the extreme edge of the cross section. The internal and external forces will balance at either of these points. However, the value of EI found by equation 4.2 will not correspond to the value of EI calculated by using the second moment of the axial stiffness about that particular point.

It is known that EI, determined using transformed section properties, will vary for different reference points in a parabolic fashion over the cross section. This will be shown by

equation 4.5. From mechanics of sections, it is known that EI will be a minimum at the transformed elastic-centroid, ($EI_{\min} = EI_{cg}$). This transformed elastic centroid is found by considering the summation of the first moment of the element axial stiffnesses about any initial point, i . The centroid will then be referenced to that point by equation 4.3.

$$d_{cg} = (EAd)_i / EA \quad 4.3$$

The value EI_{cg} can be found by

$$EI_{cg} = EI_i - (EA)(d_j - d_{cg})^2 \quad 4.4$$

The quantities EI_i , $(EAd)_i$, d_i and d_{cg} are all referenced to the same calculation point. Now the value of the second moment of transformed area at any point, j , is found as follows:

$$EI_j = EI_{cg} + EA(d_j - d_{cg})^2 \quad 4.5$$

The curvature used in equation 4.2 is a constant at any point on the plane of strain. However, the moment due to eccentrically applied load varies linearly depending on the reference point over the cross section, as long as P is greater than zero. Thus EI , determined by this manner, will also vary linearly. The moment will be calculated about the same initial point, i . Therefore, the moment at any point, j , will be:

$$M_j = M_i - P(d_j - d_i) \quad 4.6$$

Then, by using equation 4.2

$$EI_j = (M_i - P(d_j - d_i)) / \phi \quad 4.7$$

Unlike equation 4.5, equation 4.7 has no minimum. The value of EI_j can seemingly be calculated by two methods. However, the two methods result in different values for EI_j . Both methods vary due to a change in the calculation reference point. Equation 4.5 will always vary, no matter what the external loads may be. Equation 4.7 is invariant only for the case of zero axial load. For zero axial load, equation 4.7 becomes equation 4.2.

All methods of elastic structural analysis depend on the members of the structure being defined along their elastic centroids, even simple columns. In the analysis, the axial forces are determined such that they will act along the centroidal axis of the member. The bending moment forces are also defined in reference to this axis. The value of EI_j , when calculated by using element axial stiffnesses is a minimum by definition at the transformed elastic centroid. Thus it appears to be necessary to define all stiffness properties and to have all locations of forces referenced to this centroid.

Using equations 4.1 to 4.11, the values of EI_{cg} determined by the curvature method are found to be identical to those determined by using the element axial stiffnesses at the transformed centroid. In addition, the value of EA calculated by equation 4.1 is identical to the value based on the summation of the element axial stiffnesses if the axial strain is taken as

Therefore, it is now stated that the values for the stiffness properties EA and EI must be defined at the transformed elastic centroid for use in any structural analysis program. For this reference point, the values of EI and EA could be found by either method. However, the non-linear thermal expansion produces what is in effect the same thing as a non-linear strain distribution. Thus only the method based on element axial stiffness is used in this investigation.

4.2. Calculation of Stiffness Properties

The calculation of EA and EI proceeds in a manner analogous to the method used in obtaining element force on the cross section. The procedural steps are identical until the summation. At this point, the concrete element force is divided by the total strain or the "contact strain" as it is referred to in this study. The contact strain is the sum of the apparent strain as can be measured, plus the internal strain due to thermal expansion. If the concrete is cracked due to external forces, there is neither strain nor stress in the element. Thermal expansion at this element could cause a net compressive strain to occur as the element comes into contact at the crack. Similarly, the addition of expansion strain could cause an element already in compression to crush, losing all strength. This contact strain is a measure of the actual effective internal strain occurring in the concrete element.

The result of dividing the element force by the contact strain gives the element axial stiffness property. This can also be defined as the secant modulus for the element multiplied by the

the effective area. The following summations are carried out at the mid-depth of the cross section.

$$EA = \sum_{i=1}^n \sum_{j=1}^n \left(\frac{P_{cij}}{\xi_{cij}} \right) + \sum_{k=1}^m (E_{sk} A_{sk}) \quad 4.8$$

$$EAd_{\frac{1}{2}t} = \sum_{i=1}^n \sum_{j=1}^n \left(\frac{P_{cij}}{\xi_{cij}} d_{ij} \right) + \sum_{k=1}^m (E_{sk} A_{sk} d_{sk}) \quad 4.9$$

$$EI_{\frac{1}{2}t} = \sum_{i=1}^n \sum_{j=1}^n \left(\frac{P_{cij}}{\xi_{cij}} (d_{ij}^2 + \frac{(t/n)^2}{12}) \right) + \sum_{k=1}^m (E_{sk} A_{sk} d_{sk}^2) \quad 4.10$$

Since the properties are calculated about the mid-depth, the value of EI_{cg} can be found as follows:

$$EI_{cg} = EI_{\frac{1}{2}t} - (EAd_{\frac{1}{2}t})^2 / EA \quad 4.11$$

The values of EA and EI_{cg} are now ready for the structural analysis program.

4.3 Load-Deformation Relationships

The behaviour of the internal cross section strains have been examined in relation to the external loads. For this study, the standard sixteen inch square cross section described in section 3.5, was used. The effect of temperature on strains was not included in this section of the investigation since increased temperature will only affect the magnitudes of forces and not the general concepts involved. Figure 4.1 shows the material properties for the concrete and steel as defined in section 2.6. Also shown is the interaction diagram obtained at

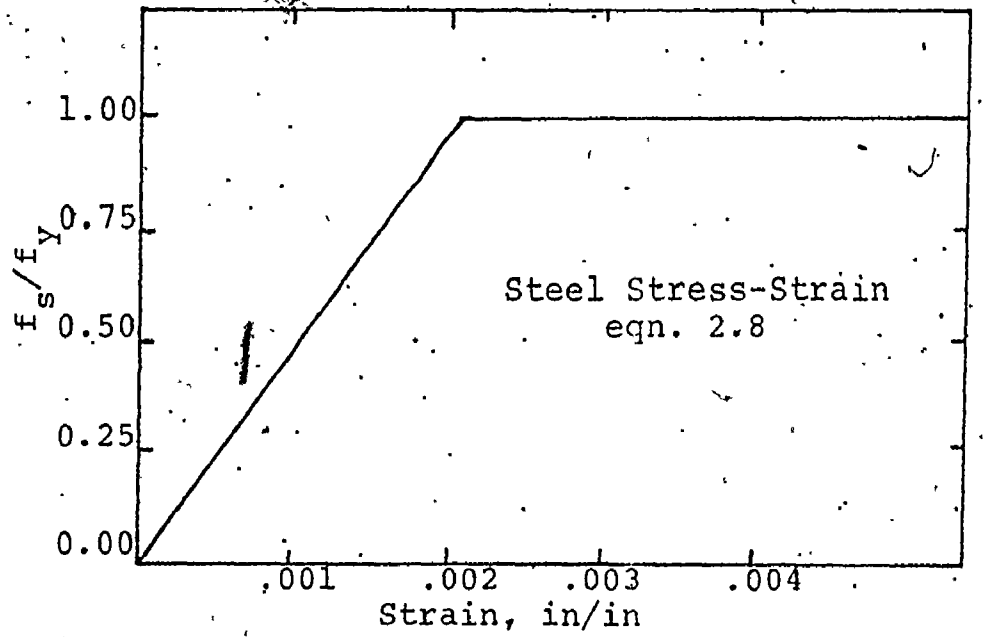
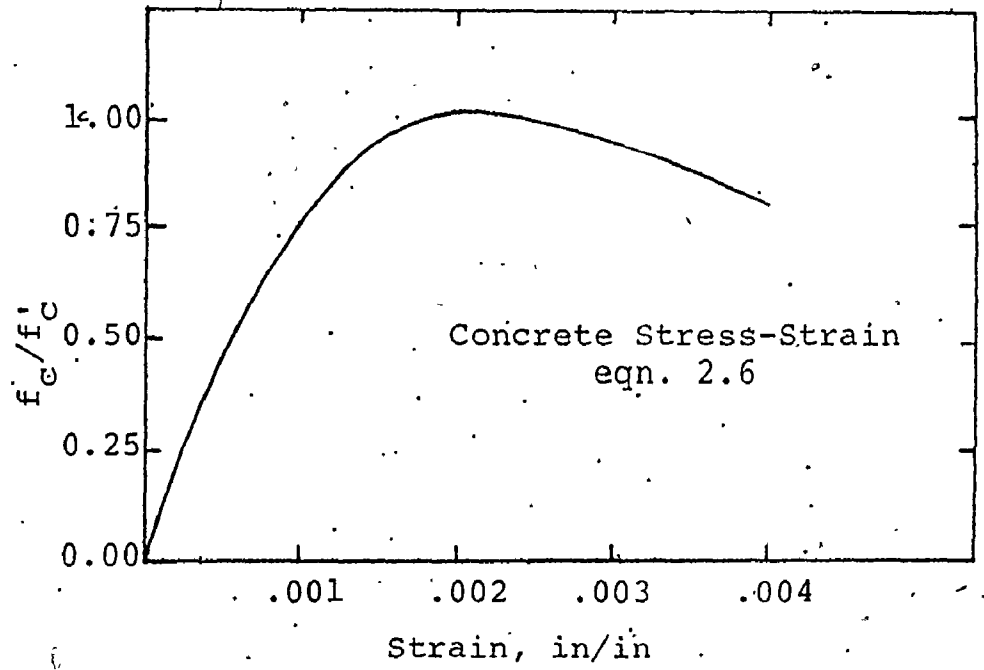
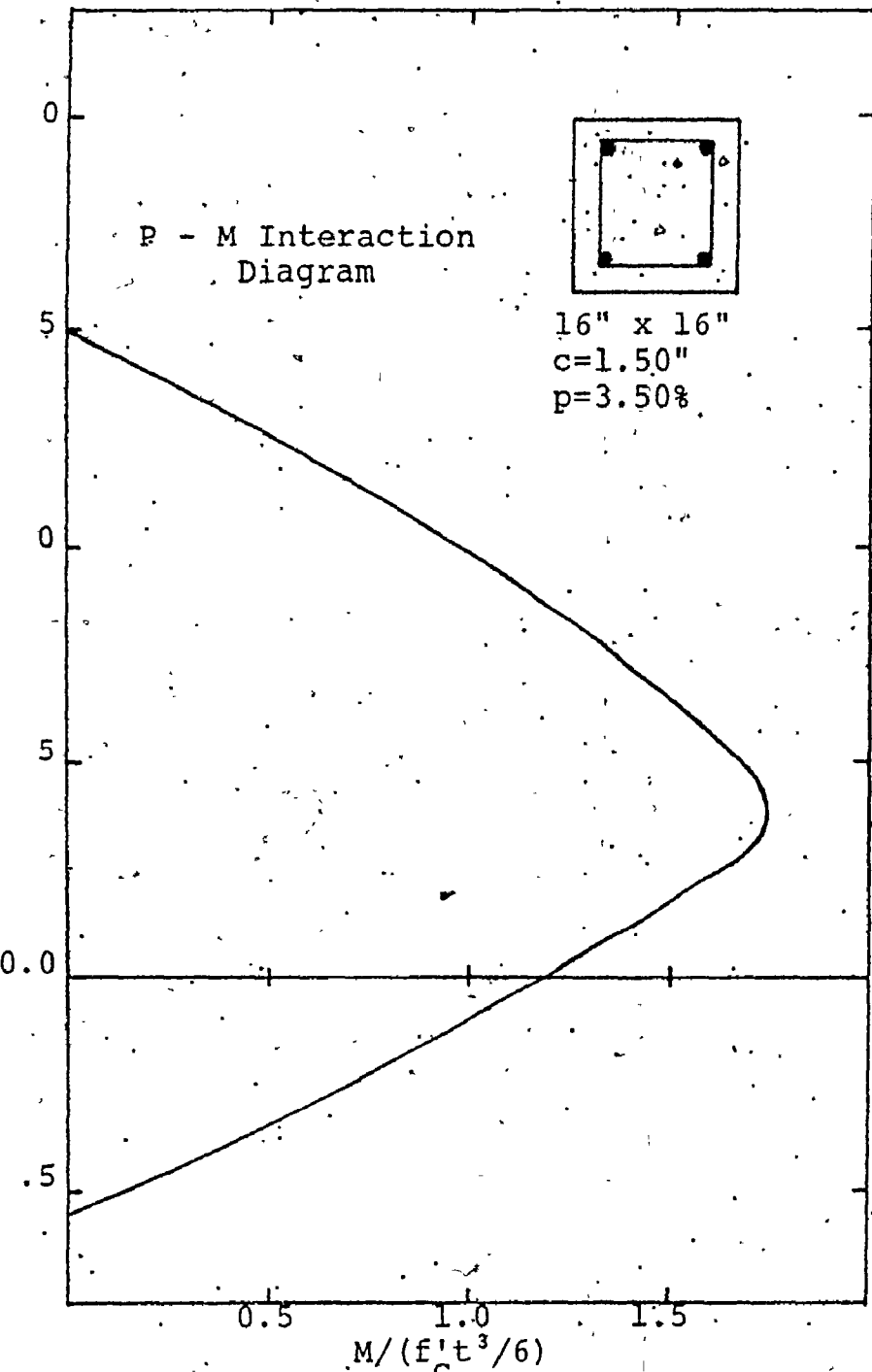


Figure 4.1 Interaction Diagram and Material Properties for Standard 16 inch Column

graphs lie within this interaction diagram.

Three distinct characteristics for load-deformation curves will be seen. The most obvious characteristic is the point of initial tension cracking of the concrete. This point is especially evident on the moment-curvature graph (Figure 4.2). The other characteristics to notice are the points of tension yield of steel and compression yielding of the section. A large amount of ductile behaviour occurs after steel yielding and before section failure.

4.3 (a). Moment-Curvature Relationship

The moments calculated in this section were those taken about the transformed elastic centroid. From Figure 4.2; it can be seen that the intensity of the axial load strongly influences the moment-curvature relationship.

For zero axial load, the moment-curvature relationship is close to being a straight line until reaching the point of tension steel yielding. The curve then exhibits very ductile behaviour up to the concrete crushing and hence, failure. As the axial load is increased, the initial straight line portion of the curve becomes steeper. This increase in the steepness stops at a point between a value of P' of 0.25 and 0.50. Looking at the interaction diagram, this particular value of P' where this increase stops, corresponds to the balanced conditions. After this point of balanced conditions has been exceeded, the straight line portion begins to lose steepness and moves in the direction of the zero axial load curve. This behaviour caused by increased axial load indicates that for a section with a low axial load, an

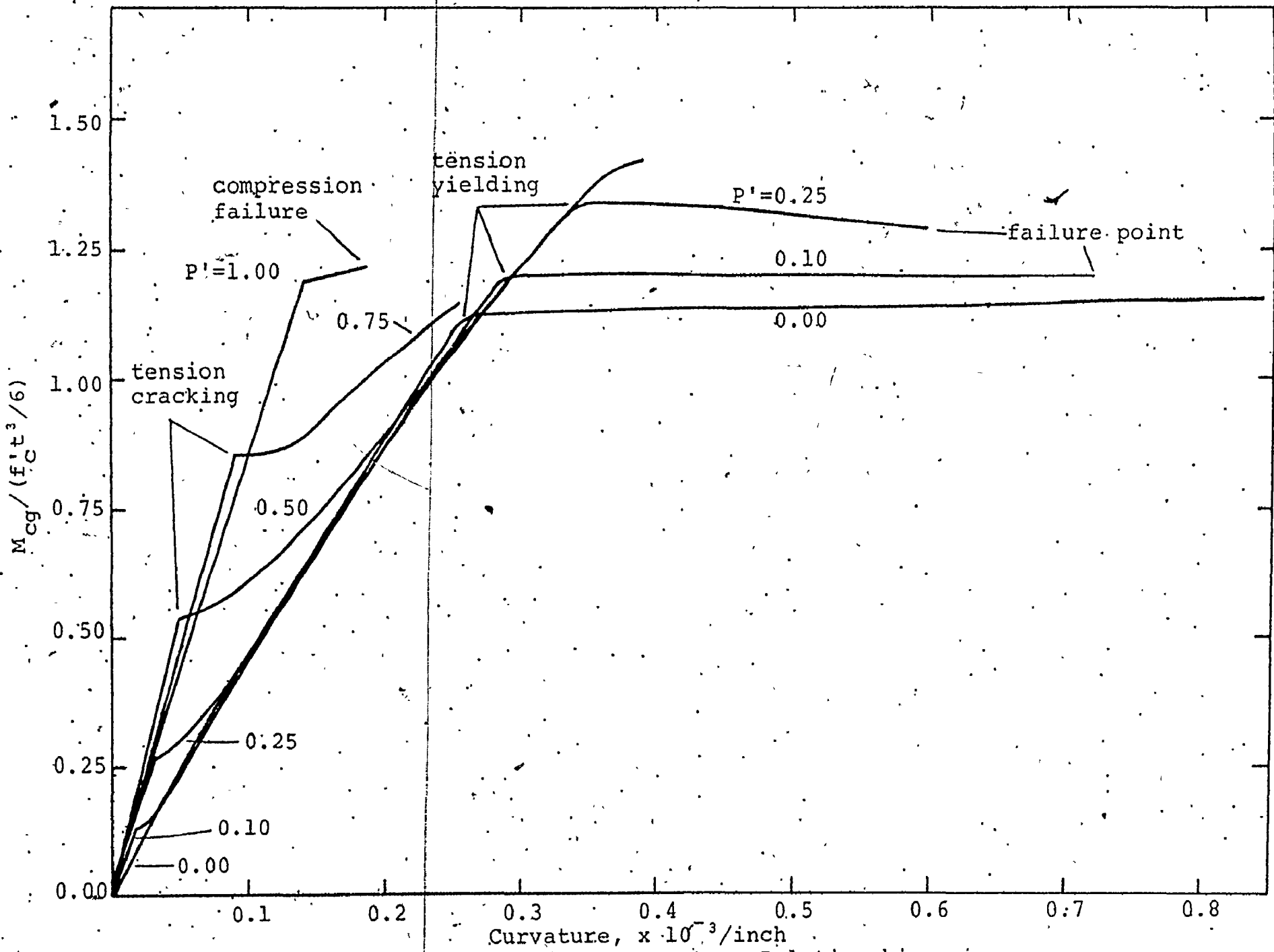


Figure 4.2 Moment-Curvature Relationship

increase in that load allows the section to carry more bending moment at the same curvature. However, after passing the balanced load point, an increase in axial load is detrimental to the moment capacity.

With increases in axial load above zero, the point of tension cracking is more evident. This cracking moment increases as the axial load is increased.

For low axial loads, a great amount of ductile behaviour can occur once the tension steel yields. The ductile behaviour continues beyond yielding of compression steel and up to the point of concrete crushing when failure occurs.

4.3 (b) Axial Load-Axial Strain Relationship

The axial load has been allowed to go into the tensile region on the graph in figure 4.3 which describes the axial load-axial strain behaviour for various constant moments. The axial strain plotted is the strain at the transformed elastic centroid.

As would be expected, all curves pass through the origin. The curve for zero bending moment is a straight line in the tensile region, since the concrete is completely cracked. When the axial load is compressive, the graph follows a line resembling the shape of the concrete stress-strain curve. The strain at maximum concrete stress is the point of failure for this curve. It is noted that the steel yields at very nearly the same strain.

Up to M' equal to 1.15, there exists the possibility of a tensile axial load. Above this moment, the axial load must be compressive to avoid failure. In the tensile region, the curves approach the straight line for $M' = 0.0$. Deviation from a

if

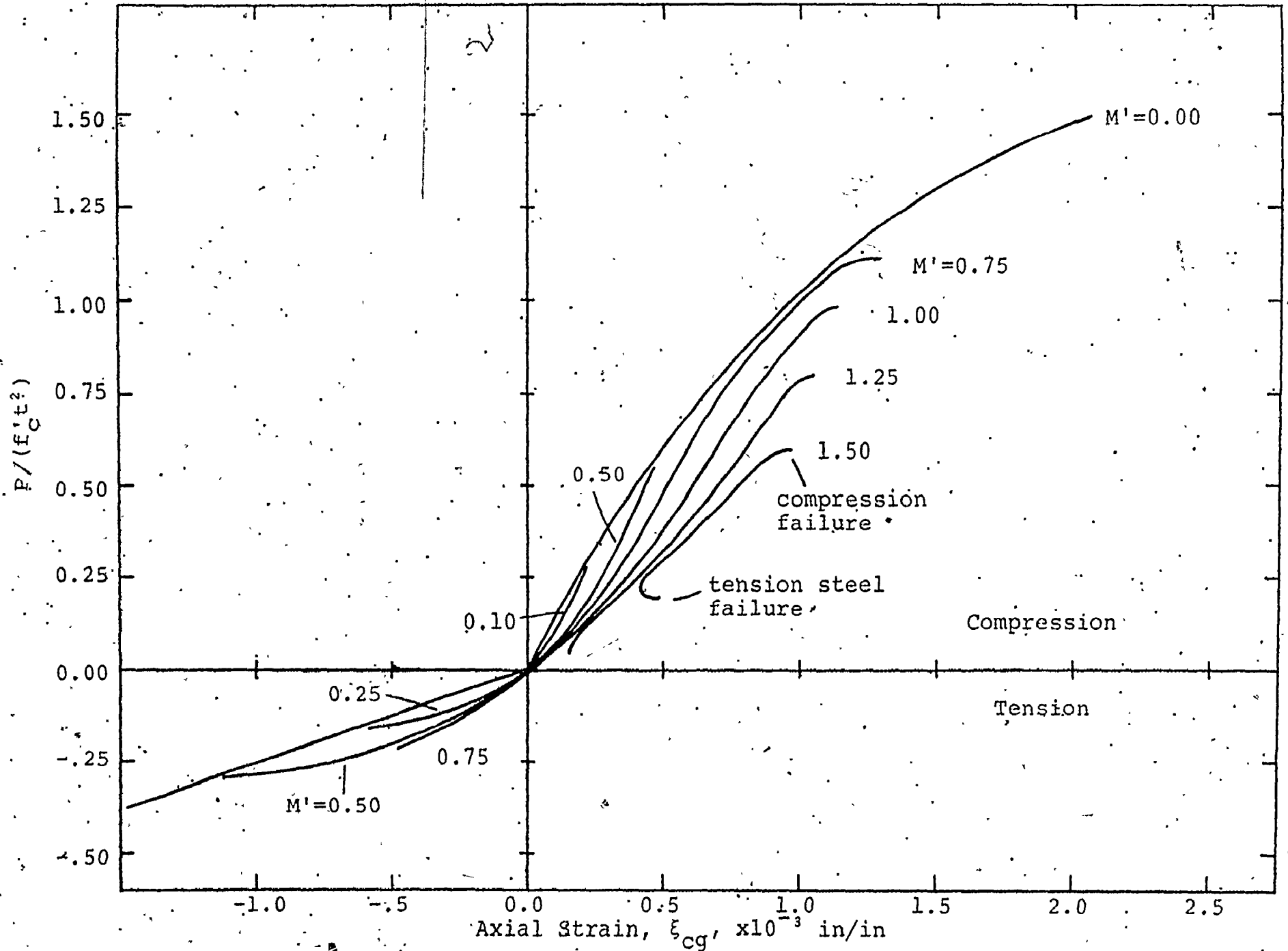


Figure 4.3 Axial Load-Axial Strain Relationship

For the compression region, as long as the strains on the entire cross section remain in compression, there is little deviation from the zero moment curve. When the axial load is low, tension strains can develop even for small M' ratios (ie. when $M/P > t/6$). As the axial load is increased for the low moment curves, they will approach the zero moment curve again. Moment values above 0.75 will always result in tension cracking of the concrete and hence, larger deviation from the zero moment curve. High M' values of 1.25 or 1.50 show two different yield points at both ends of their curves. The yield point at low axial load indicates plastic deformation in the tension steel. The yield point at high axial load is caused by compression steel plastic deformation and by the loss in compression strength of the concrete after the ultimate strength has been exceeded.

4.3 (c) Axial Load-Curvature Relationship

The first feature noted on Figure 4.4 is the fact that for any value of axial load, an increase in the bending moment causes an increase in the curvature. As the moment is increased for a constant axial load, the rate of change in the curvature also increases.

For any constant axial load, the curvature has two local maximum values. Starting at low axial loads (tension if permitted), there is a maximum due to tension yielding. As the axial load is increased, at constant moment, the curvature decreases. The addition of compressive axial load places more of the cracked section under compression. This increases the effective area up to the point where there is no cracked concrete

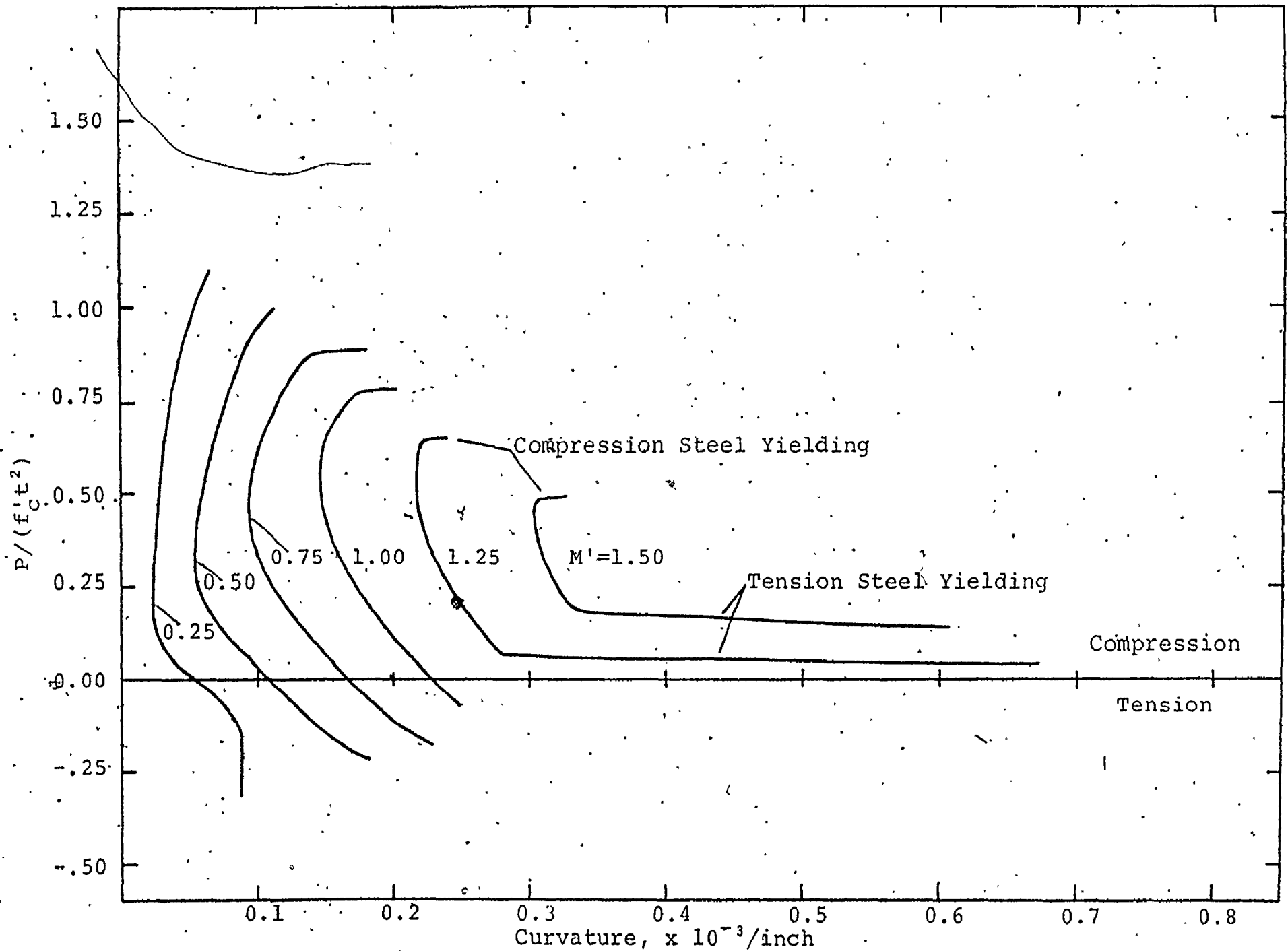


Figure 4.4 Axial Load-Curvature Relationship

remaining or until the concrete under highest compression reaches the maximum strength. The curvature gradually increases as the axial load is further increased because of the non-linear concrete stress-strain relationship.

The ductile behaviour at low axial loads and high moments due to yielding of the tension steel is indicated. The post yield behaviour associated with high axial load exhibits less ductility. Also, the yielding of the compression steel coincides with a rapid decrease in concrete capacity. These two features result in a more abrupt failure. The curve representing a constant M' of 0.25 is of special interest. When the concrete section is fully cracked, the curvature is a constant related to the steel behaviour. Failure due to increased tension is abrupt since little plastic distribution of forces can take place when all the tension steel yields at the same time. For a large compressive axial load coupled with low bending moments, the failure is again abrupt. In this case it is the combined result of compression steel yielding and concrete crushing.

4.4. Variation of EA and EI with External Loads

The behaviour of the transformed section properties relative to the external loads has been examined. As in section 4.3, analysis have been made using the standard sixteen inch square cross section.

The values of EA and EI from the graphs in figures 4.5 and 4.6 were obtained using the transformed section method of calculation. The axial load is both tensile and compressive, resulting in a full definition of the section properties for any

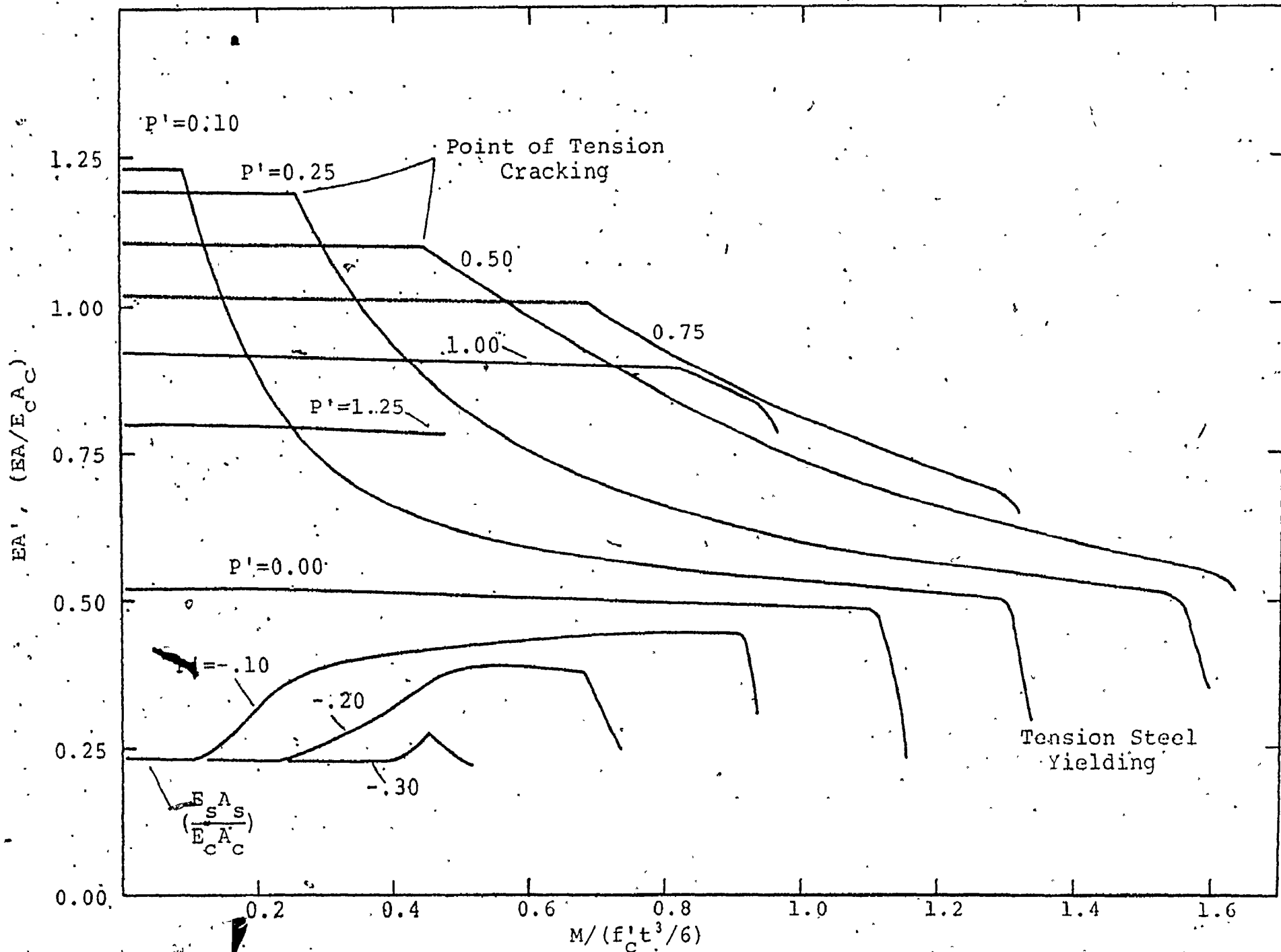


Figure 4.5. Variation of EA at Constant Axial Load

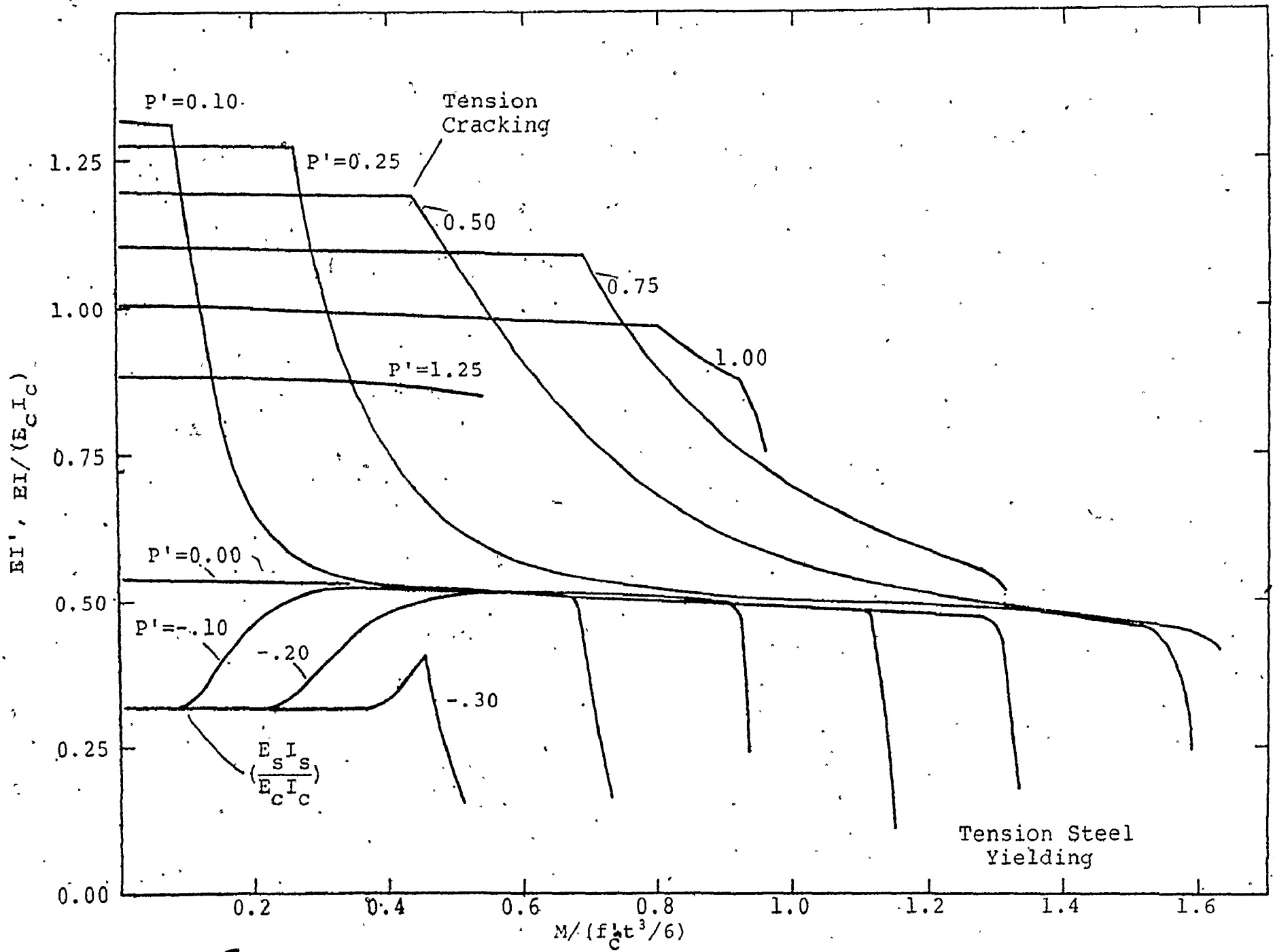


Figure 4.6 Variation of EI at Constant Axial Load

load combination. It will be noted that the point of tension cracking is the most important aspect in determining the transformed section properties.

The values of EA and EI at any load and moment are normalized by dividing by the respective values of $E_c A_c$ and $E_c I_c$. E_c is the value of the elastic modulus of concrete calculated at low axial strains. The stress-strain curve for low strains is close to being linear. A_c and I_c are the area and moment of inertia respectively of the uncracked section.

4.4 (a) Variation of EA and EI with Moment

The normalized curves for EA and EI shown in figure 4.5 and figure 4.6 are very similar in appearance as would be expected. EA' and EI' are plotted for a constant value of P', with M' varying from zero to the maximum associated with that axial load.

For cross sections with a compressive axial force, there are three distinct segments to each curve. For each curve for both EA' and EI', there is an initial high value, then a transitory stage followed by a relatively constant low value as the moment increases.

The initial high plateau for EA' or EI' with compressive axial load, is the result of the cross section being fully effective. The extent of this high plateau up to the start of the transitory stage is directly proportional to the axial load, the larger the load is, then the greater is the extent. The secant modulus for the concrete stress-strain curve is greatest for very small strains. This results in maximum values for EA' and EI'. At concrete cracking, there is a drop in the values of EA' and EI'. The slope of this transitory stage is steepest for

low axial loads. The slope is more severe for EI' than for EA' . With low axial loads, the cracked section stabilizes rapidly to the relatively flat segment of the curve. With high compression, the transitory stage is more gradual and failure may occur before EA' and EI' reach relatively constant values.

After the transitory stage, the values of EI' and EA' for low axial compression, are nearly constant but gradually decrease for increases in the moment. At the yield moment for low compression loads, there is a sudden drop in the stiffness properties which is indicative of a plastic behaviour. At high compression loads, the failure is sudden due to concrete crushing and compression steel yielding.

For axial tension, the values for EA' and EI' correspond to $(E_s A_s)'$ and $(E_s I_s)'$, the normalized stiffness properties for the steel only. As long as the concrete is wholly cracked, EA' and EI' remain constant. When compression in the concrete begins, as the moment is increased, then EI' rises to the previously mentioned nearly constant value for cross sections under compression. The values remain nearly constant until tension yielding occurs.

As a comparison, the value of EI was calculated using the moment about the geometric centroid divided by the curvature. The comparative graph is plotted in Figure 4.7. Although the general shape is similar, there is substantial differences in the actual values. The changes in EI values are more gradual.

The differences between the two sets of EI curves in figure 4.7 are due to the movement of the transformed elastic centroid. The effect on moment is shown in Figure 4.8. Here the moment

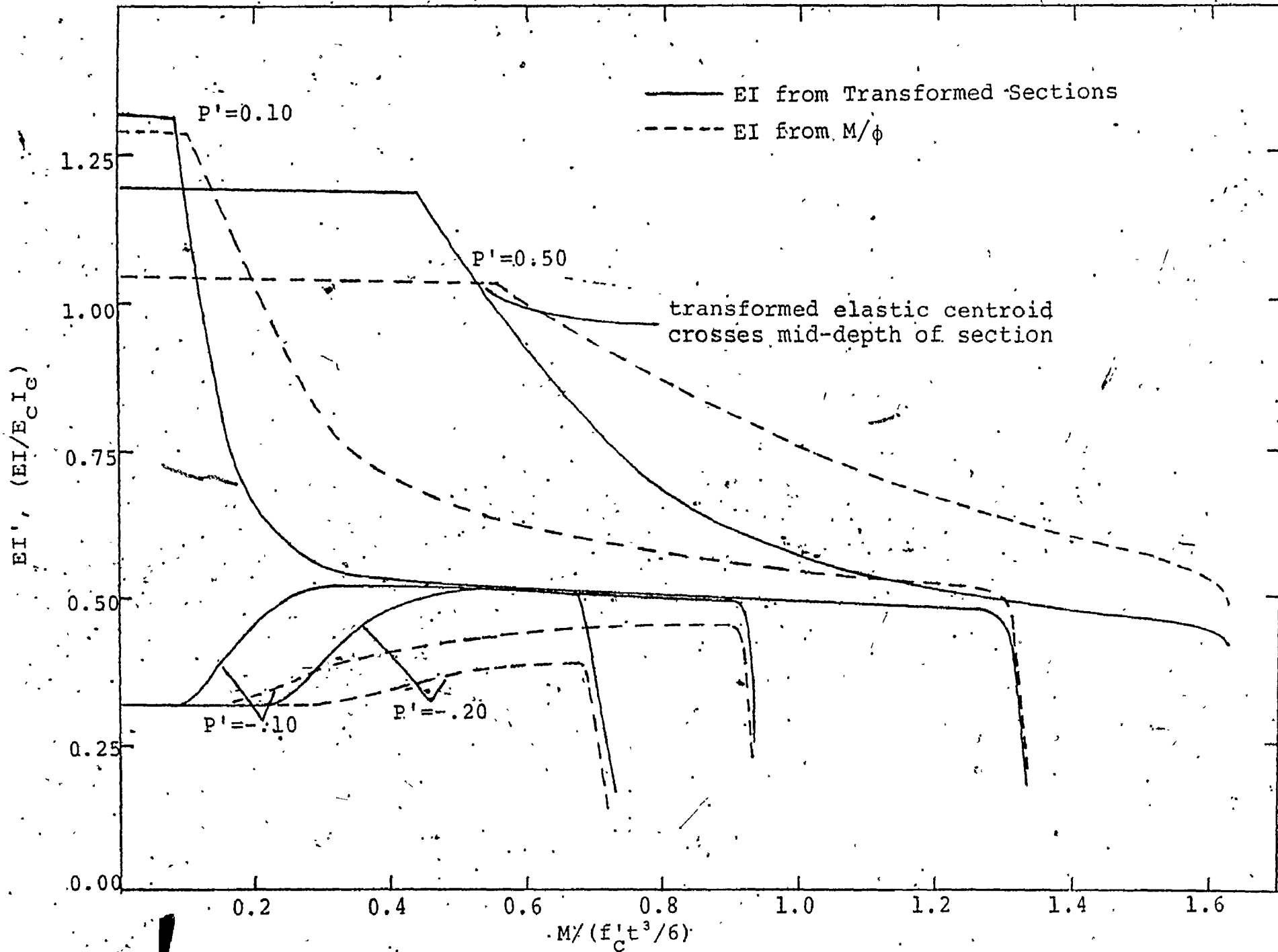


Figure 4.7 Comparison for EI Method of Calculation

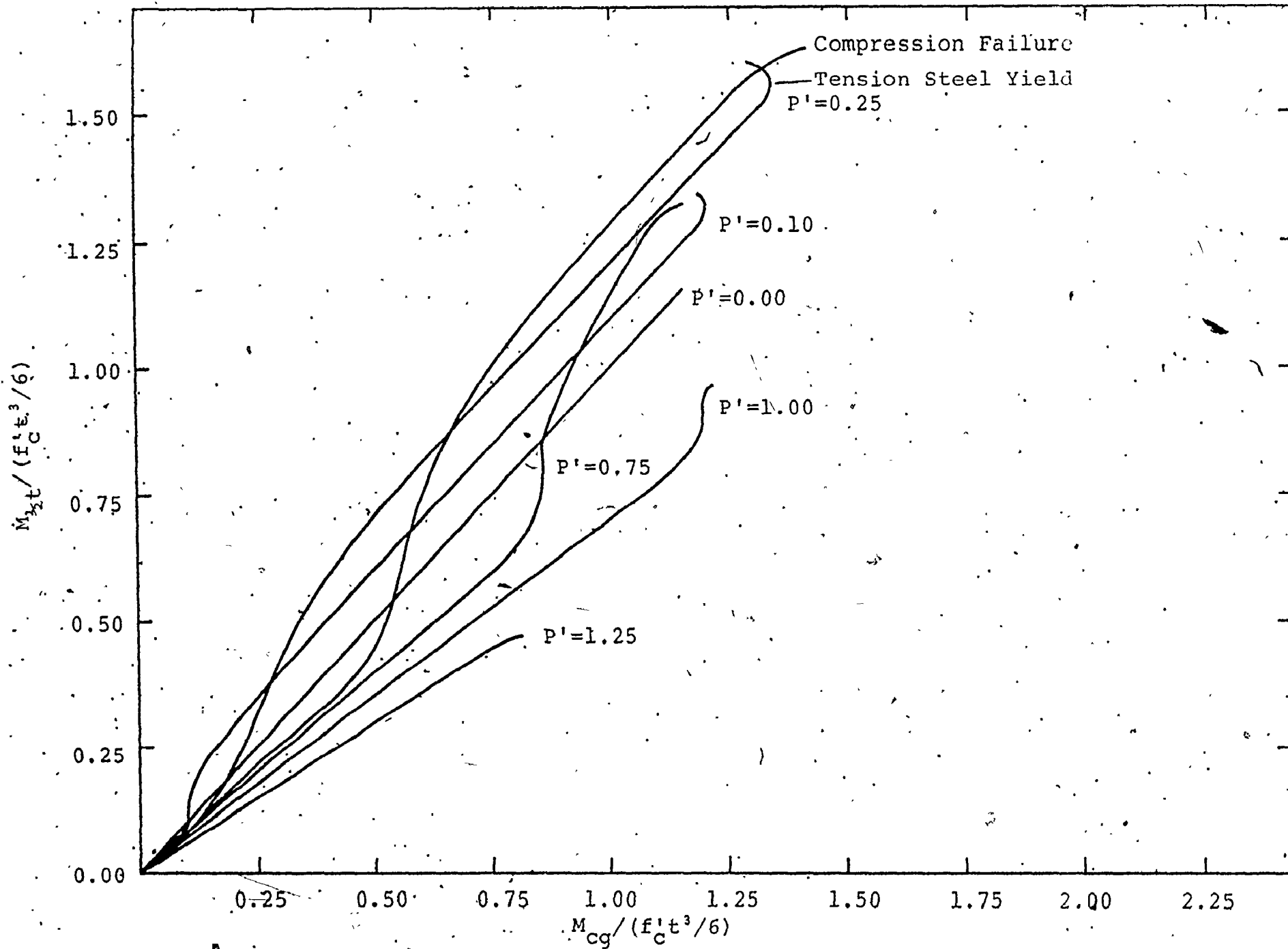


Figure 4.8 Plot of M_{xt} versus M_{cg}

about the geometric centroid is plotted against the moment about the elastic centroid. Only for the case of zero axial load is there a one to one collation. For low axial loads, there is a rapidly increasing difference for a portion of the curve until the elastic centroid becomes stable. A stable centroid is indicated by the constant offset of the parallel lines for P' up to 0.5. Up to P' equal to 0.5, the elastic centroid of the transformed area moves several inches towards the compression zone. As the axial load is increased, the effective area also increases, pulling the centroid away from the compression steel. At high axial loads, the concrete secant modulus is larger on the tension side moving the elastic centroid to the tension side of the geometric centroid. The tails at the ends of each curve on Figure 4.8 indicate the mode of failure. A tail to the left indicates tension failure while a tail to the right indicates compression failures. The elastic centroid moves away from the failure side.

4.4 (b) Variation of EA and EI with Axial Load

The curves for EI' and EA' are plotted for constant M' with varying P' in figures 4.9 and 4.10. The value of P' goes from a minimum (negative if feasible) to a maximum in compression.

For a negative axial load, the EA' and EI' values are close to the $(E_s A_s)'$ and $(E_s I_s)'$ values, respectively. As the axial load is increased, increasing the effective area, all curves up to M' of 0.75 approach the boundary curve defined by M' equal to 0.0. The ductile nature of the yielding cross section is again evident.

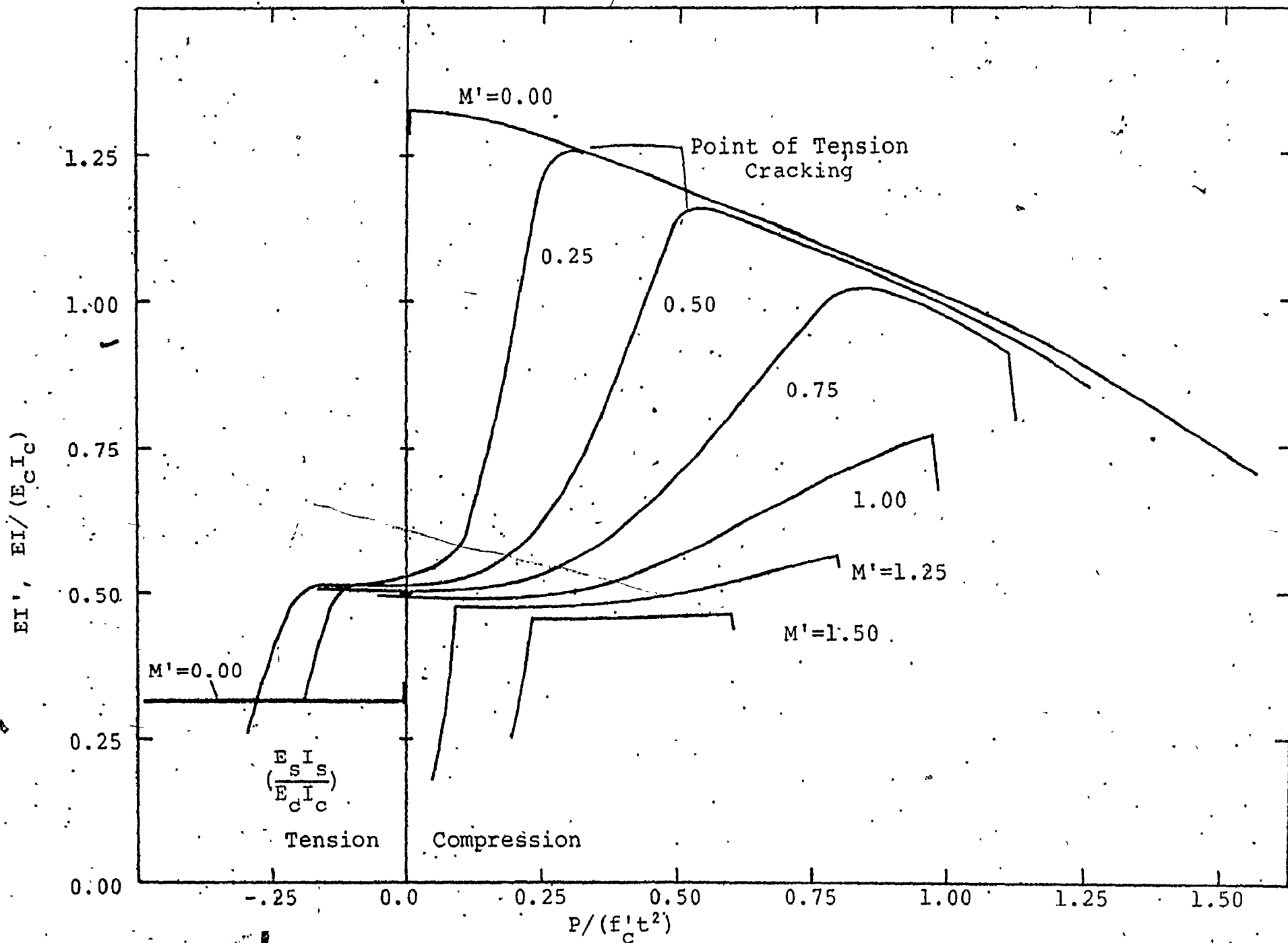
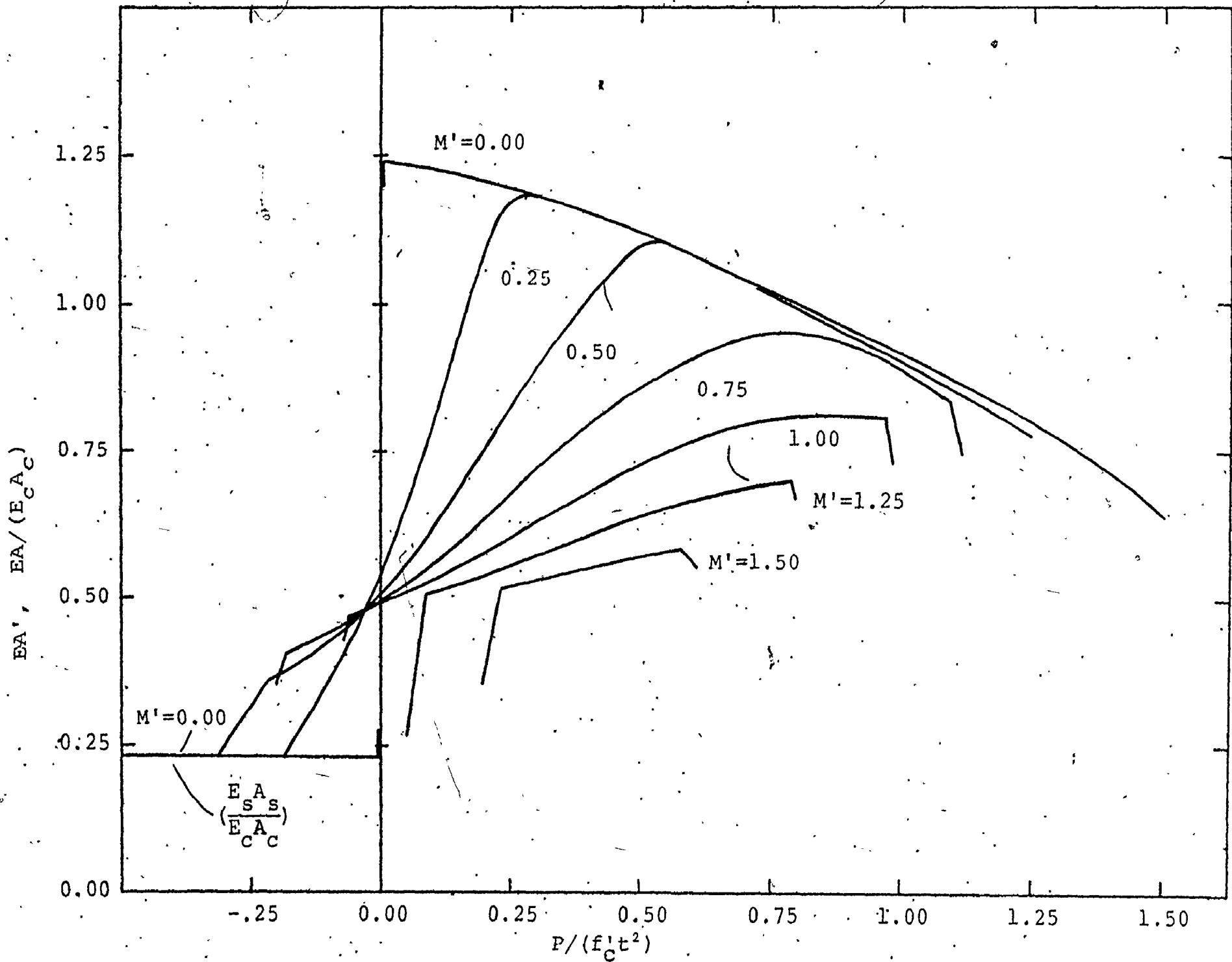


Figure 4.9 Variation of EI at Constant Moment



4.5 Method of Structural Analysis

For a reinforced concrete frame there is a problem with defining the geometry. The transformed elastic centroid is dependent on the magnitude and the eccentricity of the axial load and on the magnitude of the bending moment. This causes a continuous shifting of the centroid as the forces change. For instance, at the onset of tension cracking in the concrete there is a very rapid movement of the centroid towards the compression zone.

For an elastic structure, the centroid location does not change, but for the non-linear structure, the centroid will change. This necessitates adjusting the member stiffness and transformation matrix as the joints defining the centroidal axis move. This would complicate the analysis.

To determine the importance of this movement of the centroid, two analyses were performed using a single-bay, single storey reinforced concrete frame. One analysis used the mid-depth of the cross section as the centroidal axis (the straight frame), while the other analysis used the actual elastic centroid (the crooked frame). At first appearance, the results shown in Figure 4.11 for forces seemed to be greatly different, but this was due to a different reference point for moments for each analysis. For comparison, the forces in the crooked frame were transposed to the mid-depth of the cross section which was the centroidal axis for the straight frame. Now the bending moments are in close agreement, as are the deflections and the transformed section properties. It is noted that the frame shown in Figure 4.11 is a small frame. As the dimensions of the frame are increased, the effect of movement of the centroidal axis will

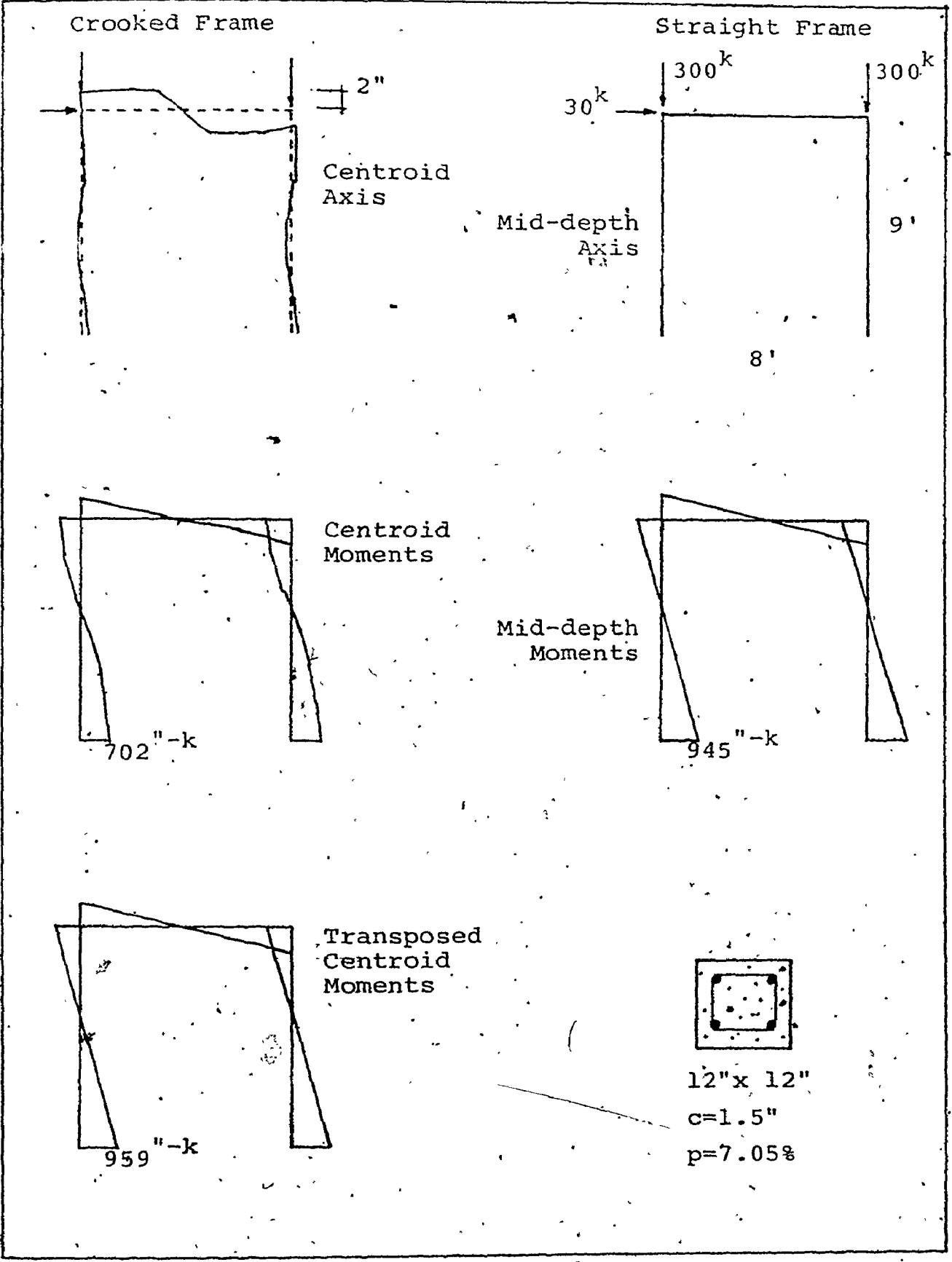


Figure 4.11
Frame Analysis Based on Centroid Axis

decrease. For this study, the effect of the movement of the centroidal axis will be ignored. Therefore, all moments, forces and stiffness properties will be calculated for convenience, at the cross section mid-depth. The resulting stiffness properties are transposed to the centroid to obtain the actual minimum value for EI . The value of EI at the centroid is used in the frame analysis which is referenced to the mid-depth of members. Errors no larger than the one or two percent convergence tolerance should occur.

A further consideration is the secondary bending moment (P- Δ effect) due to joint translation under applied loads. This effect can only be taken into account for a multi-storey building by making use of the deflected shape of the entire structure. Thus the deflected shape of the centroidal axis becomes the input geometry of the frame. By an iteration process, carried out at the same time as the forces and section properties are being adjusted, a final deflected shape is attained. Each iterative cycle produces new deflections which are referenced to the original geometry. As the cycles proceed, the change in deflection decreases approaching a stable configuration if there is no buckling. Also the moments at the centroids change in an amount equal to the axial load multiplied by the reference deflection. The reference deflection is defined here as the displacement of the load on the frame relative to the joint being investigated. Figure 4.12 illustrates the P- Δ effect more clearly.

The final configuration of the frame is the sum of the initial geometry and the joint deflections. This final configuration is

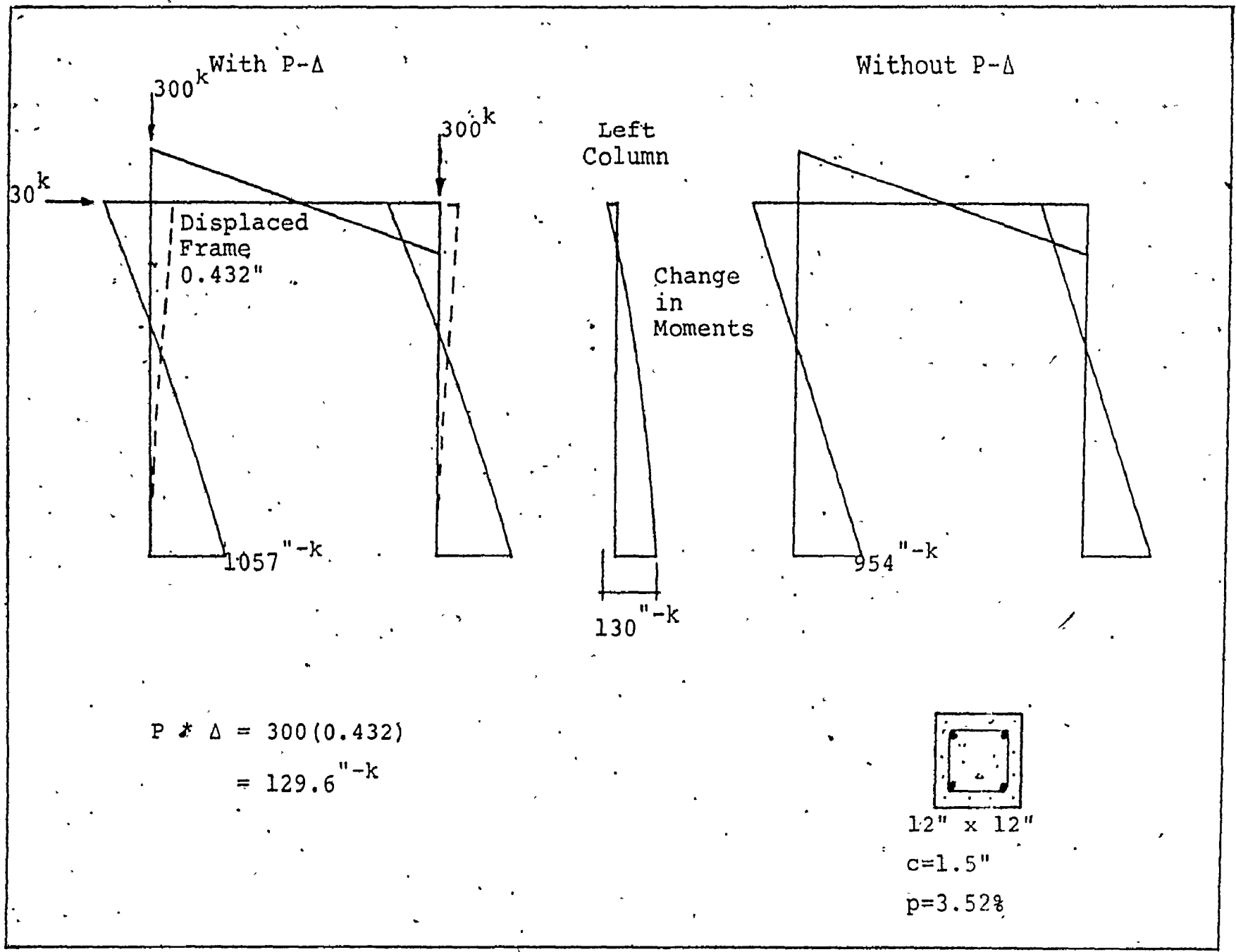


Figure 4.12 P- Δ Effect

is close to the deflected shape obtained after only one cycle of analysis. It should be noted that if the frame loads were reversed at this deflected shape then the frame would move back to its original geometry with only one iteration cycle.

Examining the base moments for the left column shows that the change in moment due to deflection is 11%. This is a large variation and is quite important. Moreover, the effect of secondary bending moments will increase greatly as the number of floors in a building increases. In the present study, only the primary effects of fire exposure are examined. To include the secondary effects of joint translation could possibly hide the desired information. Comparisons in this chapter are for different heights of building. Clearly, the secondary effects would be different for the different building heights. Therefore, the P- Δ effect has been left out of the frame analysis. An actual design should include this effect.

The foregoing has dealt with how an inelastic frame is defined with regard to its stiffness properties and its geometry. A method of successive linear approximations of the inelastic frame has been developed to analyze the inelastic frame. An initial approximation to the stiffness properties is made. These stiffnesses are used in an elastic structural analysis resulting in member forces. These forces are used to determine the cross section strains which are in turn used to obtain new estimates to the member stiffness properties. This cycle continues until convergence has been obtained, if possible. A more detailed explanation of the program is available in Appendix A section A.6 (b).

4.6 Results and Observations of Frames Subjected to Fire Exposure

4.6 (a) Frame Details

Differential thermal expansion over a cross section is more detrimental to the section capacity than is a uniform expansion. In a similar manner, expansion of only a few selected members in a rigid frame will have more serious effects on these members and on the remaining frame than if all members of the frame were exposed to fire. There is also a great expenditure of computing time required to analyze a complete frame rather than a portion of that frame.

Restraint of thermal expansion must never be ignored. Even at temperatures just above room ambient there can be difficulties in a frame due to expansion. The expansions resulting from fire exposure can have major structural significance. The seriousness of the expansion corresponds with the degree of restraint at the member ends. If all members of a frame are expanding there will be little restraint on the individual members except at foundation locations. However, if only a few members are expanding, then elastic restraint is afforded by the members which are not expanding.

A three-bay building with varying building heights has been examined with two lower floor columns exposed to fire. The columns chosen were one interior column and one exterior column. The interior column was heavily restrained by the short floor beam spanning the building hallway. The exterior column had much less restraint since the floor beam attached to it spanned a longer distance.

The height effect has been studied using two, four and eight floors.. (see Figure 4.13) The restraint function should increase as the number of floors increases. Since the expansion is resisted by frame action, it follows that the greater the distance from the expanding member, the lesser will be the effect of the restraint function. Therefore, the addition of extra floors will not proportionately increase the restraint function.

Some simplifications have been allowed in these analyses. The cross section has been made equal for all members. After the initial force-strain-stiffness balance at zero time, the cross section stiffness properties of all members not exposed to fire have been set as an elastic constant, for all following times of exposure. A set of representative design values for floor and wind loads have been applied to the frame. These loads are also set as constants. If the external wind and internal live loads varied, then it would be difficult to determine the effect of the fire.

The lower column axial reactions would normally vary as the building height changes. However, the stiffness properties of the cross sections would also vary with the changing axial reactions. Likewise, with a change in stiffness characteristics, the thermal expansion force would also change. As before, all of these changing variables will hide the effects of the degree of restraint associated with different building heights. To make up for the loss of axial load due to the removal of upper floors, point loads equal to the loss have been added to the columns on the top floor. Now all three frames will have similar reactions and can be compared to study the restraint effect.

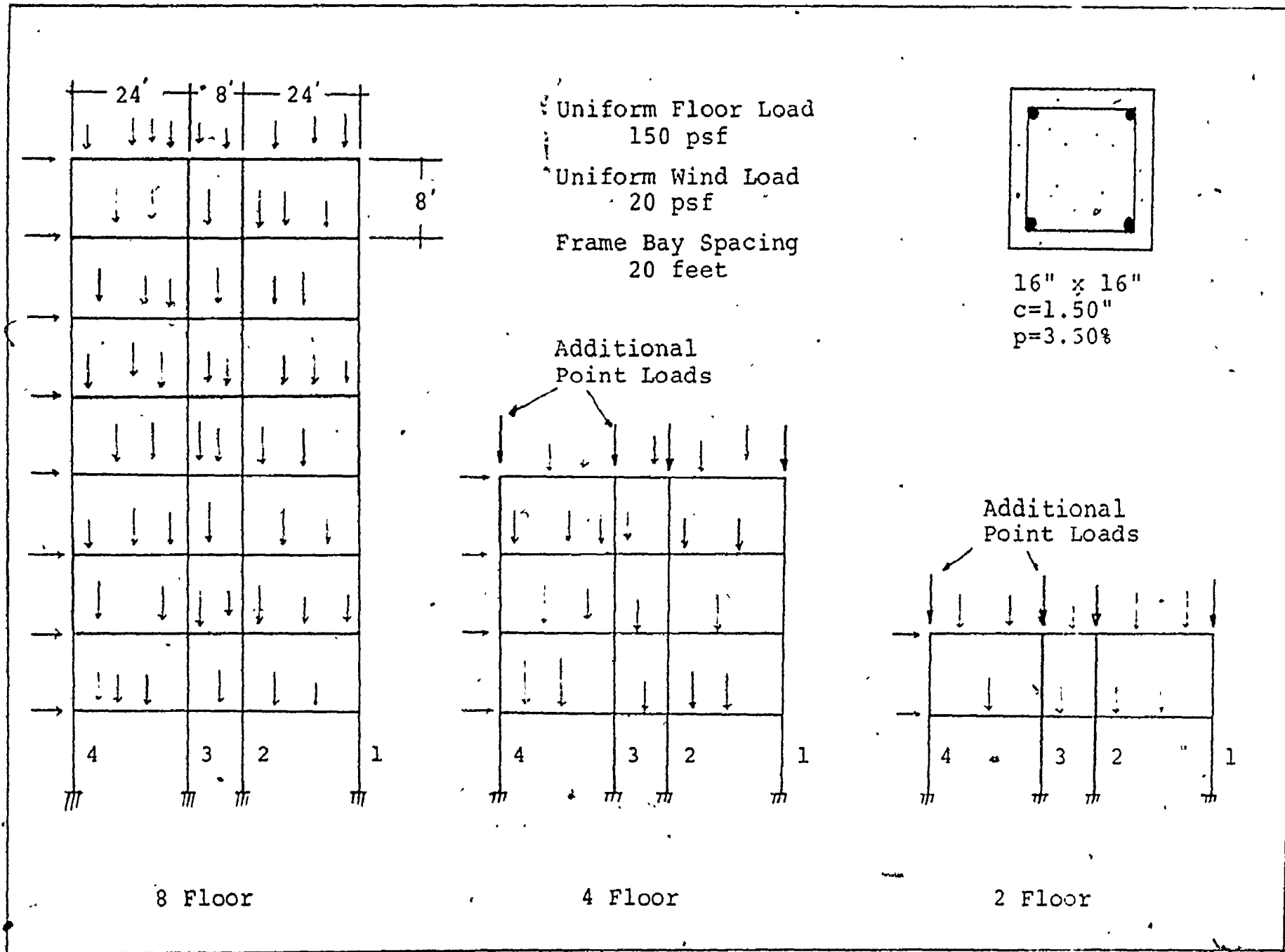


Figure 4.13 Details of Frames Analyzed

The four lower floor columns have been studied in detail in the following tables. Columns one and two are the columns exposed to the fire. Columns three and four were not exposed.

4.6 (b) Force Redistribution Due to Fire Exposure

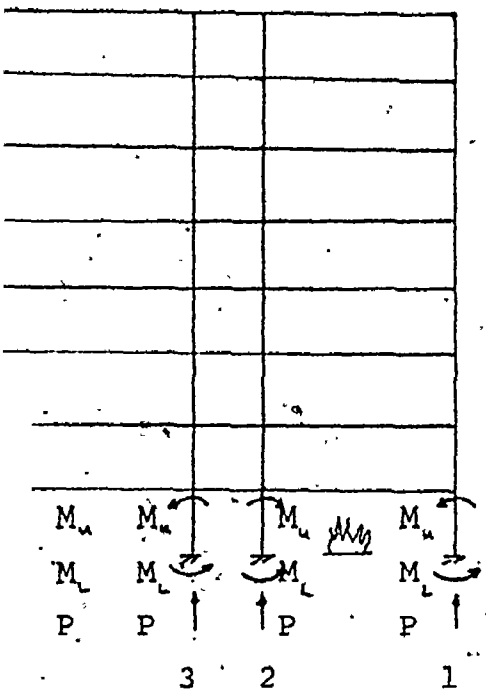
The normalized axial and bending moment forces are shown in tables 4.1, 4.2 and 4.3 for the analyses of the eight, four and two storey frames. Two cases, one with expansion and one without, were studied for each building height.

The effect of moment redistribution is evident for both cases. The moment is substantially reduced in the fire exposed columns as the period of exposure is increased. Some of this moment is transferred to the adjoining columns and some to the floor beams. The total moments are not greatly affected by the inclusion of expansion in the columns. This is partly because the large part of the column moment is caused by the lateral forces. This loss of column moment is beneficial to the fire endurance of the exposed columns. However, the increase in moments in the unexposed columns causes them to be overloaded.

The column axial loads are affected by the inclusion of thermal expansion in the analysis. Without expansion effects, the heated columns may lose a small portion of their axial loads due to the decline of EA. However, columns with thermal expansion included have large increases in axial load.

The increase in axial load is not restricted to the column length between the floors where the fire exists. The expansion in the lower column affects the whole building column from the foundation to the roof. This is shown in Table 4.4. The initial

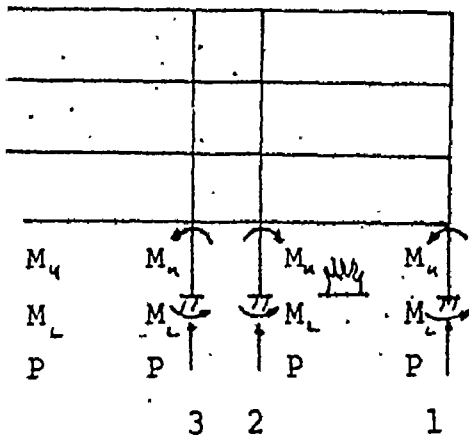
Refer to Figure 4.13
or Frame and Loading
etails.



| | Column | Force | Initial Force Level | FORCE LEVEL AFTER FIRE EXPOSURE | | | | | |
|-------------------|--------|----------------|---------------------|---------------------------------|--------|--------|--------|--------|--------|
| | | | | 30 | 60 | 90 | 120 | 150 | 180 |
| WITHOUT EXPANSION | 1 | P | 0.291 | 0.291 | 0.292 | 0.292 | 0.293 | 0.295 | 0.297 |
| | | M _u | 0.272 | 0.262 | 0.231 | 0.199 | 0.168 | 0.133 | 0.101 |
| | | M _l | 0.294 | 0.285 | 0.257 | 0.226 | 0.192 | 0.153 | 0.117 |
| | 2 | P | 0.404 | 0.403 | 0.399 | 0.393 | 0.386 | 0.376 | 0.368 |
| | | M _u | 0.077 | 0.074 | 0.066 | 0.058 | 0.049 | 0.040 | 0.030 |
| | | M _l | 0.081 | 0.075 | 0.057 | 0.041 | 0.029 | 0.019 | 0.126 |
| | 3 | P | 0.345 | 0.346 | 0.351 | 0.356 | 0.364 | 0.374 | 0.387 |
| | | M _u | 0.264 | 0.268 | 0.285 | 0.304 | 0.324 | 0.349 | 0.374 |
| | | M _l | 0.288 | 0.291 | 0.299 | 0.307 | 0.315 | 0.321 | 0.324 |
| | 4 | P | 0.272 | 0.272 | 0.271 | 0.270 | 0.269 | 0.268 | 0.266 |
| | | M _u | 0.006 | 0.010 | 0.027 | 0.046 | 0.067 | 0.095 | 0.124 |
| | | M _l | 0.219 | 0.217 | 0.208 | 0.198 | 0.186 | 0.172 | 0.159 |
| WITH EXPANSION | 1 | P | 0.291 | 0.281 | 0.275 | 0.292 | 0.290 | 0.286 | 0.286 |
| | | M _u | 0.272 | 0.128 | 0.083 | 0.083 | 0.054 | 0.046 | 0.037 |
| | | M _l | 0.294 | 0.188 | 0.153 | 0.138 | 0.076 | 0.060 | 0.047 |
| | 2 | P | 0.404 | 0.484 | 0.548 | 0.470 | 0.438 | 0.439 | 0.431 |
| | | M _u | 0.077 | 0.050 | 0.040 | 0.031 | 0.027 | 0.020 | 0.124 |
| | | M _l | 0.081 | -0.036 | -0.072 | -0.042 | -0.019 | -0.008 | -0.004 |
| | 3 | P | 0.345 | 0.264 | 0.193 | 0.258 | 0.302 | 0.312 | 0.321 |
| | | M _u | 0.264 | 0.291 | 0.284 | 0.304 | 0.362 | 0.387 | 0.400 |
| | | M _l | 0.288 | 0.436 | 0.546 | 0.495 | 0.456 | 0.441 | 0.437 |
| | 4 | P | 0.272 | 0.284 | 0.296 | 0.293 | 0.282 | 0.276 | 0.274 |
| | | M _u | 0.006 | -0.033 | -0.092 | -0.034 | 0.051 | 0.084 | 0.101 |
| | | M _l | 0.219 | 0.196 | 0.185 | 0.160 | 0.145 | 0.146 | 0.140 |

Table 4.1 Eight Storey Frame Analysis

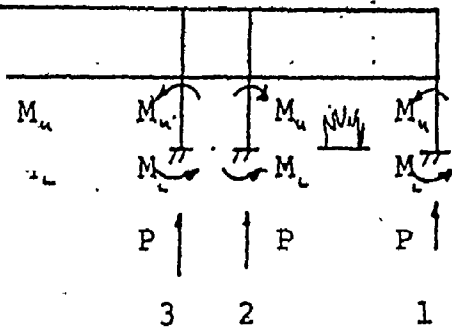
Refer to Figure 4.13
for Frame and Loading
Details



| | Column | Force | Initial Force Level | FORCE LEVEL AFTER FIRE EXPOSURE | | | | | |
|-------------------|--------|----------------|---------------------|---------------------------------|--------|--------|--------|--------|--------|
| | | | | 30 | 60 | 90 | 120 | 150 | 180 |
| WITHOUT EXPANSION | 1 | P | 0.286 | 0.286 | 0.287 | 0.287 | 0.288 | 0.289 | 0.290 |
| | | M _L | 0.271 | 0.261 | 0.230 | 0.199 | 0.168 | 0.134 | 0.103 |
| | | M _u | 0.293 | 0.285 | 0.256 | 0.226 | 0.192 | 0.154 | 0.118 |
| | 2 | P | 0.400 | 0.399 | 0.397 | 0.393 | 0.388 | 0.380 | 0.371 |
| | | M _L | 0.077 | 0.074 | 0.066 | 0.058 | 0.050 | 0.040 | 0.030 |
| | | M _u | 0.079 | 0.073 | 0.055 | 0.040 | 0.029 | 0.019 | 0.013 |
| | 3 | P | 0.351 | 0.352 | 0.355 | 0.359 | 0.364 | 0.371 | 0.381 |
| | | M _L | 0.263 | 0.268 | 0.284 | 0.303 | 0.324 | 0.349 | 0.374 |
| | | M _u | 0.288 | 0.291 | 0.298 | 0.306 | 0.313 | 0.319 | 0.319 |
| | 4 | P | 0.275 | 0.275 | 0.274 | 0.274 | 0.273 | 0.272 | 0.271 |
| | | M _L | 0.005 | 0.010 | 0.026 | 0.046 | 0.068 | 0.096 | 0.127 |
| | | M _u | 0.219 | 0.216 | 0.207 | 0.197 | 0.186 | 0.172 | 0.158 |
| WITH EXPANSION | 1 | P | 0.286 | 0.279 | 0.273 | 0.284 | 0.285 | 0.283 | 0.283 |
| | | M _L | 0.271 | 0.124 | 0.077 | 0.080 | 0.054 | 0.046 | 0.037 |
| | | M _u | 0.293 | 0.187 | 0.150 | 0.136 | 0.078 | 0.060 | 0.047 |
| | 2 | P | 0.400 | 0.459 | 0.510 | 0.456 | 0.426 | 0.423 | 0.419 |
| | | M _L | 0.077 | 0.049 | 0.039 | 0.031 | 0.027 | 0.020 | 0.013 |
| | | M _u | 0.079 | -0.041 | -0.081 | -0.046 | -0.021 | -0.008 | -0.005 |
| | 3 | P | 0.351 | 0.292 | 0.238 | 0.285 | 0.321 | 0.330 | 0.334 |
| | | M _L | 0.263 | 0.289 | 0.279 | 0.301 | 0.359 | 0.386 | 0.400 |
| | | M _u | 0.288 | 0.444 | 0.566 | 0.512 | 0.460 | 0.439 | 0.437 |
| | 4 | P | 0.275 | 0.282 | 0.291 | 0.288 | 0.281 | 0.277 | 0.276 |
| | | M _L | 0.005 | -0.039 | -0.107 | -0.046 | 0.046 | 0.084 | 0.101 |
| | | M _u | 0.219 | 0.195 | 0.185 | 0.160 | 0.144 | 0.144 | 0.139 |

Figure 4.2 Four Storey Frame Analysis

er to Figure 4.13
Frame and Loading
ails



| | Column | Force | Initial Force Level | FORCE LEVEL AFTER FIRE EXPOSURE | | | | | |
|-------------------|--------|-------|---------------------|---------------------------------|--------|--------|--------|--------|--------|
| | | | | 30 | 60 | 90 | 120 | 150 | 180 |
| WITHOUT EXPANSION | 1 | P | 0.283 | 0.283 | 0.283 | 0.283 | 0.284 | 0.284 | 0.285 |
| | | M_u | 0.259 | 0.250 | 0.221 | 0.191 | 0.161 | 0.129 | 0.100 |
| | | M_u | 0.266 | 0.258 | 0.234 | 0.206 | 0.176 | 0.142 | 0.109 |
| | 2 | P | 0.388 | 0.388 | 0.386 | 0.384 | 0.382 | 0.378 | 0.372 |
| | | M_u | 0.090 | 0.087 | 0.077 | 0.067 | 0.057 | 0.045 | 0.034 |
| | | M_u | 0.046 | 0.041 | 0.029 | 0.019 | 0.011 | 0.007 | 0.004 |
| | 3 | P | 0.364 | 0.364 | 0.365 | 0.367 | 0.370 | 0.374 | 0.380 |
| | | M_u | 0.244 | 0.249 | 0.266 | 0.286 | 0.307 | 0.333 | 0.359 |
| | | M_u | 0.260 | 0.263 | 0.271 | 0.279 | 0.286 | 0.292 | 0.292 |
| | 4 | P | 0.278 | 0.278 | 0.273 | 0.277 | 0.277 | 0.276 | 0.275 |
| | | M_u | 0.011 | 0.016 | 0.033 | 0.052 | 0.075 | 0.104 | 0.136 |
| | | M_u | 0.185 | 0.182 | 0.173 | 0.163 | 0.152 | 0.139 | 0.126 |
| WITH EXPANSION | 1 | P | 0.283 | 0.279 | 0.274 | 0.279 | 0.282 | 0.281 | 0.281 |
| | | M_u | 0.259 | 0.116 | 0.065 | 0.069 | 0.051 | 0.044 | 0.036 |
| | | M_u | 0.266 | 0.173 | 0.138 | 0.124 | 0.073 | 0.056 | 0.044 |
| | 2 | P | 0.388 | 0.424 | 0.460 | 0.434 | 0.405 | 0.401 | 0.399 |
| | | M_u | 0.090 | 0.055 | 0.043 | 0.034 | 0.029 | 0.022 | 0.014 |
| | | M_u | 0.046 | -0.060 | -0.101 | -0.060 | -0.027 | -0.013 | -0.008 |
| | 3 | P | 0.364 | 0.328 | 0.291 | 0.314 | 0.345 | 0.351 | 0.354 |
| | | M_u | 0.244 | 0.268 | 0.252 | 0.276 | 0.339 | 0.369 | 0.383 |
| | | M_u | 0.260 | 0.420 | 0.561 | 0.519 | 0.437 | 0.410 | 0.408 |
| | 4 | P | 0.278 | 0.282 | 0.287 | 0.285 | 0.281 | 0.279 | 0.278 |
| | | M_u | 0.011 | -0.036 | -0.119 | -0.064 | 0.049 | 0.093 | 0.110 |
| | | M_u | 0.185 | 0.156 | 0.142 | 0.119 | 0.106 | 0.108 | 0.103 |

Figure 4.3 Two Storey Frame Analysis

force in the interior column (column 2) is tabulated for each floor. Compared with this initial force is the total column force at sixty minutes of exposure. This time period has the largest effect due to thermal expansion. After sixty minutes, the decrease in cross section stiffness EA has a greater influence than the thermal expansion force and a reduction in force begins. The remaining three columns in Table 4.4 contain the extra force caused by expansion in the first floor column, this extra force expressed as a percent of the initial forces and the shear transferred at each floor level.

Although the extra forces in the upper columns decrease as the height increases, the extra forces are still a large percentage of the initial axial loads. If these columns were designed with a reduced cross section at the upper levels, then these extra forces could be critical.

4.6 (c) Thermal Restraint Equation

The floor shear transfer is an indication of the degree of restraint. The shear transferred to the individual beams decrease as the number of floors is increased. Although the thermal expansion force is lower for a fewer number of floors, the individual shear transfer forces increase as the number of floors decrease. A corollary of this observation is, although doubling the number of floors may double the capacity for total vertical shear transfer, the actual restraining force is not doubled accordingly.

The thermal restraining force is definitely non-linear with respect to increased building height. This is illustrated in

| THERMAL EXPANSION EFFECTS ON COLUMN FORCES | | | | | | |
|--|-----------|----------------|-------------------|----------------|--------------|----------------------|
| No. of Floors | Floor No. | Initial Forces | Forces at 60 min. | P ^T | % of Initial | Floor Shear Transfer |
| 8 | 8 | 47.51 | 59.13 | 11.62 | 24.4 | 11.62 |
| | 7 | 95.24 | 120.90 | 25.66 | 26.9 | 14.04 |
| | 6 | 144.56 | 184.56 | 40.00 | 27.7 | 14.34 |
| | 5 | 195.42 | 251.05 | 55.63 | 28.5 | 15.63 |
| | 4 | 247.91 | 320.90 | 72.99 | 29.4 | 17.36 |
| | 3 | 302.14 | 394.84 | 92.70 | 30.7 | 19.71 |
| | 2 | 358.03 | 473.83 | 115.75 | 32.3 | 23.05 |
| | 1 | 414.26 | 560.71 | 146.45 | 35.3 | 30.70 |
| 4 | 4 | 243.15 | 265.45 | 22.30 | 9.2 | 22.30 |
| | 3 | 297.37 | 346.73 | 49.36 | 16.6 | 27.06 |
| | 2 | 353.53 | 431.06 | 77.53 | 21.9 | 28.17 |
| | 1 | 409.84 | 521.92 | 112.08 | 27.3 | 34.55 |
| 2 | 2 | 341.36 | 372.98 | 31.62 | 9.3 | 31.62 |
| | 1 | 397.47 | 470.64 | 73.17 | 18.4 | 41.55 |

Table 4.4. Thermal Expansion Effects on Column Line 2

| THERMAL RESTRAINT FORCES AT BASE | | | | | | |
|----------------------------------|--------|--------|--------|-------|--------|-------|
| No. of Floors | 30 | 60 | 90 | 120 | 150 | 180 |
| 2 | 36.34 | 78.17 | 46.58 | 17.41 | 13.63 | 11.14 |
| 4 | 60.42 | 112.08 | 57.47 | 26.17 | 23.20 | 19.08 |
| 8 | 81.71 | 146.45 | 66.77 | 34.43 | 35.10 | 27.39 |
| RESTRAINT EQUATION VALUES | | | | | | |
| S(T) | 22.685 | 36.64 | 10.095 | 8.51 | 10.735 | 8.125 |
| B(T) | 13.655 | 36.53 | 36.485 | 8.90 | 2.895 | 3.015 |

Table 4.5 Thermal Restraint Force at Column Base 2

Table 4.5, where for each duration of exposure, the thermal restraint force on the lower interior column (column 2) is listed. The increase in the restraint force must follow a curve of decreasing slope as the number of floors is increased. This suggests a logarithmic function as follows:

$$R = B(T) + S(T) \log_a (n) \quad 4,12$$

R - restraint force on lower column
 a - base of log function
 n - number of floors
 S(T) - shear transfer/floor
 B(T) - a constant

This equation is unique for every building and is dependent upon the frame stiffness, the frame loadings, mechanical and thermal properties of the materials and the length of fire exposure. This equation would be impossible to evaluate by any simple analytical method and hence, requires the computer analysis as performed in this investigation. If the base of the logarithmic function is taken as 2, then the restraint equation for time equal to sixty minutes becomes:

$$R = 36.53 + 36.64 \log_2 (n)$$

The values of the restraint equation for a log base of 2 for other times are shown in the lower half of Table 4.5. Although it is possible to arrive at a restraint equation of the type shown after a computer analysis for particular conditions, it is not possible to determine a similar equation for other conditions without performing the same type of analyses. At present, there does not seem to be any accurate method to

suggest in trying to simplify design procedures.

It is evident that position of the member in the frame has an effect on the restraining force. The exterior column in these studies, although exposed to fire, showed no increase in axial load due to restraint. The expansion of the interior column next to it, cancelled any restraint caused by the floor.

4.6 (d) Deflection of Fire Exposed Columns

With thermal expansion excluded, the axial deflections of the lower columns increased in the direction of the applied load. With expansion, the vertical deflection of the lower columns moved opposite to the applied loads. This characteristic is shown in Table 4.6. The fire exposed exterior column has little restraint and hence, tends to elongate freely. The interior fire exposed column is more heavily restrained and cannot elongate as freely. This results in the increased axial force. The other unexposed interior column is pulled up by the restrained exposed interior column. At some point, the increased axial load due to restraining forces and the "softening" of the material due to fire exposure combine to cause the EA value to begin to decline. This in turn causes a gradual return to net downward deflections.

4.7 Summary

In this chapter, a method for analyzing reinforced concrete frames subjected to fire exposure has been described and results of a few analyses have been discussed. To the author's knowledge, this type of analysis has not been attempted or reported

| | | VERTICAL DEFLECTION AT TOP OF BASE COLUMNS WITH EXPANSION | | | | | | |
|----------------|--------|---|--------|--------|--------|--------|--------|--------|
| No. of Columns | Column | 0 | 30 | 60 | 90 | 120 | 150 | 180 |
| 8 | 1 | -.0214 | 0.1098 | 0.2847 | 0.3614 | 0.1602 | 0.0181 | -.0049 |
| | 2 | -.0307 | 0.0669 | 0.1583 | 0.0981 | 0.0313 | 0.0060 | -.0054 |
| | 3 | -.0258 | -.0197 | -.0144 | -.0193 | -.0226 | -.0234 | -.0240 |
| | 4 | -.0203 | -.0212 | -.0221 | -.0219 | -.0211 | -.0206 | -.0205 |
| 4 | 1 | -.0210 | 0.1107 | 0.2855 | 0.3687 | 0.1776 | 0.0185 | -.0004 |
| | 2 | -.0304 | 0.0734 | 0.1746 | 0.1120 | 0.0354 | 0.0043 | -.0055 |
| | 3 | -.0262 | -.0218 | -.0178 | -.0213 | -.0233 | -.0246 | -.0250 |
| | 4 | -.0205 | -.0211 | -.0217 | -.0215 | -.0210 | -.0207 | -.0206 |
| 2 | 1 | -.0208 | 0.1108 | 0.2851 | 0.3724 | -.1873 | 0.0184 | -.0045 |
| | 2 | -.0298 | 0.0800 | 0.2015 | 0.1473 | 0.0420 | 0.0052 | -.0050 |
| | 3 | -.0271 | -.0244 | -.0217 | -.0234 | -.0257 | -.0262 | -.0264 |
| | 4 | -.0207 | -.0210 | -.0214 | -.0212 | -.0209 | -.0208 | -.0207 |

Table 4.6 Vertical Deflection at Top of Lower Column 2

elsewhere. It is suggested that progress in understanding the behaviour of structures exposed to fire will be greatly facilitated by use of and further development of the analytical methods developed in this investigation.

Two features are important in the analysis of reinforced concrete rigid frames, one beneficial and the other detrimental. Since a frame has continuity, when one portion of it weakens, the remainder of the frame takes up the load that is on the weakening member. This redistribution of load allows a member exposed to fire to prolong its endurance. However, any member exposed to fire is going to expand. Depending on the restraining stiffness of the remainder of the frame, the force in the expanding member will vary from zero force to a very large compressive force. Any increase in axial force could be beneficial to a beam due to the typical P - BM interaction, however, increases in column axial load may precipitate failure. Even as a reinforced concrete member starts to fail, it loses some stiffness resulting in lower forces due to redistribution. Differential expansions due to non-uniform heating of parts of a rigid frame are more serious than uniform heating of the entire frame. It should be noted that thermal expansion forces vary directly with the cross section size of the member. Therefore, if a member is larger than it is required to be, the member will develop a large thermal force. This force will be out of proportion to the design load on the member. Analysis of concrete members as part of a frame is required in order that proper values for fire endurance can be assigned to the frame.

Chapter 5

CONCLUSIONS AND RECOMMENDATIONS5.1 Conclusions

The following conclusions have been based on the investigation carried out in this report:

- (1) Concrete and steel high temperature behaviour has been sufficiently investigated by others (1,2,5,8,9,18,19) to enable structural analysis of columns and frames. Tests performed for this present study have verified the high temperature material behaviour. These tests have also shown to the author, the difficulties associated with testing at high temperatures.
- (2) Structural adequacy of reinforced concrete columns is mainly dependent on the method of support and depth of concrete cover. If the member is simply supported, assuring no axial restraint, then cover is the most critical factor in determining fire endurance, with cross section size, percent of steel, slenderness ratio and steel placement having lesser effects.
- (3) The ability of columns in frames to support the structure is dependent on the restraining effect of the structure, the loading combinations and the portion exposed to fire. In many cases, moments in exposed columns decrease, thereby increasing the axial load capacity. However, expansion causes substantial increases in axial load on some exposed columns which increases the likelihood of failure.

fire endurance of reinforced concrete structures. With this program it is possible to analyze the frame for both gravity and fire loads. Small revisions to the program would allow analysis that includes secondary bending effects and creep in the structure.

5.2 Recommendations

Much more research is required to better define the effect of fire exposure on the material properties. Although the temperature effect on the strengths of concrete and steel have been widely investigated, further research is required in areas related to deformation, such as creep, shrinkage and reduction of elastic moduli. The process of spalling should be analyzed to determine the reasons for its occurrence and the proper corrective measures to prevent its occurrence. Studies should be undertaken to determine if the concrete and steel maintain sufficient bond for shear transfer between each other at high temperatures. With better understanding of these properties, the computer program could be revised to include their effects.

Pinned end column analysis is useful in the study of how changes in design parameters affect the fire endurance. However, it is the author's opinion that analyses or standard tests⁽³⁾ of individual columns exposed to fire can only provide an approximate and not necessarily safe estimate of the effect of fire. Design provisions must be based on consideration of the behaviour of columns in structures.

References

1. Abrams, M.S. "Compressive Strength of Concrete at Temperatures to 1600°F", Temperature and Concrete, ACI Publication Sp 25. 1968. pp.33-58.
2. Abrams, M.S. and A.H. Gustaferro. "Fire Endurance of Concrete Slabs as Influenced by Thickness, Aggregate Type and Moisture", Journal of the PCA Research and Development Laboratories, Vol.10, No.2. May 1968. pp.9-24. PCA Bulletin 223.
3. ASTM. "Standard Methods of Fire Tests of Building Construction and Materials", American Society for Testing and Materials, ASTM E119-71. 1971.
4. Clarke, J.H. "Method of Assessing Probable Fire Endurance of Load-Bearing Columns", Journal, American Concrete Institute, Vol.56. 1960. pp.1223-1242.
5. Cruz, C.R. "Apparatus for Measuring Creep of Concrete at High Temperatures", Journal of the PCA Research and Development Laboratories, Vol.10, No.3. 1968. pp.36-42.
6. Drysdale, R.G. "The Behaviour of Slender Reinforced Concrete Columns Subjected to Sustained Biaxial Bending", Ph.D. Thesis, University of Toronto. 1967.
7. Gustaferro, A.H. "Factors Influencing the Fire Resistance of Concrete", Fire Technology, Vol.2 No.3. August 1966. pp.187-195.
8. Harmathy, T.Z. "Determining the Temperature History of Concrete Constructions Following Fire Exposure", Journal ACI, Vol.65 No.11. November 1968. (NRC 10429).
9. Harmathy, T.Z. and J.E. Berndt. "Hydrated Portland Cement and Lightweight Concrete at Elevated Temperatures". ACI Proceedings, Vol.63 No.1. January 1966.
10. Harmathy, T.Z. and W.W. Stanzak. "Elevated Temperature Tensile and Creep Properties of Some Structural and Prestressing Steels", ASTM, Special Technical Pub. 464. 1970. (NRC11163).
11. Lankard, D.L. et al. "Effects of Moisture Content on the Structural Properties of Portland Cement Concrete Exposed to Temperatures up to 500°F", Temperature and Concrete, ACI Pub. Sp.25. 1968. pp.59-102.
12. Lie, T.T. and D.E. Allen. "Concrete Temperatures and Properties", Private Communication, National Research Council of Canada. March 1972.

13. Lie, T.T. "Fire and Buildings", London, Applied Science Publishers Ltd. 1972.
14. Lie, T.T. and D.E. Allen. "Calculations of the Fire Resistance of Reinforced Concrete columns:", National Research Council of Canada, Division of Building Research. NRCC 12797. August 1972.
15. Lie, T.T. and W.W. Stanzak. "Fire resistance of Protected Steel Columns", Transactions of the Canadian Society for Civil Engineering, EIC Vol.17 No.A-2, in the Engineering Journal. May/June 1974.
16. Tan, K.B. "On Short-Term and Sustained-Load Analysis of Concrete Frames", M.Eng. Thesis, McMaster University. 1972.
17. Vickers, E.F. and R.G. Drysdale. "Effect of Fire on the Capacity of Reinforced Concrete Columns", Symposium on Design and Safety of Reinforced Concrete Compression Members, International Association for Bridge and Steel Engineering, Quebec. August 1974. pp.227-234.
18. Wang, C.H. "Creep of Concrete at Elevated Temperatures", Creep, Shrinkage, Temperature in Concrete Structures, ACI Sp.27. 1971. pp.387-400.
19. Zoldners, N.G. "Thermal Properties of Concrete Under Sustained Elevated Temperatures", Temperature and Concrete, ACI Pub. Sp.25. 1968. pp.1-31.

Appendix A

COMPUTER PROGRAM FOR FIRE ENDURANCE

A.1 Introduction

The analyses for the behaviour of cross sections, columns and frames have been merged to form one program. Since there is a great deal of duplication between the calculations for each type of analysis, it was decided to develop a comprehensive program to handle all cases. One advantage in using a combined program is that the subroutine for calculating equivalent EA and EI values for the frame can be used to determine a very good set of initial values for axial load, bending moment, strains and curvature when an interaction diagram for section or column behaviour is being computed. Subroutines that are not required for a particular study can be simply removed from the computer deck.

A.2 Program FIRE

This is the driving program which is used to input the section dimensions, the material properties and the code numbers which are used for direction to the parts of the program being used. The input variables are listed on the comment cards at the start of the program. The dimensions of variables input in this part of the program are in inches for length measurements and in kips per square inch (ksi) for material properties.

A.3 Subroutine TEMPER

Subroutine TEMPER is used to calculate the temperature dependent properties of each element on the cross section. The

temperature gradient over the cross section is input at the midpoints of the square elements. The temperature values supplied by the National Research Council are in degrees Rankine and require conversion to thousands of degrees Celsius. Since the temperature gradient is symmetric for a square section heated on all four sides, it is necessary to enter only one eighth of the values over a "pie-shaped" wedge, reducing the keypunching required and also the possibility of mistaken input. Since all loadings on the cross section have been assumed to be uniaxial causing stresses and strains symmetrical about a line perpendicular to the loading axis passing through the area centroid, then the temperature properties are required for only one half of the total cross section. The reduction factor for concrete strength and if required, the values for concrete thermal expansion and for increased concrete failure strain are calculated using the equations noted in section 2.6.

The temperature in the steel reinforcing must be approximated using the available concrete temperature gradients. The location of the steel is defined at initial input in program FIRE. The three closest points on the temperature gradient to the steel location are used to form a plane surface approximating the curved temperature gradient. The temperature in the steel is defined where a perpendicular line from the steel location pierces this plane. This method is slightly conservative but it eliminates the need for the very lengthy process of calculating the temperature by finite elements techniques. (see figure A.1) It has been assumed that the steel will not act as a heat sink thereby attracting a large amount of heat to its particular

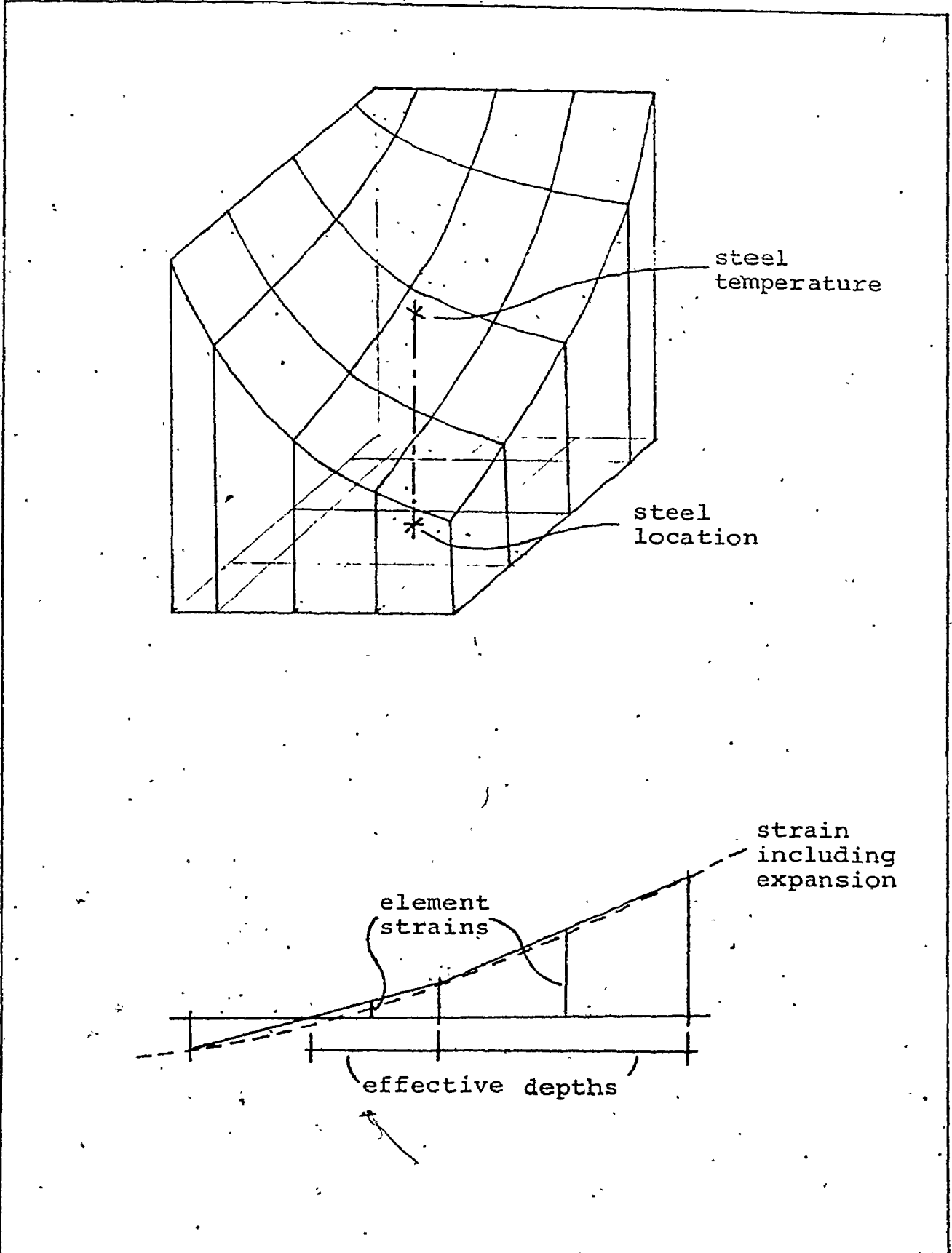
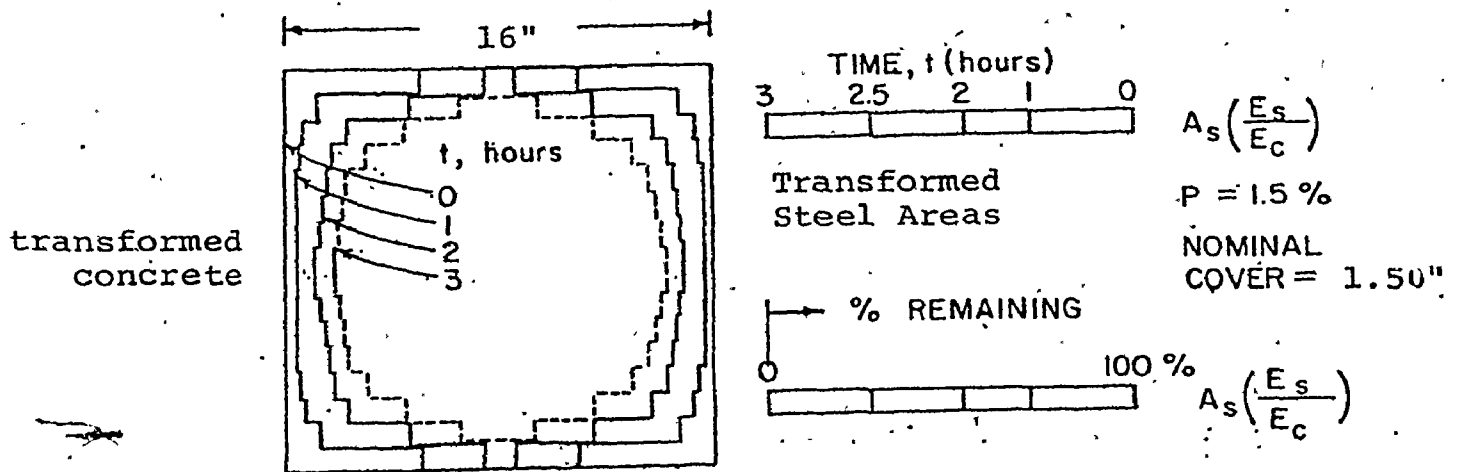


Figure A.1

Calculations For Subroutine ITERATE

position and thus distorting the uniformly varying temperature gradient in the concrete. Once the steel temperature is known, then all of its temperature properties can be calculated using equations from section 2.6.

If the effects of thermal expansion and elongation of the strain axis of the stress-strain curve are to be ignored, then only the strength reduction factors for the concrete need to be calculated. Since these strength reduction factors are symmetrical over the cross section, then an effective reduced area or reduced width can be defined such that the reduced magnitude of strength of concrete multiplied by the full area equals the unreduced strength of concrete multiplied by the reduced area, for a given strain. For this case, the cross section is treated as a series of strips parallel to the axis of bending. A summation of the strength reduction factors for each element is carried out across these strips to arrive at a factor of reduced strength or reduced area for each strip. This is possible only when thermal expansion effects are neglected. This subroutine is entered each time that the duration of fire exposure is increased. (see figure, A:2)



A.4 Subroutine ITERATE

The basis of the whole program is the ability to force the internal strains to change in a reliable fashion in order that the internal and external forces can be brought into equilibrium. There are two major problems to overcome in the balancing of the strain pattern. First, there is a problem with the materials comprising the cross section. Steel is linear elastic and hence, corrections to the strain pattern would be a single step requiring no further iteration. The major problem is the concrete itself. The material is non-linear and also has been assumed to possess no tensile strength. Due to the composite action of the two materials, it is obvious that axial load and bending moments are functions of the strain magnitude and of the curvature. This was illustrated graphically in Chapter 4 figures 4.2 and 4.3. Small changes to the magnitude or curvature of the strains will affect both axial bending forces and not just the respective individual force as would occur for an elastic cross section.

The second problem involves the financial consideration of maintaining a realistic usage of computer time. The use of either strips or small squares in the computation of internal forces requires a large number of calculations for each iteration cycle. With the case of strips (which corresponds to ignoring thermal expansion), there are $(n + m)$ calculations required for each cycle. The variable n is the number of strips which represents the number of times that the stress-strain polynomial must be evaluated and the resulting element forces totalled. The variable m represents a basic set of calculations also required with each cycle; m is much less than n . However, when the inclusion

of thermal expansion is necessitated, then the number of calculations will be $(n^2/2 + m)$ which is a substantial increase. A larger number of cycles of iteration are also required for this second case due to the non-uniformity of the stresses. Limitations of money and of user computer time forced a reduction in the number of cross section elements to a minimum at a possible sacrifice to accuracy.

In early work involving integrating the cross section capacity numerically, the calculations were performed to obtain axial capacity then a check was made to compare this force with the required force. Finally, a change was made to the strain magnitude. The same procedure was followed for bending moment, resulting in a change to the curvature. ⁽⁶⁾ This method requires a cycle of calculations of internal forces for a given strain distribution for both load and moment. Since the changes to strain are made independently for load and moment without consideration of the effect on the other, there is a strong probability of cycling about the desired pair of strain parameters. With this problem in mind, further work was done on a method of improving convergence. This consisted of extending the Newton-Raphson method to the use of two independent variables. Changes to the magnitude and curvature of the strain distribution were made simultaneously, hence cycling was reduced. ⁽¹⁶⁾ However, there is now a cycle of force integration required to obtain the forces and one cycle each to obtain the differentials of the forces due to a small change in strain magnitude or curvature. Although this method may reduce the number of cycles required to obtain convergence of stresses and strains, unfortunately,

it requires that three lengthy force summations for each cycle of iteration be performed. One summation is for calculating the total forces and two summations for the differentials of these forces. The accuracy of both of the above programs would suffer greatly if the number of strips or squares were reduced below an established minimum. Many steps have been taken in the present program to reduce time requirements, to increase the accuracy of numerical integration and to improve the convergence process.

A large time saver is achieved by performing the calculations for internal axial and bending forces at the same time. The individual element forces are totalled to arrive at the internal axial force at the same time as the first moment of each individual force is taken about the gross concrete centroid to arrive at the internal bending moment force. Error bounds are then found for each force.

Due to the method of calculating EA and EI using the section properties directly, it became necessary to develop a more accurate method of integration to determine section properties as well as forces. It should be noted that the integration process is usually based on the finite area of a strip or square and on using the strain at the centre of this element to determine the element force. This is basically sound for force calculations when the stress goes to zero as the strain goes to zero. However, to determine section properties, it should be noted that EA or EI values for a given element go to a maximum for concrete as the strain approaches zero. This fact aggravates the accuracy of the convergence process for frame analysis since, for some element areas, the values for EA and EI can switch from

maximum to zero with only the slightest change in the strain at the element centre.

In the present program, failure of the section is taken to be failure to reach convergence. This definition allows the extreme compression fibre strain to go beyond the usually limiting strain of concrete crushing, $\epsilon_{c \max}$. This factor also causes convergence problems for the force calculations since the element force can now switch from a high value to zero for a small strain pattern change. The effect on EA and EI values is less than the case of zero strain since E is not a maximum at high strains. Added to the previous two considerations is the problem of non-linearity of total strains (contact strains) due to the high thermal expansion strains involved. These thermal strains can result in only a very small area of the total cross section remaining effective due to crushing on the outer layers and tension at the core.

From consideration of the above, it was apparent that using mid-element strains and total element areas would result in using a very large number of elements if convergence was to be obtained. However, the number of elements that could be used was limited already by the available temperature information. Therefore, a different method of element integration was developed based on the strains at the element edges instead of the centroid.

In the subroutine TEMPER, the thermal expansion strains were calculated at the edges of each element using an interpolated value for the temperature. Now when the integration process is performed, the strains due to the external loads are found at the edges of the element and added to the thermal strains. The

two strains are taken to represent two points on the assumed linear strain distribution between the two element edges. The actual effective depth of the element can be found, as well as the effective strain (contact strain) as shown in Figure A.1. Referring to Figure A.3, it can be seen that the forces and EA values are close to the actual values. No attempt was made to find the position of the resultant (centroid of EA) for each element because with small elements, the increased complexity was unwarranted because of the small effect on accuracy. With this refinement, element force and section property calculations will vary uniformly from a maximum to zero as the effective element depth is reduced, adding to the accuracy without the need for many more elements. On each cycle of iteration the effects of the steel reinforcing are calculated and added to the concrete effects. The actual steel contribution to the force or section property calculation was reduced by the effect of the area of concrete that was displaced by the steel. For concrete of 4 ksi maximum strength, steel of 60 ksi yield and a percentage of steel over gross concrete area of 3.5%, the exclusion of the adjustment for displaced concrete would result in an error of 2.3% for axial force calculations. This was considered an unacceptable error when convergence is set at only 1%.

Iteration to converge to a force and strain combination that is close to zero is very time consuming. The possibility of there being no eccentricity on a cross section is remote especially with considerations such as workmanship or material variability. Therefore, a minimum value of bending moment was assumed, that was based on the section properties. The minimum

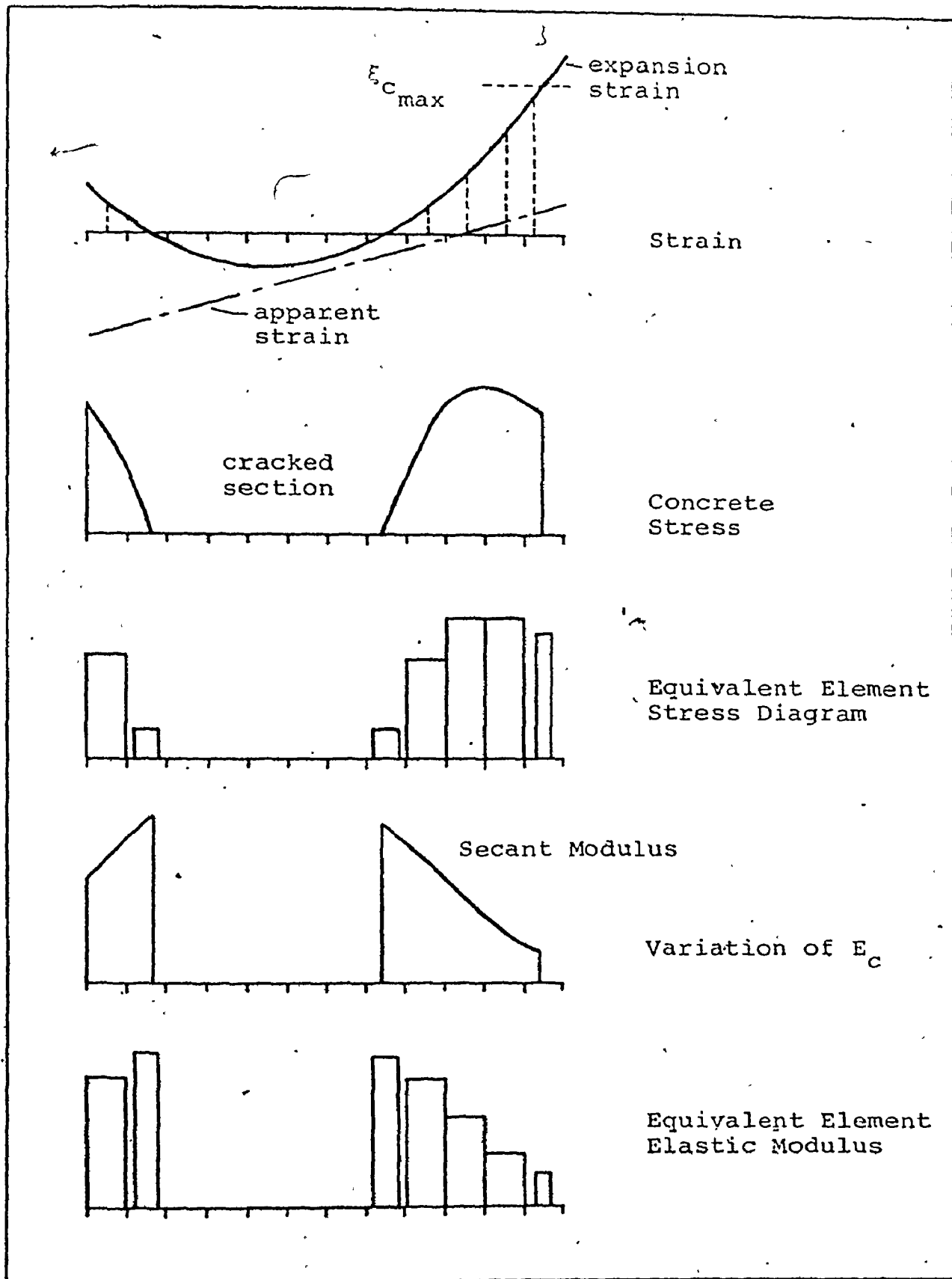


Figure A.3 Calculation Procedures for Stress and E

bending was taken as 1% of the gross concrete section modulus multiplied by the allowable concrete stress. This applies to structural analysis only and not to P vs M interaction diagrams.

In the case of axial load, a different method was followed when the load fell below certain limits. Whenever the total steel effect was tensile, the usual balancing of internal axial force with external axial force was not followed. Instead, the internal concrete axial force was balanced against the applied external axial force, which could equal zero, less the tensile force of the steel. This step always allowed easy convergence of the axial load especially for very high eccentricities.

The convergence process has two main parts. The first method of convergence is just a direct search for those strains which produce internal forces compatible with the outside forces. The calculated error bounds are used to determine the step size for the strains. There are maximum and minimum step sizes allowed. When and if the direct search method finally oversteps the desired strains and hence, the forces, the convergence process switches to a bisection method. Methods such as Newton-Raphson or Regula-falsi of which bisection is a sub group, were not used in finding the general area of feasibility of the solution strains since they have a tendency to over-project when moving to the new point. Near failure of the section, this over-projection can cause premature prediction of failure. Bisection was chosen over Newton-Raphson for the final convergence process because bisection has a higher Effectivity Index, Q . Newton-Raphson has a higher convergence power, $a = 2$ (quadratic)

compared to $a = 1.62$ for bisection. However, many more evaluations, v , of the forces and derivatives are required for the Newton-Raphson method. In this case, three are required compared to only one for bisection for each cycle of iteration.. The Effectivity Index, defined as:

$$Q = a^{\frac{1}{v}}$$

which gives $Q = 1.62$ for bisection and

$$Q = 1.26 \text{ for Newton-Raphson}$$

is strongly in favour of bisection. Although the bisection method has more ancillary calculations associated with each cycle of force determination, these extra calculations are small in number compared to the number required for each cycle of force determination.

Bisection is carried out to obtain the independent corrections to the magnitude and curvature of strain based on the error in the axial force and bending moment respectively. Since these variables are interdependent, a limitation on the number of consecutive cycles of bisection is imposed to prevent the process from hanging up on a false point.

The corrections to the magnitude and curvature of strain are added to the extreme fibre strains after they have been duly weighted to reduce any cyclic problems. The weighting ratio of corrections for curvature to axial strain was determined to be 4:3 by a number of trial runs. It was noted that after concrete tension cracks appeared due to high bending moments, convergence was aided by forcing a curvature change on the tension strain that was double that forced on the compression strain.

This is due to the movement of the centroid of the transformed area. Even when there was no change required to one of the strain parameters, due to convergence of its respective force, a weight factor of 1 was still added to the total weighting factor to reduce the magnitude of the change in strain due to the variation of the remaining force. This caused the actual strains to asymptotically approach the required strains and not cycle about the set of strains.

AS mentioned, failure is defined as the inability to converge. For a safeguard against cyclic iterations, the tolerance level for convergence is doubled after 75% of the stated maximum number of iterations has been reached. If the iteration process is going to converge, it usually will very rapidly. Otherwise divergence usually occurs very rapidly. It is only the cyclic problem sometimes associated with small error tolerances which require the larger error bounds.

A.5 Subroutine STIFF

The equivalent elastic section properties for the cross section are calculated following the method discussed in section 4.2. The method of calculation is similar to that used in computing the forces in subroutine ITERATE. Once the element force is found, it is divided by the total effective strain which has been referred to as the "contact strain". (see section 4.2)

Force divided by contact strain, defines the secant modulus multiplied by the effective area for that element. The axial section property of all elements is summed. Also summations of the first and second area moments of all the transformed
ted at the gross concrete centroid.

The effects of steel less the displaced concrete are also added to the totals.

The distance to the elastic centroid is defined by the quotient of the sum of the first moment of the transformed areas divided by the sum of the transformed areas. The sum of the second moment of the transformed areas can now be transposed to the elastic centroid where it will be at its minimum value.

With this method it is possible to obtain EA and EI values for any strain pattern including the case in which the section has yielded. It is also possible to obtain the transformed section properties even for the cases of zero, axial load or bending moment forces. This is not possible for methods based simply on the total internal forces and the strain pattern.

To obtain the thermal expansion force in the cross section, the smaller of either the thermal expansion strain or the net contact strain is multiplied by the transformed axial section property for each element. It is this thermal expansion force which causes additional deformation of the frame.

A.6 Structural Analysis Subroutines

A.6.a Subroutine COLUMN

Short or slender pinned end columns can be analyzed using subroutine COLUMN to establish the effect of increasing exposure to fire. With a predetermined column cross section input in program FIRE and with column length to thickness ratio input, the maximum axial loads for an input set of load eccentricities can be found. The effect of secondary bending moments in the reduction of axial load capacity due to the P- Δ effect is considered for columns with a finite length. The program can be used to study the effect of eccentricity of load or enough eccentricities

to be useful in sketching an axial load-bending moment interaction diagram. Although zero axial load cannot be input, it is possible to use a very large eccentricity to represent pure bending. Zero axial load is not allowed for in this subroutine because the bending moment is related to the axial load by using the eccentricity as a multiplier, thus, if axial load was zero, the bending moment would be found to be zero also.

To converge quickly to the maximum axial load, it is important to have a feasible starting point below the actual maximum. This initial starting point is found by assuming two values for extreme fibre strains and substituting these strains in subroutine STIFF to obtain a set of transformed section properties. These transformed section properties are used in equation A.2 to obtain an allowable axial load for the specified eccentricity.

$$P = \frac{0.004}{\left(\frac{1.0}{EA|e|} + \frac{t}{2EI}\right)} / e * ((3 + \frac{|e|}{4}))$$

A.2

$|e|$ - absolute value of eccentricity

The first portion of equation A.2 is based on elastic analysis. The second portion of the equation is a reduction factor used when the eccentricity is negative. A negative value for axial load is possible but bending moment is always positive.

If there is no convergence for the first estimate for the axial load it is reduced in magnitude until convergence will occur. At some high temperatures convergence may not be possible

obtained, a direct search method with expanding step size is used to increase the axial load. The current feasible set of parameters, loads and strains is stored by use of subroutine VALID. When an invalid point is attempted after an increase in axial load, the program reverts to the last feasible set of parameters stored in subroutine VALID. The step size is reduced and a further attempt is made to increase the axial load. This process can continue until the step size is less than the required accuracy. Then the maximum axial load point is assumed to have been reached.

When the column length is not zero, each increase to the axial load is followed by an analysis of the secondary bending effects. The deflection at the mid-height for the simple column is based on the curvature of each subsection along the column length. The end rotation of the column is determined. Using the tangent established at the column base, a projection from subsection to subsection is carried out. The tangent is adjusted at each subsection due to the curvature. The deflection at each subsection and at the mid-height is found. The axial load and corresponding increased bending moment are checked to determine whether equilibrium can be reached for the axial load.

When column length effects are not considered, the maximum axial load is determined by failure to obtain load convergence for any set of strain parameters. When length effects are considered, the previously stated failure criterion or the divergence for the calculation of the deflection at mid-span will define failure.

When the ratio of load eccentricity to column depth is small,

it is necessary to decrease the size of the error bound to ensure that buckling of the column will occur at very nearly the correct load. False points indicating greater column strength than is actually available could occur if the error bound on deflection is not adjusted.

A.6 (b) Subroutine FRAME

Subroutine FRAME can be used to analyze a rigid frame which has a number of its members defined as inelastic. At this stage of development of the program, the entire inelastic frame or the inelastic portion of the total frame is subjected to the same fire exposure. The cross section for all inelastic members is assumed to be identical and is input through program FIRE.

One of the most efficient methods of matrix structural analysis uses a banded stiffness matrix with the Choleski method of solution. However, this requires care in the joint numbering which may have proven restrictive for this study. It was desirable to be able to choose the inelastic structural members at random anywhere in the frame. In addition, to improve the accuracy of the analysis, each inelastic member (column or beam) is divided into a number of sub-members. The sub-members at the ends of the inelastic member are smaller in size. This is done to reduce the effect of the calculation for deformations due to the external forces being performed at the mid-length and not at the ends of members. This method of division of the inelastic members would have made systematic joint numbering difficult if different members in the same frame were chosen as inelastic for separate computer analyses. Using a standard

method of solution for simultaneous equations allows repeated use of a single set of data cards. The input requirements for this subroutine are similar to most other matrix analysis programs. A detailed sketch, as shown in Figure A.4, indicating all joint and member numbering is required.

The three global forces are input on only the loaded joints. Inputting only loaded joints allows for more flexibility for changes to the load pattern. The input load values are calculated to represent a standard floor loading with all forces and moments in the correct ratio to each other. The load values are in kips/foot and in inch-kips/foot. The input values are converted to kips and inch-kips by means of a parameter representing the frame bay spacing in feet. The loads on the loaded joints are placed in their correct locations in the external load vector. The use of the bay spacing variable allows different load intensities with no change to the input load data.

The member information for the inelastic members are input first. The inelastic sub-members can be in any order but systematic input aids the understanding of the results. The first input variable is the member or sub-member identification number. Following this number is a displacement vector representing the position of the second joint relative to the first joint of the member. This vector is in global directions and is in foot units. For a rectangular frame, this joint displacement vector represents the column or floor spacing, a simple form of input requiring only two numbers. This method was used because standard joint coordinates based on the global require a great deal of calculation and additional input.

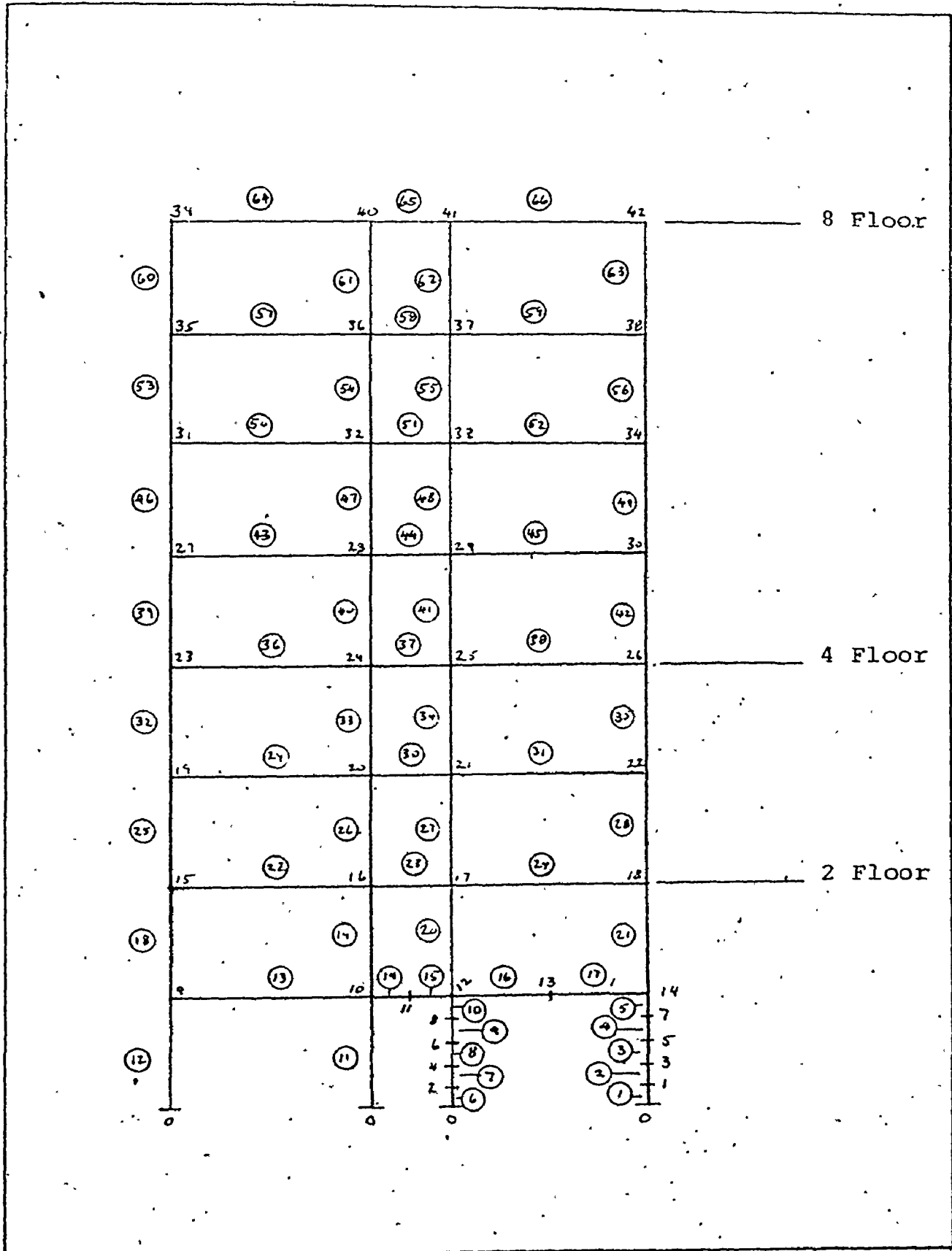


Figure A.4 Joint and Member Numbering

Note: Member end one is always the smaller joint number and is always the origin for the displacement vector.

For inelastic members only, a pair of extreme fibre strains are input. These strains should be estimated so that the magnitude and curvature will be similar to the expected strains. That is, if the moment is large, the curvature should be large also and vice-versa. If the axial force is large, then both extreme fibre strains should indicate compression. However, if the axial load is small and the moment is high, then the strain on the tension fibre will be negative.

The transformed axial and flexural section properties are input in kips and in inches²-kips as equal for all members. As each member is input, the transfer matrix relating global and member coordinates is calculated using subroutine TRANSF.

With all input complete, the study of the effects of temperature exposure on the frame is begun. The first temperature must always be zero time, that is, no fire applied, in order that the initial member section properties can be correctly calculated for all of the inelastic and elastic members. At the end of each cycle, for zero time only, the average section properties over all of the inelastic sub-members are found. The section properties of each sub-member is found by using STIFF. The average section property is used for all members that are not exposed to fire and hence, are assumed to remain elastic. When the frame has reached convergence for zero time, the section properties of all elastic members are set as constants for the remaining fire exposure. It should be noted that as long as the case of zero fire exposure is run first, as it must be, then

the remaining fire exposures can be run in any order with convergence to the identical results within the allowable error bounds. Although order of exposure is not important, convergence will be obtained faster if the exposures are applied in increasing time.

When the effects of thermal expansion and concrete softening are neglected, then the iteration cycles are simple. With the section properties calculated for each member, a structural analysis is performed to obtain the member axial and bending forces. These forces are calculated at the member ends, hence, the average of these forces is used to obtain fibre strains which are assumed to be uniform along the member. These strains are used by subroutine STIFF to obtain new approximations to the inelastic member section properties. With new section properties, a new structural analysis is performed. This cycle is repeated until convergence of both axial and flexural section properties is found. A simple weighting procedure is again used to prevent fluctuations. Convergence to a set of section properties is required for this program. Failure is defined by inability of internal and external forces to reach equilibrium. After convergence, the time of exposure is increased.

If the forces from the preceding converged state are used directly for the first iterative cycle after temperature increase, then a false failure may be predicted. It is noted that as the fire progresses, the affected member section properties will decrease. Associated with this decrease is usually a corresponding decrease in actual member bending force. Therefore, it is ~~adv~~ to use the strains from the preceding converged

state with the new thermal properties to obtain a new set of section properties. These new section properties are then used for the first frame analysis following increased exposure to fire. This aspect points out another advantage in calculating EI and EA values using the section geometry coupled with strains rather than simply using the total forces with the strains. With the latter, new strains and forces can only be obtained after a new frame analysis has been carried out. If the forces have not been adjusted from the previous converged state, a false failure could be predicted whereas the structure would actually have sufficient strength due to load redistribution.

The problem of thermal expansion causes new loads to be applied to the frame. As the fire progresses, the concrete and steel tend to expand greatly. For the pinned end column program free expansion was allowed because there was no additional restraint. However, for a rigid frame, there is a large resistance to the expansion of any single member due to adjacent member stiffnesses. The thermal restraint force is calculated for each inelastic sub-member in subroutine STIFF. The reverse of this restraint force is applied to the frame causing the deflection and the force redistribution that would be associated with the expanding member. However, as far as the expanding member is concerned, the restraint force is pushing along its axis. Therefore, to the final results of the structural analysis, a force equal but opposite to the restraint force must be added to the forces in the inelastic sub-member. With each cycle of structural analysis, new restraints are calculated and applied to the frame.

Convergence is defined when all axial and flexural section properties of the frame have converged to within the specified error tolerance. The axial and bending forces are not checked since they are a function of the frame section properties. When the frame section properties reach a convergent point, they no longer change and the forces from the frame analysis cannot change. As a general rule, the effect of a change in the member section properties on member forces will be much smaller than the change in the section properties. It has been found that after the first cycle of iteration, only a few members will still have varying section properties.

A.6 (c) Subroutine RIGID

Subroutine RIGID performs the actual structural analysis for a vector of load values and a set of member stiffnesses. The subroutine assembles the general frame stiffness matrix making use of the subroutine GLOBAL which transforms the member stiffness matrix from member coordinates into global coordinates.

Once the frame stiffness matrix has been formed, the solution to find joint global displacements is performed using the McMaster Computer Centre library subroutine SIMQ. After these global displacements have been transformed into member joint displacements, member forces can be found using the individual member stiffness matrices. After the effects of any thermal restraint forces have been added to the member forces, a full listing of the deflections and member forces is printed, if desired. The average forces in each inelastic sub-member are calculated and then transferred to the calling routine FRAME

for subsequent equilibrium checks.

No attempt has been made to study the effects of secondary bending moments due to the P- Δ effect in FRAMES. For the relatively short columns used in this study of frames this omission will not cause significant error.

A.7 Program Listing

The computer program is listed on the following pages. The subroutines are listed in the order that they were first mentioned in the preceding sections. As mentioned on the comment cards in program FIRE the subroutines not required for the structure being analyzed may be removed from the card deck.


```

24, ITER, NTEMP, IPRINT
COMMON /BLOCK2/ T(3,3,66), DIST(66), SF(6,6), FI(66), FA(66), STF11(3,3
1,66), STF12(3,3,66), STF21(3,3,66), STF22(3,3,66)
COMMON /BLOCK3/ PDD(126), IFORM(66), ITD(66), DF(10), SYF(10), PT(10), U
IN(10), UP(10)

```

```

PRINT 120
PRINT 160
PRINT 40
PRINT 160
READ 60, X,Y,FC,FS,FD,ETAII, TOLCD
READ 60, NX,NY,NSTL,ITER,IPRINT,ITHERM,NTEMP
PRINT 70, X,Y,NX,NY,FC,FS,FD,ETAII

```

```
DX=X/NX
```

```
DY=Y/NY
```

```
X2=X/2.0
```

```
Y2=Y/2.0
```

```
ACONC=2*DX*DY*FC
```

```
PRINT 80
```

```
DO 10 I=1,NSTL
```

```
READ 50, (STL(I,J),J=1,3)
```

```
PRINT 90, (STL(I,J),J=1,3)
```

```
STL(I,0)=STL(I,2)-Y2
```

```
STL(I,1)=STL(I,1)/X
```

```
STL(I,2)=STL(I,2)/Y
```

```
CONTINUE
```

```
IF (ITHERM.EQ.0) PRINT 100
```

```
IF (ITHERM.EQ.1) PRINT 110
```

```
N=NX=NX/2
```

```
IF (ITHERM.EQ.0) NX=1
```

```
INPUT AND WRITE ALPHANUMERIC TITLE FIELD
```

```
PRINT 120
```

```
PRINT 160
```

```
READ (5,130) (TITLE(I),I=1,13), ITYPE
```

```
GO TO (20,30), ITYPE
```

```
WRITE (6,140) (TITLE(I),I=1,13)
```

```
PRINT 160
```

```
CALL FRAME
```

```
WRITE (6,150) (TITLE(I),I=1,13)
```

```
PRINT 160
```

```
CALL COLUMN
```

```
STOP
```

```

40 FORMAT (1H0, //, 17X, *A FORTRAN PROGRAM FOR THE ANALYSIS OF REINFORC
IED CONCRETE FRAMES AND COLUMNS*///, 26X, *UNDER THE INFLUENCE OF GRA
2VITY LOADS IN A FIRE ENVIRONMENT*///, 25X, *WRITTEN AS A PORTION OF
3THE THESIS SUBMITTED FOR THE DEGREE*///, 44X, *MASTER OF ENGINEERIN
4G*///, 41X, *BY E. F. VICKERS, B. ENG.*//, 44X, *MCMASTER UNIVERSITY*//, 4
55X, *HAMILTON, CANADA*///)

```

```
50 FORMAT (7F10.0)
```

```
60 FORMAT (7I10)
```

```

70 FORMAT (//5X, *SECTION PROPERTIES*//10X, *MEMBER DIMENSIONS*, F5.1, *
1BY*, F5.1, * (INCHES) DIVIDED INTO*, I3, * BY*, I3, * DIVISIONS*//10X, *C
2ONCRETE STRENGTH*, F5.1, * (KSI)*//10X, *STEEL YIELDS*, F6.1, * (KSI) S
3TEEL IS ELASTO-PLASTIC*//10X, *STEEL ELASTIC MODULUS*, F8.1, * (KSI)*
4RUPTURE STRAIN*, F9.6, * (INCH/INCH)*///)
) AND

```



```

FT(I,J)=0.0
DO 60 I=1,N
  READ 330, (TEMP(I,J),J=1,N)
  DO 30 J=1,N
    T=((TEMP(I,J)-492.0)*A-20.0)/1000.0
    TEMP(I,J)=TEMP(J,I)=T
    IF (ITHERM.EQ.0) GO TO 30
    C=0.002724+0.01276*T
    IF (C.LT.EFAIL) C=EFAIL
30  EU(I,J)=EU(J,I)=C
    IF (ITHERM.EQ.0) GO TO 50
    T=TEMP(I,1)*1.5-TEMP(I,2)/2
    ET(I,1)=(0.008*T+0.006)*T
    FT(I,N+1)=(0.008*TEMP(I,N)+0.006)*TEMP(I,N)
    DO 40 J=2,N
      T=(TEMP(I,J-1)+TEMP(I,J))/2
      ET(I,J)=(0.008*T+0.006)*T
40  CONTINUE
50  DO 60 J=1,N
      NR=NY+1-J
      TEMP(I,NR)=TEMP(I,J)
      FT(I,NR+1)=FT(I,J)
60  EU(I,NR)=EU(I,J)
    PRINT 290
    PRINT 340, ((TEMP(I,J),J=1,N),I=1,N)

CALCULATE STEEL TEMPERATURE PROPERTIES WITH OR WITHOUT
EXPANSION EFFECTS
DO 90 I=1,NSTL
  A=STL(I,1)*X
  B=STL(I,2)*Y
  IF (A.GT.X?) A=X-A
  IF (B.GT.Y?) B=Y-B
  NA=A/DX+0.5
  NR=B/DY+0.5
  A=A/DX-NA+0.5
  B=B/DY-NR+0.5
  IF (NA.GE.N) GO TO 70
  STL(I,5)=(TEMP(NA,NB)*(1-B)+TEMP(NA,NB+1)*B)*(1-A)+(TEMP(NA+1,NB)*
1 (1-B)+TEMP(NA+1,NB+1)*B)*A
  GO TO 80
70  STL(I,5)=TEMP(NA,NR)*(1-B)+TEMP(NA,NR+1)*B
80  STL(I,12)=1.0
  STL(I,10)=STL(I,11)=0.0
  IF (ITHERM.EQ.0) GO TO 90
  STL(I,10)=(0.004*STL(I,5)+0.012)*STL(I,5)
  STL(I,11)=(0.008*STL(I,5)+0.006)*STL(I,5)-STL(I,10)
  STL(I,12)=(0.002724+0.01276*STL(I,5))/EFAIL
  IF (STL(I,12).LT.1.0) STL(I,12)=1.0
90  CONTINUE
  DO 110 I=1,N
    DO 100 J=1,N
      R=2.011-2.353*TEMP(I,J)
      IF (R.GT.1.0) R=1.0
      IF (R.LT.0.0) R=0.0
      TEMP(I,J)=TEMP(J,I)=R
100
100

```

```

10  NR=NY+1-J
    TEMP(I,NR)=TEMP(I,J)
    PRINT 200
    PRINT 240, ((TEMP(I,J),J=1,N),I=1,N)
    PRINT 190
    NA=N+1
    PRINT 250, ((FT(I,J),J=1,NA),I=1,N)
    PRINT 200
    PRINT 240, ((FU(I,J),J=1,N),I=1,N)
    DO 120 I=1,N
    DO 120 J=1,NY
120  FU(I,J)=FU(I,J)/EFAIL
    PRINT 210
    PRINT 240, ((EU(I,J),J=1,N),I=1,N)
    PRINT 220
    PRINT 210, (STL(I,5),I=1,NSTL)
    DO 150 I=1,NSTL
    T=STL(I,5)
    STL(I,5)=STL(I,7)=STL(I,8)=0.0
    E=ES*(1.0-2.04*T*T)
    IF (E.LF.0.0) GO TO 130
    F=FS*(1.0-0.78*T-1.89*T**4)
    IF (F.LF.0.0) GO TO 130
    STL(I,7)=F/E
    STL(I,8)=F
130  A=2.011-2.353*T
    IF (A.GT.1.0) A=1.0
    IF (A) 150,150,140
140  STL(I,5)=A
150  CONTINUE
    PRINT 220, (STL(I,8),I=1,NSTL)
    PRINT 230, (STL(I,7),I=1,NSTL)
    PRINT 240, (STL(I,10),I=1,NSTL)
    PRINT 250, (STL(I,11),I=1,NSTL)
C
C   IF THERMAL EXPANSION IS NOT CONSIDERED TRANSFORM FROM USING
C   SQUARE ELEMENTS TO STRIPS (IE. USE EFFECTIVE WIDTH)
    IF ((THERM.NE.0) GO TO 180
    DO 170 J=1,N
    T=0.0
    DO 160 I=1,N
    T=T+TEMP(I,J)
160  CONTINUE
    TEMP(1,J)=TEMP(1,NY+1-J)=T
170  CONTINUE
    PRINT 260
    PRINT 270, (TEMP(1,J),J=1,N)
180  RETURN
190  FORMAT (1H ,/5X,*CONCRETE THERMAL EXPANSION STRAINS*/)
200  FORMAT (1H ,/5X,*CONCRETE MAX. YIELD STRAINS*/)
210  FORMAT (1H ,/5X,*CONCRETE EUMAX AT ELEV TEMP/EUMAX AT ROOM TEMP*/)
220  FORMAT (1H1,/55X,*STEEL REINFORCING BAR TEMPERATURE DEPENDENT PROP
    VEPTIFS*/)
230  FORMAT (1HC,25X,*STEEL ELASTIC YIELD STRAIN*,6F11.6)
240  FORMAT (1HC,20X,*STEEL THERMAL EXPANSION STRAINS*,6F11.6)
250  FOR (1HC,6X,*THERMAL STRAIN DIFFERENTIAL AT LEVEL OF STEEL*,6F1
1

```

```

240  FORMAT (1H ,/5X,*ACCUMULATED CONCRETE STRENGTH REDUCTION FACTORS*/
1)
250  FORMAT (1H ,8F11.4)
260  FORMAT (13A6)
270  FORMAT (1H ,/5X,*THOUSANDS OF DEGREES C. ABOVE ROOM TEMP.*/ )
280  FORMAT (1H ,/5X,*REDUCTION FACTORS FOR CONCRETE STRENGTH*/ )
290  FORMAT (1H ,5X,*THOUSANDS OF DEGREES C. ABOVE ROOM TEMPERATURE*,6F
111.6)
300  FORMAT (1H ,19X,*REDUCED ELASTIC MODULUS OF STEEL*,6F11.1)
310  FORMAT (8F10.1)
320  FORMAT (1H ,8F11.6)
330  FORMAT (1H ,9F11.6)
END

```

```

SUBROUTINE ITERATE (P,BM,U1,U2,KOUNT)

```

```

*****

```

```

SUBROUTINE ITERATE ADJUSTS THE MAGNITUDE AND CURVATURE OF
STRAIN ON THE CROSS-SECTION TO BALANCE THE INTERNAL CAPACITY
AGAINST THE EXTERNAL APPLIED LOADS

```

```

*****

```

```

S S S SUBROUTINE ITERATE BEGINS S S S

```

```

DIMENSION UA(2,3), UX(2,3)
COMMON /BLOCK1/ TEMP(8,16),ET(8,17),EU(8,16),STL(6,12),X,Y,DX,DY,N
IX,NY,NSTL,X2,Y2,TOLER,EFAIL,FC,FS,PCAL,BMCAL,PSTL,ES,N,ACONC,ITER
2M,ITER,NTEMP,IPRINT

```

```

EXPRESSION FOR THE CONCRETE STRESS-STRAIN FUNCTION
FCONC(X)=(((((-1.797E+10*X+2.126E+8)*X-9.304E+05)*X+1.2E+3)*X+3.529
101)/4.0

```

```

WA=WX=WC=1.0

```

```

DO 10 I=1,2

```

```

DO 10 J=1,3

```

```

10 UA(I,J)=UX(I,J)=0.0

```

```

K=0

```

```

ACCUR=TOLER

```

```

BISECTA=BISECTX=C

```

```

IF (BM.FO.0.0) U1=U2=ABS(U2*P)/P

```

```

DO 170 KOUNT=1,ITER

```

```

IF (KOUNT.GT.0.75*ITER) ACCUR=2*TOLER

```

```

PCAL=PSTL=BMCAL=0.0

```

```

U12=(U1-U2)/NY

```

```

DO 90 I=1,NX

```

```

DO 90 J=1,NY

```

CALCULATE THE STRAIN AT THE EDGES OF EACH ELEMENT

$UL = (U1 - U12 * (J - 1) + FT(I, J)) / FU(I, J)$

$UR = (U1 - U12 * J + FT(I, J + 1)) / FU(I, J)$

DETERMINE THE AVERAGE COMPRESSIVE STRAIN IN THE CONCRETE ELEMENT
DETERMINE THE PROPORTION OF ELEMENT AREA THAT IS IN COMPRESSION
BUT HAS NOT CRUSHED

IF $(UL > 0 \text{ AND } UR > 0)$ GO TO 40

IF $(UR > 0)$ GO TO 20

IF $(UL > 0)$ GO TO 30

GO TO 90

$D = UR / (UR - UL)$

$U = UR / 2$

GO TO 70

$D = UL / (UL - UR)$

$U = UL / 2$

GO TO 70

IF $(UL > EFAIL \text{ AND } UR > EFAIL)$ GO TO 90

IF $(UL > EFAIL)$ GO TO 50

IF $(UR > EFAIL)$ GO TO 60

$U = (UL + UR) / 2$

GO TO 80

$D = (EFAIL - UR) / (UL - UR)$

$U = (UR + EFAIL) / 2$

GO TO 70

$D = (EFAIL - UL) / (UR - UL)$

$U = (UL + EFAIL) / 2$

$C = C * D$

$R = (J - 0.5) * DY - Y2$

PERFORM THE AXIAL AND BENDING MOMENT FORCE SUMMATIONS

$F = FCONC(U - 0.00127367) * C * TEMP(I, J)$

$PCAL = F + PCAL$

$BMCAL = BMCAL + F * B$

CONTINUE

REPEAT ABOVE OPERATIONS FOR THE NET STEEL AREAS

$U12 = U1 - U2$

DO 100 I = 1, NSTL

$A = STL(I, 4) = U1 - U12 * STL(I, 2) + STL(I, 10)$

$F = STL(I, 6) = STL(I, 3) * STL(I, 8) * (ABS(A + STL(I, 7)) - ABS(A - STL(I, 7))) / 2$

$U = (A + STL(I, 11)) / STL(I, 12)$

IF $(U > 0 \text{ AND } U < EFAIL)$, $F = F - FCONC(U - 0.00127367) * STL(I, 5) * STL(I, 13) * FC$

$PSTL = PSTL + F$

$BMCAL = BMCAL + F * STL(I, 9)$

CONTINUE

DETERMINE THE ERROR BOUNDS FOR THE AXIAL LOAD

IF $(P * PSTL > 0.0)$ GO TO 110

$PA = P - PSTL$

GO TO 120

$PA = 0$

$PCAL = PCAL + PSTL$

$CORR = (PCAL - PA) / ABS(PA)$

IF $(P * PSTL < 0.0)$ $PCAL = PCAL + PSTL$

IF .LT GO TO 130

```

K=0
WA=2.0
IF (ABS(CORR).GT.1.0) CORR=ABS(CORR)/CORR

```

```

DETERMINE THE CORRECTION TO THE MAGNITUDE OF STRAIN BY USING
A STEPPING ROUTINE FIRST AND THEN BY USING A BISECTION METHOD

```

```

U=(U1+U2)/2
DU=CORR*ABS(U)
I=1
IF (DU.LT.0) I=2
IF (ABS(U).LT.0.00025) DU=0.00025*CORR
IF (ABS(DU).GT.0.0006) DU=0.0006*ABS(DU)/DU
UA(I,1)=U
UA(I,2)=DUA=DU
UA(I,3)=1.0
IF ((UA(1,3)+UA(2,3)).NE.2.0) GO TO 140
DUA=DU*(UA(1,1)-UA(2,1))/(UA(1,2)-UA(2,2))
IF (DUA/DU.LT.0.05) DUA=0.05*DU
IF (DUA/DU.GT.1.0) DUA=DU
BISECTA=BISECTA+1.0
IF (BISECTA.GT.6) BISECTA=UA(1,3)=UA(2,3)=0.0
UA(I,3)=1.0
GO TO 140
130 K=K+1
DUA=0.0

```

```

DETERMINE THE ERROR BOUNDS FOR THE PENDING MOMENT LOAD

```

```

140 IF (BM.EQ.0.0) GO TO 150
CORR=(BMCAL-BM)/BM
IF (ABS(CORR/ACCUR).LT.1.0) GO TO 150
WX=4.0
K=0
IF (ABS(CORR).GT.1.0) CORR=ABS(CORR)/CORR

```

```

DETERMINE THE CORRECTION TO THE CURVATURE OF STRAIN BY A STEP
METHOD FOLLOWED BY A BISECTION METHOD

```

```

U=(U2-U1)/2
DU=CORR*ABS(U)
I=1
IF (DU.LT.0) I=2
IF (ABS(U).LT.0.00005) DU=0.00005*CORR
IF (ABS(DU).GT.0.0006) DU=0.0006*ABS(DU)/DU
UX(I,1)=U
UX(I,2)=DUX=DU
UX(I,3)=1.0
IF ((UX(1,3)+UX(2,3)).NE.2.0) GO TO 160
DUX=DU*(UX(1,1)-UX(2,1))/(UX(1,2)-UX(2,2))
IF (DUX/DU.LT.0.05) DUX=0.05*DU
IF (DUX/DU.GT.1.0) DUX=DU
BISECTX=BISECTX+1.0
IF (BISECTX.GT.6) BISECTX=UX(1,3)=UX(2,3)=0.0
UX(I,3)=1.0
GO TO 160

```

```

150 K=K+1
DUX=0.0
160 IF (K.GE.2) GO TO 180

```

LT

TO THE STRAIN PATTERN TO AVOID ANY CYCLING

PROBLEMS, CURVATURE CORRECTIONS ARE GIVEN A LARGER WEIGHTING FACTOR, WEIGHTING FACTOR IS ALWAYS USED EVEN WHEN THE CORRESPONDING CORRECTION IS EQUAL TO ZERO TO PREVENT OVER-CORRECTION.

IF (U1.LT.0.0) WC=2.0

IF (U2.LT.0) WC=1.0

U1=U1-(DUA*WA-DUX*WX*WC)/W

U2=U2-(DUA*WA+DUX*WX)/W

WX=WA=WC=1.0

IF (IPRINT.GT.0) PRINT 107, PCAL, PA, PM, PMCAL, U1, U2, ACCUR, KOUNT
CONTINUE

RETURN TO THE CALLING PROGRAM WITH THE CONVERGED STRAINS, IF POSSIBLE, AND THE CORRESPONDING CONVERGENCE INTEGER 'KOUNT'
KOUNT=0

RETURN

FORMAT (1H, 4F10.2, 2F10.6, 55.2, 15)
END

SUBROUTINE STIFF (U1,U2,FA,FI,CG,PT).

SUBROUTINE 'STIFF' CALCULATES THE CROSS-SECTION STIFFNESS PROPERTIES BY NUMERICAL INTEGRATION ACROSS THE CROSS-SECTION. THE FORCE DUE TO THERMAL EXPANSION IS ALSO CALCULATED IF REQUIRED

\$\$\$ SUBROUTINE STIFF BEGINS \$\$\$

COMMON /BLOCK1/ TEMP(8,16), FT(8,17), FU(8,16), STL(6,12), X, Y, DX, DY, N1X, NY, NSTL, X2, Y2, TOLER, EFAIL, FC, FS, PCAL, BMCAL, PSTL, ES, N, ACONC, IITER, IITER, NTEMP, IPRINT

EXPRESSION FOR THE CONCRETE STRESS-STRAIN FUNCTION
FCONC(X)=((((-1.797E+10*X+2.126E+8)*X-9.304E+05)*X+1.2E+3)*X+3.529E+10)/4.0

FA=FI=FAY=0.0

U12=(U1-U2)/NY

PT=0.

DO 80 I=1,NX

DO 80 J=1,NY

C=ACONC

CALCULATE THE STRAIN AT THE EDGES OF EACH ELEMENT

U1=(U1-U12*(J-1)+FT(I,J))/FU(I,J)
U2=(U1-U12*(J-1)+FT(I,J))/FU(I,J)

DETERMINE THE AVERAGE COMPRESSIVE STRAIN IN THE CONCRETE ELEMENT
 DETERMINE THE PROPORTION OF ELEMENT AREA THAT IS IN COMPRESSION
 BUT HAS NOT CRUSHED

IF (UL.GT.0.AND.UR.GT.0) GO TO 30

IF (UR.GT.0) GO TO 10

IF (UL.GT.0) GO TO 20

GO TO 80

D=UR/(UR-UL)

U=UR

GO TO 50

D=UL/(UL-UR)

U=UL

GO TO 60

IF (UL.GT.EFAIL.AND.UR.GT.EFAIL) GO TO 80

IF (UL.GT.EFAIL) GO TO 40

IF (UR.GT.EFAIL) GO TO 50

U=(UL+UR)/2

D=DY*DY/12

GO TO 70

D=(EFAIL-UR)/(UL-UR)

U=(UR+EFAIL)/2

GO TO 60

D=(EFAIL-UL)/(UR-UL)

U=(UL+EFAIL)/2

C=C*D

D=D*D*DY*DY/12

R=(J-0.5)*DY-Y2

IF (U.LT.0.0001) U=0.0001

DETERMINE THE AXIAL STIFFNESS OF EACH ELEMENT USING THE SECANT
 ELASTIC MODULUS, PERFORM THE SUMMATION TO FIND THE AXIAL AND
 BENDING STIFFNESS DETERMINED ABOUT THE GROSS CONCRETE CENTROID
 $F = FCONC(U - 0.00127367) * C * TEMP(I, J) / U$

EA=EA+F

FAY=FAY+F*R

FI=FI+F*(D+R*R)

IF (ITHERM.EQ.0) GO TO 80

R=(ET(I, J)+ET(I, J+1))/2

U=U*FU(I, J)

IF ((U-R).GT.0.0) U=R

PT=PT+F*U

CONTINUE

U12=U1-U2

REPEAT ABOVE OPERATIONS FOR THE NET STEEL AREAS

DO 90 I=1,NSTL

A=STL(I,4)=U1-U12*STL(I,2)+STL(I,10)

F=STL(I,8)*STL(I,3)

IF (ABS(A).GT.ABS(STL(I,7))) F=F*STL(I,7)/ABS(A)

U=(A+STL(I,11))/STL(I,12)

IF (U.GT.0.AND.U.LT.0.0001) U=0.0001

IF (U.GT.0.AND.U.LT.EFAIL) F=F-FCONC(U-0.00127367)*STL(I,5)*STL(I,
 13)*FG/U

EA=EA+F

FAY=FAY+F*STL(I,9)

FI=FI+F*STL(I,9)*STL(I,9)

TRANSFORM THE BENDING STIFFNESS CALCULATED ABOUT THE GROSS
CENTROID TO THE 'ELASTIC' CENTROID
CG=FAY/FA

FI=FI-FAY*CG
RETURN
END

SUBROUTINE COLUMN

SUBROUTINE 'COLUMN' READS THE DATA FOR THE PINNED COLUMN, PERFORMS
THE NECESSARY CALCULATIONS AND PRINTS THE FINAL INFORMATION FOR
EACH ECCENTRICITY.

INPUT VARIABLES IN THE FOLLOWING ORDER

NPTS - NUMBER OF ECCENTRICITIES TO BE INVESTIGATED
NSECT - NUMBER OF EQUAL SECTIONS THE COLUMN LENGTH WILL BE DIVIDED
INTO (NSECT MUST BE EVEN AND GREATER THAN ZERO EVEN FOR
THE CASE WHERE LENGTH IS NOT BEING CONSIDERED)
COL - COLUMN LENGTH EXPRESSED AS A RATIO OF LENGTH TO DEPTH 'Y'
RAT(I) - LOAD ECCENTRICITIES EXPRESSED AS RATIO TO DEPTH 'Y'

\$\$\$ SUBROUTINE COLUMN BEGINS \$\$\$

COMMON /BLOCK1/ TFMP(8,15),FT(8,17),EU(8,16),STL(6,12),X,Y,DX,DY,N
1X,NY,NSTL,X2,Y2,TOLER,EFAIL,FC,FS,PCAL,BMCAL,PSTL,ES,N,ACONC,ITHR
2M,ITER,NTEMP,IPRINT
COMMON /BLOCK2/ DEFL(11),CUR(11),EYY(30),RAT(30)

DATA CARDS FOR COLUMN ANALYSIS

READ 140, NPTS,NSECT,COL

PRINT 160, COL,NSECT

COL=COL*Y

PRINT 170, NPTS

READ 150, (RAT(I),I=1,NPTS)

DO 10 I=1,NPTS

EYY(I)=RAT(I)*Y

CONTINUE

PRINT 180, (RAT(I),I=1,NPTS)

HSQ=(COL/NSECT)**2

NMID=NSECT/2+1

HINT=COL/NSECT

NC=NSECT+1

```

DO 120 ITEMP=1, NITEMP
CALL TEMPER
PRINT 220

```

```

INITIAL ESTIMATES TO STRAINS AND FORCES USING SUBROUTINE 'STIFF'
IS=NY/2

```

```

U2=FFAIL*FU(IS,1)-FT(IS,1)

```

```

U1=-2*FFAIL*FU(IS,1)-FT(IS,1)

```

```

CALL STIFF (U1,U2,FA,FI,CG,PT)

```

```

DO 130 KOUNT=1, NPTS

```

```

FY=FY(KOUNT)

```

```

P=FFAIL/(1/(FA*ABS(FY))+Y/FI/2)/FY*(3+ABS(FY)/FY)/4

```

```

U2=FFAIL*FU(IS,1)/4-FT(IS,1)

```

```

U1=-FFAIL*FU(IS,1)/2-FT(IS,1)

```

```

PRINT=-0.09

```

```

PRINT 210, EY, RAT(KOUNT)

```

```

BMX=P*EY

```

```

CALL VALID (P, BMX, U1, U2, 1)

```

```

BMX=P*FY

```

```

ATTEMPT FORCE AND STRAIN CONVERGENCE FOR BASE MOMENTS

```

```

CALL ITERATE (P, BMX, U1, U2, KNT)

```

```

IF (KNT) 110, 110, 30

```

```

CALCULATE DEFLECTION CURVE AND INCREASED BENDING MOMENTS AT
VARIOUS POINTS UP THE COLUMN FROM BASE TO MID-HEIGHT, IF REQUIRED

```

```

IF (COL.EQ.0.0) GO TO 100

```

```

UA=U1

```

```

UB=U2

```

```

DO 40 I=1, NC

```

```

CUR(I)=(UB-UA)/Y

```

```

CONTINUE

```

```

DEFL(1)=DM=DEFL(NC)=0.0

```

```

DO 90 IO=1, 10

```

```

D=0.0

```

```

DO 50 I=2, NC

```

```

D=CUR(I-1)*(NSECT-I+1.5)+(CUR(I)-CUR(I-1))*(NSECT-I+4.0/3.0)/2.0+D

```

```

CONTINUE

```

```

TAU=D/NSECT

```

```

DO 70 J=2, NMID

```

```

D=0.0

```

```

DO 60 I=2, J

```

```

D=CUR(I-1)*(J-I+0.5)+(CUR(I)-CUR(I-1))*(J-I+1.0/3.0)/2.0+D

```

```

CONTINUE

```

```

DEFL(J)=DEFL(NC+1-J)=(TAU*(J-1)-D)*HSQ

```

```

CONTINUE

```

```

DO 80 I=2, NMID

```

```

BMXD=P*(FY+DEFL(I))

```

```

CALL ITERATE (P, BMXD, UA, UB, KNT)

```

```

IF (KNT) 110, 110, 80

```

```

CUR(I)=CUR(NC+1-I)=(UB-UA)/Y

```

```

D=DEFL(NMID)

```

```

TOL=TOLFR

```

```

IF ((FY/Y).LE.0.175) TOL=TOLER/2.0

```

```

PRINT 200, P, BMXD, UA, UB, DEFL(NMID)

```

MID-HEIGHT DEFLECTION

MODE=0

```

00 CONTINUE
   GO TO 110
C   FIND NEW ESTIMATE TO AXIAL LOAD BY STEPPING, STEP SIZE EXPANDS
C   AFTER EACH SUCCESSFUL INCREASE AND DECREASES AFTER EACH INVALID
C   ATTEMPT AT INCREMENTING
100 CALL VALID (P,BMX,U1,U2,1)
   PRINT 190, P,BMX,U1,U2
   PINT=1.1*ABS(PINT)
   P=P*(1.0+PINT)
   GO TO 20
110 CALL VALID (P,BMX,U1,U2,2)
   IF (ABS(PINT).LT.TOLFR) GO TO 120
   PINT=0.4*PINT
   IF (PINT.LT.0.0) PINT=4.0*PINT
   IF (PINT.LE.-1.0) GO TO 120
   P=P*(1.0+PINT)
   GO TO 20
120 CALL VALID (P,BMX,U1,U2,2)
   PRINT 190, P,BMX,U1,U2
130 PRINT 220
   STOP
C
140 FORMAT (2I10,F10.0)
150 FORMAT (8F10.0)
160 FORMAT (1H,5X,*RATIO OF COLUMN LENGTH TO THICKNESS IS*,F5.1,* DIV
  110ED INTO *,I3,* EQUAL VERTICAL SECTIONS*//)
170 FORMAT (1H,5X,*NUMBER OF P VS. BM POINTS TO BE FOUND IS*,I3//)
180 FORMAT (1H,5X,*Y - ECCENTRICITIES OVER THICKNESS RATIOS*//,(10X,F
  110.4))
190 FORMAT (1H0,2F12.4,2F12.6)
200 FORMAT (1H,50X,2F12.4,3F12.6)
210 FORMAT (1H,5X,*ECCENTRICITY =*,F8.3,* FOR THE E/T RATIO OF*,F8.3/
  17,5X,*PRIMARY EFFECTS*,43X,*MID-HEIGHT SECONDARY EFFECTS CONVERGEN
  2CE SERIES (IF CONSIDERED)*//,11X,*P*,11X,*BM*,10X,*U1*,10X,*U2*,16
  2X,*P*,8X,*TOTAL BM*,7X,*U1*,10X,*U2*,6X,*MID-HEIGHT DEFL*//)
220 FORMAT (1H1)
   END

```

SUBROUTINE VALID (P,BMX,U1,U2,MODE)

SURROUTINE VALID STORES THE MOST RECENT SET OF CONVERGED VARIABLES
GO TO (10,20), MODE

```

10 A=U1
   C=U2
   F=P
   F=BMX
   RETURN
20 U1=A
   U2=C
   P=F
   BMX=F
   RETURN
END

```

SUBROUTINE 'FRAME' READS THE STRUCTURAL FRAME INPUT, PERFORMS THE NECESSARY CALCULATIONS, AND CALLS THE APPROPRIATE SUBROUTINES TO ARRIVE AT A STABLE SET OF FRAME FORCES AND STIFFNESSES IF POSSIBLE

INPUT VARIABLES IN THE FOLLOWING ORDER

NJOIN - NUMBER OF JOINTS IN THE STRUCTURE, BASE JOINTS ALL EQUAL 0
 NELEM - NUMBER OF STRUCTURAL MEMBERS IN THE FRAME, INCLUDING THE INELASTIC SUB-MEMBERS

LDJNT - NUMBER OF JOINTS ACTUALLY LOADED

INELAST - NUMBER OF INELASTIC SUB-MEMBERS, MUST BE GREATER THAN 0

BAY - SPACING OF THE RIGID FRAMES ALONG BUILDING LENGTH

J - LOADED JOINT NUMBER

FORCE(I) - LOADS ON THE LOADED JOINTED 'J', IN THE GLOBAL X, Y, AND Z-DIRECTIONS, RESPECTIVELY

EII - INITIAL APPROXIMATION TO THE MEMBER BENDING STIFFNESS

EAA - INITIAL APPROXIMATION TO THE MEMBER AXIAL STIFFNESS

K - MEMBER NUMBER BEING INPUT

XP - RELATIVE GLOBAL DISPLACEMENT OF END 2 OF THE MEMBER IN THE X-DIRECTION

YP - RELATIVE GLOBAL DISPLACEMENT OF END 2 OF THE MEMBER IN THE Y-DIRECTION

IFROM(J) - JOINT NUMBER AT END 1 OF THE MEMBER, ALWAYS SMALLER THAN ITO(J).

ITO(J) - JOINT NUMBER AT END 2 OF MEMBER

FOLLOWING TWO VARIABLES ARE FOR INELASTIC MEMBERS ONLY

UN(J) - INITIAL FIBRE STRAIN ON TENSION SIDE OF CROSS-SECTION

UP(J) - INITIAL FIBRE STRAIN ON COMPRESSION SIDE

\$\$\$ SUBROUTINE FRAME BEGINS \$\$\$

COMMON /BLOCK1/ TEMP(8,16), ET(8,17), EU(8,16), STL(6,12), X, Y, DX, DY, N1X, NY, NSTL, X2, Y2, TOLER, EFAIL, FC, FS, PCAL, BMCAL, PSTL, ES, N, ACONC, ITHR2M, ITER, NTEMP, IPRINT

COMMON /BLOCK2/ T(3,3,66), DIST(66), SF(6,6), F1(66), EA(66), STF11(3,3,1,66), STF12(3,3,66), STF21(3,3,66), STF22(3,3,66)

COMMON /BLOCK3/ PDD(126), IFROM(66), ITO(66), PF(10), BMF(10), PT(10), UN(10), UP(10)

DIMENSION FORCE(3)

INPUT THE PREVIOUSLY MENTIONED DATA
 READ 220, NJOIN, NELEM, LDJNT, INELAST
 PRINT 210, NELEM, INELAST, NJOIN, LDJNT

JOINT=3*NJOIN

READ 230, BAY

PRINT 240, BAY

DO 10 I=1, JOINT

PDD(I)=0.0

CONTINUE

DO 20 I=1, LDJNT

READ 250, J, FORCE

PRINT 250, J, FORCE

```

DO 20 J=1,3
DOO(K+J)=FORCE(J)*RAY
PRINT 200
PRINT 260
READ 270, FII,FAA
DO 30 J=1,INFLAST
READ (5,280) K,XP,YP,IFROM(K),ITO(K),UN(K),UP(K)
FI(K)=FII
EA(K)=FAA
WRITE (6,290) K,XP,YP,IFROM(K),ITO(K),FI(K),EA(K),UN(K),UP(K)
CALL TRANSF (XP,YP,K)
CONTINUE
IF (INFLAST.EQ.NELEM) GO TO 50
L=INFLAST+1
PRINT 300
DO 40 J=L,NELEM
READ (5,280) K,XP,YP,IFROM(K),ITO(K)
EI(K)=FII
FA(K)=FAA
WRITE (6,290) K,XP,YP,IFROM(K),ITO(K),EI(K),FA(K)
CALL TRANSF (XP,YP,K)
CONTINUE
40
50
C
C BEGIN INVESTIGATION OF EACH THERMAL GRADIENT
DO 170 NTM=1,NTEMP
PRINT 200
CALL TEMPER
C
C CALCULATE INITIAL MEMBER STIFFNESSES, PERFORM INITIAL ANALYSIS
DO 60 K=1,INFLAST
CALL STIFF (UN(K),UP(K),FA(K),EI(K),CG,PT(K))
60
CONTINUE
CALL RIGID (NELEM,JOINT,IPRINT,INELAST,ITHERM)
PRINT 310
C
C ITERATION CYCLE BEGINS TO OBTAIN CONVERGENCE OF MEMBER STIFFNESS
C AND HENCE FORCES
DO 130 KOUNT=1,10
PRINT 320, KOUNT
KNT=INELAST
DO 90 K=1,INFLAST
SIGN=1.0
IF (RMF(K).LT.0.0) SIGN=-1.0
RM=SIGN*RMF(K)
IF (RM.LT.BMXMIN) RM=BMXMIN
CALL ITERATE (PF(K),RM,UN(K),UP(K),MODE)
IF (MODE) 180,180,70
70
RMCAL=RMCAL*SIGN
CALL STIFF (UN(K),UP(K),FAA,EII,CG,PT(K))
CG=CG*SIGN
C
C CHECK TOLERANCE LEVEL, CHANGES TO STIFFNESSES ARE WEIGHTED TO
C AVOID CYCLING CAUSED BY OVER-CORRECTION
EA(K)=(EA(K)+3*FAA)/4
FI(K)=(FI(K)+3*FII)/4
IF (ABS((EA(K)-FAA)/FAA).GT.TOLER/4.0) GO TO 80
IF .LT. GO TO 90

```

```

90 KNT=KNT+1
PRINT 230, PF(K),RMF(K),PCAL,BMCAL,UN(K),UP(K),CG,FI(K),FA(K),K
90 KNT=KNT-1
IF (NTM.GT.1) GO TO 120
IF (NFLFM.EQ.INFLAST) GO TO 120
FII=EAA=0.0
DO 100 I=1,INFLAST
FII=EII+FI(I)
FAA=FAA+FA(I)
100 CONTINUE
FII=FII/INFLAST
FAA=FAA/INFLAST
DO 110 I=L,NELEFM
FI(I)=EII
EA(I)=FAA
110 CONTINUE
120 IF (KNT.EQ.0) GO TO 140
CALL RIGID (NFLFM,JOINT,IPRINT,INELAST,ITHERM)
130 CONTINUE
C
C PRINTOUT OF RESULTS AFTER CONVERGENCE OR WHEN THE MAXIMUM NUMBER
C OF CYCLES HAS BEEN EXCEEDED
140 PRINT 340, KOUNT,KNT
DO 150 J=1,INFLAST
PRINT 250, PF(J),RMF(J),UN(J),UP(J),FI(J),EA(J),J
150 CONTINUE
IF (INFLAST.EQ.NELEFM) GO TO 160
PRINT 260, FI(L),FA(L),L,NELEFM
160 CALL RIGID (NELEFM,JOINT,1,INFLAST,ITHERM)
170 CONTINUE
GO TO 190
180 PRINT 270
190 STOP
C
200 FORMAT (1H1)
210 FORMAT (1H0,*STRUCTURE CONSISTS OF *,I3,* MEMBERS INCLUDING *,I3,*
1 INELASTIC MEMBERS*//,5X,*FRAME HAS *,I3,* JOINTS OF WHICH *,I3,*
2 ARE LOADED*//)
220 FORMAT (6I10)
230 FORMAT (F10.0)
240 FORMAT (//5X,*INPUT LOADED JOINTS ONLY, (INPUT ORDER IS NOT IMPORT
1 ANT) BAY SIZE = *,F5.1,* FT*//.* JOINT X-ACTION Y-ACTION
2 Z-ACTION (KIPS AND INCH-KIPS)*//)
250 FORMAT (I10,3F10.2)
260 FORMAT (1H,5X,*MEMBER X*,10X,*Y FROM TO EI*,9X,*E
1A*,6X,*STRAINS (TENSION AND COMPRESSION),FOR INELASTIC MEMBERS*//)
270 FORMAT (2F20.0)
280 FORMAT (I5,2F10.0,2I5,2F10.0)
290 FORMAT (5X,I5,2F11.4,2I6,2F11.0,2F11.5)
300 FORMAT (1H0,5X,*MEMBER X*,10X,*Y FROM TO EI*,9X,*E
1A*,6X,*FOR ELASTIC MEMBERS*//)
310 FORMAT (1H1,5X,*START ITERATION CYCLE*//9X,*P*,8X,*RM*,6X,*PCAL
1 BMCAL *,5X,*U1*,8X,*U2*,8X,*CG*,8X,*FI*,10X,*FA*//)
320 FORMAT (1H0,I7)
330 FORMAT (5X,2(F8.2,F9.2),3F10.6,F12.0,F10.0,* MEMBER NO.*,I3)
340 FORMAT (1H1,5X,*FINAL RESULTS AFTER*,I3,* CYCLES OF ITERATION, LEA
1 VING*,I3,* UNSATISFIED VARIABLES*//10X,*P*,7X,*RM*,9X,*U1*,8X,*U2*

```

```

350 FORMAT (1H ,F13.2,F9.2,2F12.6,F12.0,F10.0,* MEMBER NO.*,I3/)
360 FORMAT (1H),42X,F12.0,F10.0,* MEMBER NO.*,I3,* TO*,I3)
370 FORMAT (5X,*NO CONVERGENCE*)
END

```

SUBROUTINE RIGID (NELEM,JOINT,IPRINT,INELAST,ITHERM)

STRUCTURAL ANALYSIS OF THE RIGID FRAME
NOTE ALL JOINTS INCLUDING BASE ARE RIGID, SOLUTION BY
SIMULTANEOUS EQUATIONS DUE TO FACT THAT EXTRA MEMBERS AND
JOINTS CAN BE ADDED TO OR DELETED FROM THE INPUT DATA DECK
AS DESIRED WITHOUT DISTURBING PREVIOUS DATA

\$\$\$ SUBROUTINE RIGID BEGINS \$\$\$

```

DIMENSION STIFF(78,78), PD(78)
DIMENSION GD1(3), GD2(3), FORC1(3), FORC2(3), D1(3), D2(3)
DIMENSION RK(3,3), SK(3,3), QK(3,3), UK(3,3)
COMMON /BLOCK2/ T(3,3,66),DIST(66),SF(6,6),FI(66),EA(66),STF11(3,3
1,56),STF12(3,3,66),STF21(3,3,66),STF22(3,3,66)
COMMON /BLOCK3/ PDD(126),IFROM(66),ITO(66),PF(10),BMF(10),PT(10)
DO 10 I=1,JOINT
DO 10 J=1,JOINT
STIFF(I,J)=0.0

```

MEMBER STIFFNESS MATRIX IN MEMBER COORDINATES

```

DO 70 KNT=1,NELEM
DO 20 I=1,3
DO 20 J=1,3
RK(I,J)=SK(I,J)=0.0
QK(I,J)=UK(I,J)=0.0,
BL=DIST(KNT)
RK(1,1)=UK(1,1)=FA(KNT)/BL
RK(2,2)=UK(2,2)=12.0*EI(KNT)/BL**3
RK(2,3)=RK(3,2)=6.0*EI(KNT)/BL/BL
RK(3,3)=UK(3,3)=4.0*EI(KNT)/BL
UK(2,2)=UK(3,2)=-RK(2,3)
SK(1,1)=QK(1,1)=-RK(1,1)
SK(2,2)=QK(2,2)=-RK(2,2)
SK(2,3)=QK(3,2)=RK(2,3)
SK(3,2)=QK(2,3)=-RK(3,2)
SK(3,3)=QK(3,3)=RK(3,3)/2.0

```

STORE MEMBER STIFFNESS MATRIX (MEMBER COORD'S) IN 3-DIMENSIONAL
ARRAY. THIRD SUBSCRIPT DEFINES MEMBER NUMBER

```

DO 30 J=1,3
STF11(I,J,KNT)=RK(I,J)
STF12(I,J,KNT)=SK(I,J)

```

```

U STF21(I,J,KNT)=OK(I,J)
DO STF22(I,J,KNT)=UK(I,J)
IT00=3*IT0(KNT)-3

```

```

C
C TRANSFORM MEMBER STIFFNESS MATRIX TO BE REFERENCED BY GLOBAL
C COORDINATES USING SUBROUTINE 'GLOBAL'
C FOR MEMBERS CONNECTING TO BASE JOINTS, ONLY K22 REQUIRED
CALL GLOBAL (UK,3,3,KNT)
IF (IFROM(KNT).EQ.0) GO TO 50
IFRO=3*IFROM(KNT)-3

```

```

C
C ADD K11, K12, K21, K22 TO ASSEMBLY MATRIX AT CORRECT LOCATION.
C LOCATION DEFINED BY JOINT NUMBERS OF MEMBER ENDS.

```

```

CALL GLOBAL (PK,0,0,KNT)
CALL GLOBAL (SK,0,3,KNT)
CALL GLOBAL (OK,3,0,KNT)

```

```

DO 40 I=1,3
IF=I+IFRO
IT=I+IT00
DO 40 J=1,3
JF=J+IFRO
JT=J+IT00
STIFF(IF,JF)=STIFF(IF,JF)+SF(I,J)
STIFF(IF,JT)=STIFF(IF,JT)+SF(I,J+3)
STIFF(IT,JF)=STIFF(IT,JF)+SF(I+3,J)
STIFF(IT,JT)=STIFF(IT,JT)+SF(I+3,J+3)
GO TO 70

```

```

C
C ADD K22 TO ASSEMBLY MATRIX FOR MEMBERS CONNECTING TO BASE JOINTS

```

```

DO 60 I=1,3
IT=I+IT00
DO 60 J=1,3
JT=J+IT00
STIFF(IT,JT)=STIFF(IT,JT)+SF(I+3,J+3)
70 CONTINUE

```

```

C
C TRANSFORM MEMBER THERMAL EXPANSION FORCES INTO GLOBAL FORCES

```

```

DO 80 KO=1,JOINT
PD(KO)=PDD(KO)

```

```

CONTINUE
IF (ITHERM.EQ.0) GO TO 100

```

```

DO 100 I=1,INFLAST
P1=T(1,1,I)*PT(I)
P2=T(1,2,I)*PT(I)
J=3*IFROM(I)-2
IF (J.LE.0) GO TO 90

```

```

PD(J)=PD(J)-P1
PD(J+1)=PD(J+1)-P2
J=3*IT0(I)-2
PD(J)=PD(J)+P1
PD(J+1)=PD(J+1)+P2

```

```

CONTINUE

```

```

C
C ALL MEMBERS HAVE BEEN PROCESSED, PROCEED WITH SOLUTION
C OF THE SIMQ

```

```

110 CALL SIMO (STIFF,PD,78,ISING)
WRITE TITLES FOR SUBSEQUENT DATA OUTPUT
IF (IPRINT.GT.0) PRINT 210
IF (IPRINT.GT.0) WRITE (6,220)
IF (IPRINT.GT.0) WRITE (6,230)

C
C INITIATE DO-LOOP TO CALCULATE MEMBER FORCES AND DISPLACEMENTS
DO 200 K=1,NFLEM
ITOO=3*ITO(K)-3
IFRO=3*IFROM(K)-3
IF (IFRO.LT.0) GO TO 130
DO 120 I=1,3
IF=I+IFRO
IT=I+ITOO
GD1(I)=PD(IF)
GD2(I)=PD(IT)
120 CONTINUE
GO TO 150
130 DO 140 I=1,2
IT=I+ITOO
GD1(I)=0.0
GD2(I)=PD(IT)
140 CONTINUE
150 CONTINUE
IF (IPRINT.GT.0) WRITE (6,240) (GD1(I),I=1,2),K
IF (IPRINT.GT.0) WRITE (6,250) (GD2(I),I=1,3)
DO 160 I=1,3
D1(I)=D2(I)=0.0
FORC1(I)=FORC2(I)=0.0
160 CONTINUE

C
C CALCULATE MEMBER DISPLACEMENTS FROM GLOBAL VALUES, VIA T WHICH
C WAS PREVIOUSLY STORED IN 3-DIMENSIONAL ARRAY FOR THIS PURPOSE.
DO 170 L=1,3
DO 170 M=1,3
D1(L)=D1(L)+T(L,M,K)*GD1(M)
170 D2(L)=D2(L)+T(L,M,K)*GD2(M)

C
C CALCULATE MEMBER FORCES IN MEMBER COORDINATES
DO 180 I=1,3
DO 180 J=1,3
FORC1(I)=FORC1(I)+STF11(I,J,K)*D1(J)+STF12(I,J,K)*D2(J)
180 FORC2(I)=FORC2(I)+STF21(I,J,K)*D1(J)+STF22(I,J,K)*D2(J)
IF (K.GT.INELAST) GO TO 190
FORC1(I)=FORC1(I)+PT(K)
FORC2(I)=FORC2(I)-PT(K)
190 CONTINUE
IF (IPRINT.GT.0) WRITE (6,260) (FORC1(I),I=1,3)
IF (IPRINT.GT.0) WRITE (6,270) (FORC2(I),I=1,3)
IF (K.GT.INELAST) GO TO 200
PF(K)=(FORC1(1)-FORC2(1))/2
BMF(K)=(FORC1(3)-FORC2(3))/2
200 CONTINUE
RETURN

C
210 FORMAT (JH1)
220 FORMAT (5X,*,MEMBER DISPL. (INCHES) IN GLOBAL COORDES. AND MEMBER #//)

```

```

230  FORMAT (23X,19HX5 AND X DIRECTIONS,6X,19HY5 AND Y DIRECTIONS,6X,19
240  FORMAT (140,4X,*DISPLC FND 1*,3E25.5,5X,*MEMBER NO.*,12)
250  FORMAT (5X,*DISPLC FND 2*,3E25.5)
260  FORMAT (5X,*FORCES FND 1*,3E25.5)
270  FORMAT (5X,*FORCES FND 2*,3E25.5)
      FND

```

```

SUBROUTINE GLOBAL (A, I1, J1, KNT)

```

```

*****

```

```

C THIS SUBROUTINE ACTUATES A SIMILARITY TRANSFORM OPERATING ON THE
C PRIMARY 3X3 MATRICES. THESE ARE SUBSEQUENTLY STORED IN PROPER
C LOCATIONS IN THE STIFFNESS MATRIX, SF.

```

```

*****

```

```

C $ $ $ SUBROUTINE GLOBAL BEGINS $ $ $

```

```

C DIMENSION A(3,3), B(3,3), D(3,3)
C COMMON /BLOCK2/ T(3,3,66),DIST(66),SF(6,6)
C DO 10 I=1,3
C DO 10 J=1,3
C B(I,J)=0.0
C D(I,J)=0.0
C CONTINUE

```

```

C CALCULATE (B) = (A)(T)
C DO 20 I=1,3
C DO 20 J=1,3
C DO 20 K=1,3
20 B(I,J)=B(I,J)+A(I,K)*T(K,J,KNT)

```

```

C CALCULATE (D) = (TT)(A)(T). MATRIX D THEN REPRESENTS MATRIX A,
C IN GLOBAL COORDINATES (OR D IS EQUAL TO 'A-PAR')

```

```

C DO 30 I=1,3
C DO 30 J=1,3
C DO 30 K=1,3
30 D(I,J)=D(I,J)+T(K,I,KNT)*B(K,J)

```

```

C POPULATE STIFFNESS MATRIX WITH SUBMATRICES WHICH ARE NOW
C EXPRESSED IN GLOBAL COORDINATES. RESULT IS MEMBER STIFFNESS
C MATRIX IN GLOBAL COORDINATES, READY FOR ADDITION TO STIFF.

```

```

C DO 40 I=1,3
C II=I1+I
C DO 40 J=1,3
C JJ=J1+J
40 SF(II,JJ)=D(I,J)
C RETURN

```

SUBROUTINE TRANSF (XP,YP,K)

CALCULATE MEMBER LENGTH FROM COORDINATES
STORE TRANSFORMATION MATRIX IN 3-DIMENSIONAL ARRAY. THIRD
SUBSCRIPT DEFINES MEMBER NUMBER, AS COUNTED BY PROGRAM FRAME.

\$\$\$ SUBROUTINE TRANSF BEGINS \$\$\$

COMMON /BLOCK2/ T(3,3,66),DIST(66)

AL=(XP*XP+YP*YP)**0.5

T(1,1,K)=T(2,2,K)=XP/AL

T(1,2,K)=YP/AL

T(1,3,K)=T(3,1,K)=0.0

T(2,1,K)=-T(1,2,K)

T(2,3,K)=T(3,2,K)=0.0

T(3,3,K)=1.0

TRANSFORM MEMBER LENGTH FROM FEET TO INCHES FOR DIMENSIONAL
CONTINUITY

DIST(K)=12.0*AL

RETURN

END